

**Addenda Published on this Book's  
Website Only**



## Addendum N

---

---

# ***Comparison of the Characteristic Function Method and Sheppard's Approach***

In this addendum we will briefly overview Sheppard's ideas that resulted in his famous corrections, and will discuss the differences between his approach and the characteristic function method of this book.

Rather than following Sheppard's original paper (Sheppard, 1898) step by step, we will present a more straightforward derivation, based on the ideas of (Cramér, 1946) and (Stuart and Ord, 1994).

Sheppard made use of the Euler-Maclaurin summation formula. Therefore, we start with a discussion of this.

### **N.1 THE EULER-MACLAURIN SUMMATION FORMULA**

The Euler-Maclaurin formula (Cramér, 1946; Korn and Korn, 1968; Milne-Thomson, 1960) is a relation between the integral of a function over a given range and the sum of uniformly spaced samples of this function over the same range multiplied by the sampling interval. The formula is

$$\begin{aligned} \sum_{m=0}^s g(a + mq) &= \frac{1}{q} \int_a^b g(x) dx \\ &+ \frac{1}{2} (g(a) + g(b)) \\ &+ \sum_{k=1}^K \frac{B_{2k}}{(2k)!} q^{2k-1} (g^{(2k-1)}(a) - g^{(2k-1)}(b)) \\ &+ S_{2K} . \end{aligned} \tag{N.1}$$

**W3**

The difference between the integral and the sum is evident. In this formula,  $B_{2k}$  is the  $(2k)$ th Bernoulli number<sup>1</sup>,  $K \geq 1$ ,  $b = a + sq$ , and  $g^{(2k-1)}(x)$  being the  $(2k - 1)$ th derivative of the function  $g(x)$ .

The remainder  $S_{2K}$  can be expressed according to (Korn and Korn, 1968) as

$$S_{2K} = \frac{s B_{2K+2}}{(2K + 2)!} q^{2K+2} g^{(2K+2)}(a + \vartheta(b - a)), \quad (\text{N.2})$$

where  $\vartheta$  is a properly chosen real number,  $0 < \vartheta < 1$ , assuming that  $g^{2K+2}(x)$  is continuous in  $[a, b]$ . The integer  $K$  can be any number greater than or equal to 1. Once  $K$  is chosen, there will always be a number  $\theta$  in the range  $(0, 1)$  that will make Eq. (N.1) be an equality.

A numerically somewhat more usable form of the remainder was given by (Cramér, 1946), as

$$S_{2K} = (-1)^{K+1} q^{2K} \int_a^b \sum_{n=1}^{\infty} \frac{1}{2^{2K} (n\pi)^{2K+1}} \sin\left(2\pi n \frac{x-a}{q}\right) g^{(2K+1)}(x) dx. \quad (\text{N.3})$$

For other forms, see (Milne-Thomson, 1960, Sect. 7.5).

The formula (N.1) makes use of the samples at the edges of the intervals (see Fig. N.1(a)), therefore it is not directly applicable for the analysis of quantization. It has however a modified version (Stuart and Ord, 1994; Milne-Thomson, 1960), which uses the samples at the center points of the intervals (Fig. N.1(b)).

$$\begin{aligned} \sum_{m=0}^{s-1} g(a + (m + 0.5)q) &= \frac{1}{q} \int_a^b g(x) dx \\ &+ \sum_{k=1}^K \frac{B_{2k}(0.5)}{(2k)!} q^{2k-1} \left( g^{(2k-1)}(a) - g^{(2k-1)}(b) \right) \\ &+ S_{2Km}, \end{aligned} \quad (\text{N.4})$$

with

$$S_{2Km} = \frac{sq^{2K}}{(2K)!} B_{2K}(0.5) g^{(2K)}(a + \vartheta(b - a)), \quad 0 < \vartheta < 1, \quad (\text{N.5})$$

<sup>1</sup>see Eq. (N.11.FN1) in the footnote of Exercise 4.25 in page S51

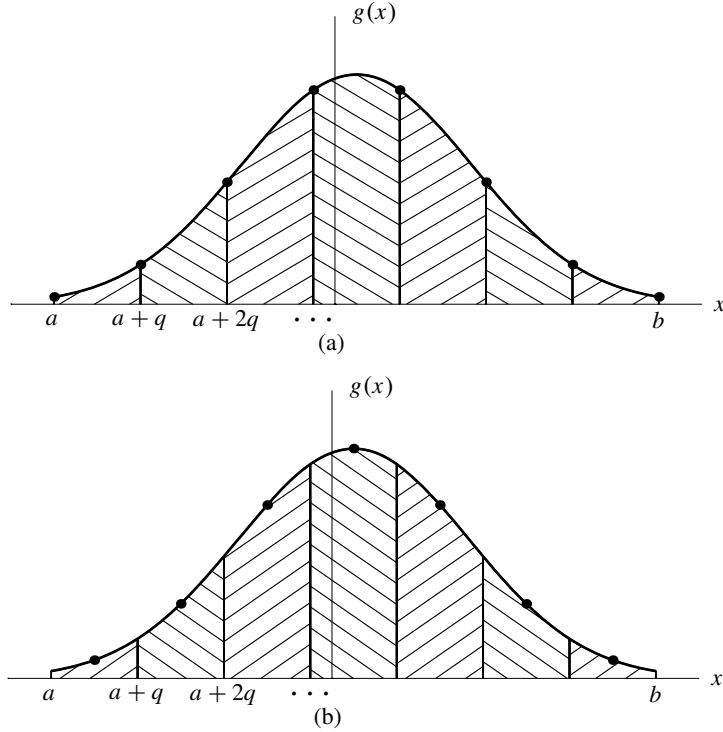


**Figure N.1** Samples and integration limits for the different forms of the Euler-Maclaurin formula: (a) the standard form, using samples at the borders of the intervals; (b) the modified form, using samples at centers of the intervals.

assuming that  $g^{2K}(x)$  is continuous in  $[a, b]$ , and  $B_{2K}(0.5)$  being the Bernoulli polynomial<sup>2</sup> at  $z = 0.5$ . When  $g^{2K}(x)$  exists, but it is not continuous,  $g^{2K}(a + \vartheta(b - a))$  may be substituted by “some value between the minimum and the maximum of  $g^{2K}(x)$  in  $[a, b]$ ”.

<sup>2</sup>The Bernoulli polynomials are defined (Abramowitz and Stegun, 1972) by the coefficients of  $t^n/n!$  in

$$\frac{te^{zt}}{e^t - 1} = \sum_{n=1}^{\infty} B_n(z) \frac{t^n}{n!}, \quad |t| < 2\pi.$$

The value of the Bernoulli polynomials for  $x = 0.5$  is  $B_{2n}(0.5) = -(1 - 2^{1-2n})B_{2n}$ , where  $B_{2n}$  is the Bernoulli number of index  $2n$ . This value can be bounded as

$$\frac{2(2n)!}{(2\pi)^{2n}} > (-1)^n B_{2n}(0.5) > \frac{2(2n)!}{(2\pi)^{2n}} (1 - 2^{1-2n}), \quad n = 1, 2, \dots \quad (\text{N.6})$$

## N.2 DERIVATION OF SHEPPARD'S CORRECTIONS

Let us investigate now the expressions for the moments of the quantized variable  $x'$ . Let the  $m$ th quantization interval be  $[a + mq, a + (m + 1)q]$ , and let the quantized variable values associated to this interval be  $x_m = a + (m + 0.5)q$ . Accordingly,

$$E\{(x')^r\} = \sum_{m=-\infty}^{\infty} x_m^r \int_{-q/2}^{q/2} f_x(x_m + \zeta) d\zeta. \quad (\text{N.7})$$

We can recognize Eq. (N.7) as a sum of samples of the function

$$g(x) = x^r \int_{-q/2}^{q/2} f_x(x + \zeta) d\zeta, \quad (\text{N.8})$$

taken at the points  $x = x_m = a + (m + 0.5)q$ . Therefore, the sum in Eq. (N.7) can be expressed by the integral of the function  $g(x)$  plus some residual terms. This idea was followed by Cramér (1946).

Sheppard chose a different approach. He assumed that the PDF

- is of finite range  $(a, b)$
- is smooth
- has a high level of contact with the  $x$ -axis at the terminals.

He assumed the interval  $(a, b)$  be divided into  $s$  intervals, and sought an expression of

$$E\{(x')^r\} = \sum_{m=0}^{s-1} x_m^r \int_{-q/2}^{q/2} f_x(x_m + \zeta) d\zeta \quad (\text{N.9})$$

in terms of the  $r$ th moment of  $x$ ,

$$E\{x^r\} = \int_a^b x^r f_x(x) dx. \quad (\text{N.10})$$

The Euler-Maclaurin formula (N.1) cannot be directly applied, since the integral is to be calculated in  $(a, b)$ , while the samples are taken not on the grid  $\{a + mq\}$ , but on  $\{a + (m + 0.5)q\}$ . Therefore, Sheppard developed a modification to the summation formula. Within the same derivation, he also managed to obtain expressions of  $E\{x^r\}$

in terms of  $E\{(x')^m\}$ ,  $m = 1, 2, \dots, r$ . This is a tedious exercise. Alternatively, we will follow the reasoning of Stuart and Ord (1994).

By choosing

$$g(x) = x^r \int_{-q/2}^{q/2} f_x(x + \zeta) d\zeta, \quad (\text{N.11})$$

and accepting Sheppard's assumptions for  $g(x)$ , the sum and the term  $S_{2Km}$  disappear in Eq. (N.4), and we obtain from Eqs. (N.9) and (N.4):

$$\begin{aligned} E\{(x')^r\} &= \sum_{m=0}^{s-1} x_m^r \int_{-q/2}^{q/2} f_x(x_m + \zeta) d\zeta \\ &= \frac{1}{q} \int_a^b x^r \int_{-q/2}^{q/2} f_x(x + \zeta) d\zeta dx \\ &\quad + \sum_{k=1}^K \frac{B_{2k}(0.5)}{(2k)!} q^{2k-1} \left( g^{(2k-1)}(a) - g^{(2k-1)}(b) \right) \\ &\quad + S_{2Km} \\ &\approx \frac{1}{q} \int_a^b x^r \int_{-q/2}^{q/2} f_x(x + \zeta) d\zeta dx \\ &\approx \frac{1}{q} \int_a^b \int_{-q/2}^{q/2} (y - \zeta)^r f_x(y) d\zeta dy \\ &= \frac{1}{q} \int_a^b \frac{(y + q/2)^{r+1} - (y - q/2)^{r+1}}{r + 1} f_x(y) dy \\ &= \sum_{n=0}^{\lfloor r/2 \rfloor} \binom{r}{2n} \left(\frac{q}{2}\right)^{2n} \frac{1}{2n + 1} E\{x^{r-2n}\}, \end{aligned} \quad (\text{N.12})$$

where  $\lfloor \cdot \rfloor$  denotes the "floor function", the integer part of the argument.

Equation (N.12) can be used to express the moments of  $x$  in terms of moments of  $x'$ , and thus Sheppard's corrections can be obtained.

The result is approximate not only because of the neglected terms of the Euler-Maclaurin formula, but also because we changed the integration surface by the variable transformation of the integral. The integration was to be done originally over the surface illustrated in Fig. N.2(a). This was transformed by introduction of  $y = x + \zeta$

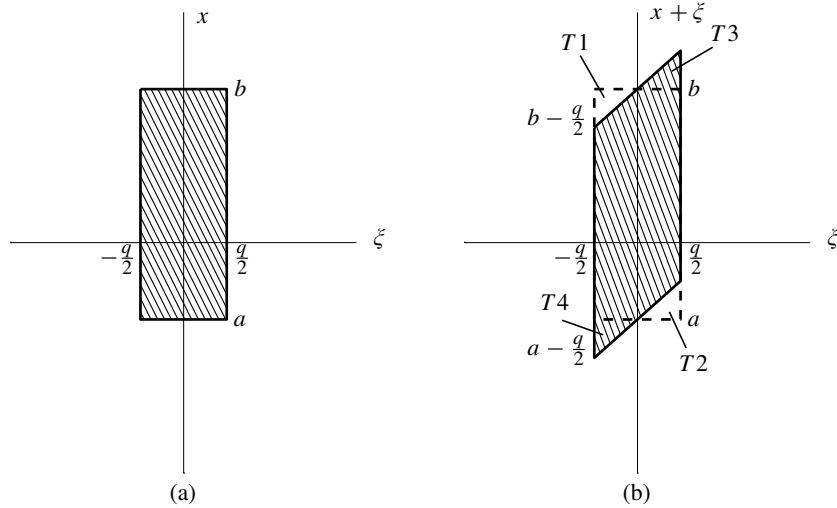


**Figure N.2** Integration surfaces in Eq. (N.12).

to a parallelogram shown in Fig. N.2(b). We approximate this integral by an integral over the rectangle. This is usually a good approximation. The integral over the dotted triangles ( $T_3$  and  $T_4$ ) is zero since  $f_x(x) = 0$  for  $x < a$  or  $b < x$ ; and the integral over the triangles marked by + marks ( $T_1$  and  $T_2$ ) is small since  $f_x(x)$  is small close to  $a$  and  $b$  as required by Sheppard.

### N.3 APPROXIMATIONS IN THE DERIVATION OF SHEPPARD'S CORRECTIONS

In order to investigate the quality of the results, we have to consider the approximations made in (N.12). We have neglected three quantities:

1. the sum containing the  $(2k - 1)$ th derivatives
2. the remainder  $S_{2Km}$
3. the difference of the integration surfaces, as illustrated in Fig. N.2.

Let us consider these terms one by one.

1. The sum

$$\sum_{k=1}^K \frac{B_{2k}(0.5)}{(2k)!} q^{2k-1} \left( g^{(2k-1)}(a) - g^{(2k-1)}(b) \right) \quad (\text{N.13})$$



is small if the PDF has a high order contact with the  $x$ -axis at  $x = a$  and  $x = b$ , that is, the value of the function and the first few derivatives are zero there (or are very close to zero there). It is not necessary to keep  $a$  and  $b$  finite: letting  $a \rightarrow -\infty$  and  $b \rightarrow \infty$  the derivatives usually disappear. The general condition is

$$\lim_{x \rightarrow \pm\infty} \frac{d^{2k-1} (x^r f_x(x))}{dx^{2k-1}} = 0 \quad k = 1, 2, \dots, K. \quad (\text{N.14})$$

For PDFs which are zero outside a finite interval, this is obviously fulfilled for a large enough integration range.

2. The remainder  $S_{2Km}$  (see (N.5)) can be bounded, using the bounds for the Bernoulli polynomials (N.6), given on page W5, and  $(b - a) = sq$ , as

$$\begin{aligned} |S_{2Km}| &< \frac{2(b-a)}{(2\pi)^{2K}} q^{2K-1} \left| g^{(2K)}(a + \vartheta(b-a)) \right| \\ &\leq \frac{2(b-a)}{(2\pi)^{2K}} q^{2K-1} \max_{x \in [a,b]} \left| g^{(2K)}(x) \right|. \end{aligned} \quad (\text{N.15})$$

with  $0 < \vartheta < 1$ , and  $g(x)$  is defined by Eq. (N.11). Therefore, when the  $(2K)$ th derivative is bounded,  $S_{2Km}$  can be made arbitrarily small for small enough values of  $q$ .

When  $a \rightarrow -\infty$  or  $b \rightarrow \infty$ , (N.15) is not usable, and another form has to be used. It can be shown that for large enough values of  $K$  and small enough  $q$ , the remainder is usually negligible (Cramér, 1946).

3. The change of the integral caused by the modification of the integration surface can be upper bounded in the following way:

$$|I| \leq q^2 \max_{T_1 \cup T_2} \{|y - \xi|^r f_x(y)\}. \quad (\text{N.16})$$

If

$$\lim_{x \rightarrow \pm\infty} x^r f_x(x) = 0 \quad (\text{N.17})$$

is fulfilled, the integral can be made arbitrarily small by choosing a large enough integration range and a small enough  $q$  value.

From the above discussion it is clear that Sheppard's approximations are usually good, and in most cases become exact with  $a \rightarrow -\infty$ ,  $b \rightarrow \infty$ , and  $q \rightarrow 0$ . However, it is difficult to numerically evaluate the deviations and their upper bounds, and there is no simple way of determining conditions from the above expressions for

Sheppard's conditions to exactly hold.  $S_{2Km}$  could be calculated by an expression similar to (N.3), but this would also be quite cumbersome to evaluate.

#### N.4 SHEPPARD'S CORRECTIONS AND THE CHARACTERISTIC FUNCTION METHOD

It is clear that both Sheppard's method and the characteristic function method yield the same results. Therefore, the assumptions and approximations should also be similar. Indeed, Sheppard's assumptions on smoothness and high order contact are strongly related to the bandlimitedness of the CF. The two kinds of assumptions are however different. The characteristic function method provides much more powerful tools for the evaluation of the approximation error, therefore it is more adequate for the evaluation of quantized measurements.

The application of the PQN model is so simple and straightforward, and its connection to bandlimitedness seems so obvious that one wonders why Sheppard did not discover it. The convolution with the uniform distribution can be immediately recognized in Eq. (N.12). In our opinion, there are important reasons for this. First, Sheppard himself never wrote his expressions in the form of Eq. (N.12). He directly obtained his corrections in the final form where the PQN model is less recognizable. Second, he did not think in terms of signals or bandlimitedness. Although the Fourier transform and the characteristic function were already known at his time, they were not yet widely used. Third, sampling and reconstruction of general signals from samples were not yet developed. It would be anachronistic to expect today a way of thinking from somebody who had a quite different background.

Nevertheless, Sheppard's derivation is a remarkable piece of mathematical work, and he deserves our admiration for deriving his corrections with tools that were quite difficult to handle.

##### Example N.1 Sheppard's Corrections for Gaussian Input

We have shown in Section 4.7 by using the characteristic function method that Sheppard's corrections are valid for Gaussian inputs with very small residual error if  $q \leq \sigma$  holds. Sheppard knew about this, and gave a numerical example illustrating the error for  $q = \sigma/\sqrt{2}$ , but did not discuss the validity of his approximations. Let us explore in this example what Sheppard's conditions tell us about this case.

First, we notice that the Gaussian distribution has infinite extent, so Sheppard's assumption about finite  $a$  and  $b$  is not valid. This could be a problem. However, we can recognize that the Euler-Maclaurin formula approximates the integral of the function  $g(x)$  over the given interval  $[a, b]$ , so the error introduced by the finite interval is equal to the integral *outside*  $[a, b]$ . Since the Gaussian PDF decays very rapidly, it is enough to assure that

$$\mu - a \gg \sigma \quad \text{and} \quad b - \mu \gg \sigma. \quad (\text{N.18})$$

For  $a \rightarrow -\infty$  and  $b \rightarrow \infty$ , this error obviously disappears. Now the approximation error terms (see N.3) will be examined.

1. Considering the sum (N.13), it can be seen that if (N.18) is valid, the sum will be small, and that it disappears for  $a \rightarrow \infty$  and  $b \rightarrow \infty$ .
2. The remainder  $S_{2Km}$  is difficult to evaluate. For small values of  $K$ , the upper bound obtained from (N.15) with the worst-case value of  $\vartheta$  is much too pessimistic.  $S_{2Km}$  could be evaluated by using an expression similar to (N.3), but even if we developed an appropriate formula, it would be cumbersome to calculate.  
For increasing values of  $K$ , numerical calculations show that the upper bound of  $S_{2Km}$  gradually decreases until it reaches the error value we had obtained in Section 4.7. These take considerable computer time, and do not give much insight about the behavior of the error.
3. The approximation of the integral causes our error to be small if (N.18) holds, and this error disappears for  $a \rightarrow -\infty$  and  $b \rightarrow \infty$ .

We have considered all the approximation errors in Sheppard's approach. We have shown that for a Gaussian variable quantized with  $q < \sigma$ , the errors in Sheppard's corrections are small, but the calculation of the errors needs significant effort.

### Example N.2 Sheppard's Example: Beta Distribution

Sheppard's first example in his paper is the quantization of a beta distribution:

$$f_x(x) = \begin{cases} \frac{(x + 4.5)^5(5.5 - x)^6}{C} & \text{for } -4.5 \leq x \leq 5.5, \\ 0 & \text{elsewhere,} \end{cases} \quad (\text{N.19})$$

with the normalizing constant  $C \approx 1.8038 \cdot 10^8$ . The quantum size is  $q = 1$  (see Fig. N.3).

Sheppard's calculated moment values are given in Table N.1. These tables nicely illustrate how small the errors are. Let us consider the error terms, to see if the same conclusion can be drawn from them.

In order to keep the integral approximation error equal to zero, let us choose  $a = -5.5$  and  $b = 6.5$  so that we have an integration interval broader than the support of the PDF,  $[-4.5, 5.5]$ . This happens to make no difference, since the PDF is zero in  $[-5.5, -4.5]$  and in  $[5.5, 6.5]$ . Over interval  $[a, b]$ , the first four derivatives of the PDF and the first five derivatives of  $g(x)$  are continuous.

Let us consider now the error terms defined in Section N.3, on page W8.

1. The sum (N.13) gives zero for the given interval  $[a, b]$ .

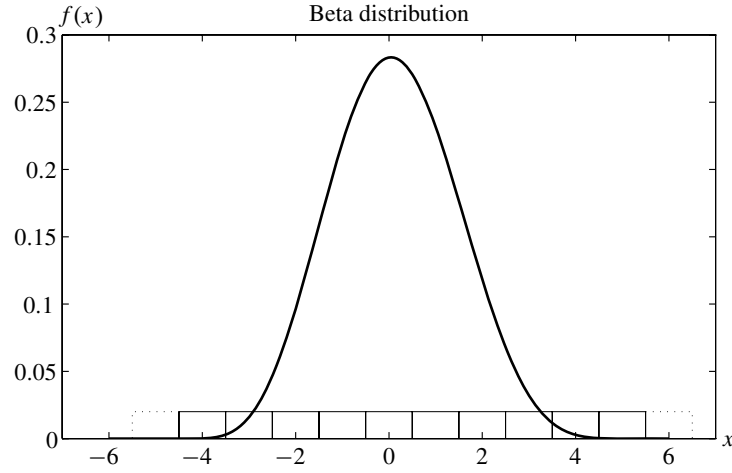


Figure N.3 Quantization of a beta distribution.

TABLE N.1 Sheppard's results for the moments of the chosen beta distribution.

	$r = 1$	$r = 2$	$r = 3$	$r = 4$	$r = 5$
$E\{x^r\}$	0.115 387	1.871 774	0.827 127	9.429 592	8.085 022
Corrected	0.115 387	1.788 441	0.798 281	8.522 872	7.412 577
$E\{x^r\}$	0.115 385	1.788 462	0.798 077	8.524 038	7.405 402
Error	$2 \cdot 10^{-6}$	$-2.1 \cdot 10^{-5}$	$2.0 \cdot 10^{-4}$	$-1.2 \cdot 10^{-3}$	$7.2 \cdot 10^{-3}$

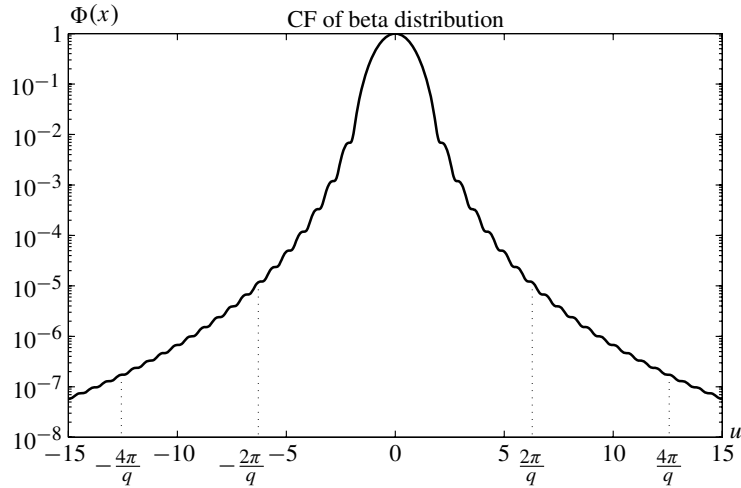
	$r = 2$	$r = 3$	$r = 4$
$E\{\tilde{x}^r\}$	1.858 47	0.182 27	9.192 04
Corrected	1.775 13	0.182 27	8.291 97
$E\{\tilde{x}^r\}$	1.775 15	0.182 07	8.298 03
Error	$-2 \cdot 10^{-5}$	$2 \cdot 10^{-4}$	$-6.1 \cdot 10^{-3}$

TABLE N.2 Upper bounds of the residual errors of the Euler-Maclaurin formula for the chosen beta distribution.

$E\{x^r\}$		$r = 1$	$r = 2$	$r = 3$	$r = 4$	$r = 5$
$ S_{2Km}  <$	$K = 1$	0.281	2.81	21.1	140	88
	$K = 2$	0.0048	0.018	0.096	0.98	12
	$K = 3$	0.0051	0.010	0.073	0.52	3.7

$E\{\tilde{x}^r\}$		$r = 2$	$r = 3$	$r = 4$
$ S_{2Km}  <$	$K = 1$	2.87	22	150
	$K = 2$	0.018	0.090	1.0
	$K = 3$	0.0099	0.070	0.49



**Figure N.4** Characteristic function of the beta distribution defined by Eq. (N.19).

2. The upper bound of the residual error can be evaluated for  $K = 1, 2, 3$  because  $g(x)$  can be differentiated six times. Numerical calculations give the values shown in Table N.2.  
It can be seen that these bounds are not very useful. Therefore, in this case the remainder itself should be evaluated, which is a difficult task.
3. The change of the integral causes no approximation because of the proper selection of the integration bounds.

Let us use now the characteristic function method for the evaluation of the errors in Sheppard's corrections. Fig. N.4 shows that the CF disappears rapidly, so QT II approximately holds, and Sheppard's corrections work almost perfectly.

A few values of the characteristic function are given in Table N.3. From these values it is clear that the residual errors can be well approximated using the  $l = 1$  terms in the appropriate error formulas. From Eqs. (B.8), (B.10), (B.13) and (B.16) we obtain

$$R_1 \approx -\frac{q}{\pi} \operatorname{Im}\left\{\Phi\left(\frac{2\pi}{q}\right)\right\} \approx 2.16 \cdot 10^{-6}. \quad (\text{N.20})$$

$$R_2 \approx -\frac{q^2}{\pi^2} \operatorname{Re}\left\{\Phi\left(\frac{2\pi}{q}\right)\right\} + 2\frac{q}{\pi} \operatorname{Re}\left\{\dot{\Phi}\left(\frac{2\pi}{q}\right)\right\} \approx 1.84 \cdot 10^{-5}. \quad (\text{N.21})$$

$$R_3 \approx 3\frac{q}{\pi} \operatorname{Im}\left\{\Phi\left(\frac{2\pi}{q}\right)\right\} \frac{q^2}{12} + \frac{3q}{\pi} \operatorname{Im}\left\{\ddot{\Phi}\left(\frac{2\pi}{q}\right)\right\}$$

**TABLE N.3** Values of the characteristic function and its first two derivatives for the chosen beta distribution.

	$u = \frac{2\pi}{q}$	$u = 2\frac{2\pi}{q}$	$u = 3\frac{2\pi}{q}$	$u = 4\frac{2\pi}{q}$
$ \Phi(u) $	$1.18 \cdot 10^{-5}$	$1.73 \cdot 10^{-7}$	$1.50 \cdot 10^{-8}$	$2.65 \cdot 10^{-9}$
$\text{Re}\{\Phi(u)\}$	$+9.66 \cdot 10^{-6}$	$-1.64 \cdot 10^{-7}$	$+1.46 \cdot 10^{-8}$	$-2.61 \cdot 10^{-9}$
$\text{Im}\{\Phi(u)\}$	$+6.77 \cdot 10^{-6}$	$-5.53 \cdot 10^{-8}$	$+3.26 \cdot 10^{-9}$	$-4.37 \cdot 10^{-10}$
$ \dot{\Phi}(u) $	$4.31 \cdot 10^{-5}$	$2.79 \cdot 10^{-7}$	$6.53 \cdot 10^{-8}$	$1.17 \cdot 10^{-8}$
$\text{Re}\{\dot{\Phi}(u)\}$	$+3.05 \cdot 10^{-5}$	$-2.49 \cdot 10^{-7}$	$+1.47 \cdot 10^{-8}$	$-1.97 \cdot 10^{-9}$
$\text{Im}\{\dot{\Phi}(u)\}$	$-3.05 \cdot 10^{-5}$	$+6.85 \cdot 10^{-7}$	$-6.36 \cdot 10^{-8}$	$+1.16 \cdot 10^{-8}$
$ \ddot{\Phi}(u) $	$2.48 \cdot 10^{-4}$	$3.62 \cdot 10^{-6}$	$3.08 \cdot 10^{-7}$	$5.42 \cdot 10^{-8}$
$\text{Re}\{\ddot{\Phi}(u)\}$	$-1.44 \cdot 10^{-4}$	$+3.11 \cdot 10^{-6}$	$-2.87 \cdot 10^{-7}$	$+5.21 \cdot 10^{-8}$
$\text{Im}\{\ddot{\Phi}(u)\}$	$-2.03 \cdot 10^{-4}$	$+1.85 \cdot 10^{-6}$	$-1.11 \cdot 10^{-7}$	$+1.50 \cdot 10^{-8}$

$$\begin{aligned}
& -\frac{3q^2}{\pi^2} \text{Im}\{\dot{\Phi}(\frac{2\pi}{q})\} - \frac{q^3}{4} \text{Im}\{\Phi(\frac{2\pi}{q})\} \left(\frac{1}{\pi} - \frac{6}{\pi^3}\right) \\
& \approx -1.84 \cdot 10^{-4}. \tag{N.22}
\end{aligned}$$

$$\begin{aligned}
R_4 \approx & \left(6\frac{q^2}{\pi^2} \text{Re}\{\Phi(\frac{2\pi}{q})\} + 2\frac{q}{\pi} \text{Re}\{\dot{\Phi}(\frac{2\pi}{q})\}\right) \frac{q^2}{12} \\
& - \frac{4q}{\pi} \text{Re}\{\ddot{\Phi}(\frac{2\pi}{q})\} + 6\frac{q^2}{\pi^2} \text{Re}\{\ddot{\Phi}(\frac{2\pi}{q})\} \\
& + q^3 \text{Re}\{\dot{\Phi}(\frac{2\pi}{q})\} \left(\frac{1}{\pi} - \frac{6}{\pi^3}\right) - \frac{q^4}{2} \text{Re}\{\Phi(\frac{2\pi}{q})\} \left(\frac{1}{\pi^2} - \frac{6}{\pi^4}\right) \\
& \approx 9.96 \cdot 10^{-4}. \tag{N.23}
\end{aligned}$$

The error values reasonably approximate the true values given in Table N.3. This demonstrates the power of the characteristic function method.

### Example N.3 Sheppard's Corrections Working in the Wrong Direction

When Sheppard's conditions are not met, Sheppard's corrections may break down. We will show that for a uniform distribution with certain parameters, Sheppard's second and fourth corrections work in the wrong direction. The sources of this example are (Stuart and Ord, 1994; Elderton, 1938).

Consider a rounding quantizer and a uniform distribution of mean  $\mu$  and amplitude  $A$ , which covers an integer number of quantization intervals, satisfying  $\mu - A = (2k_1 + 1)q/2$ , and  $\mu + A = (2k_2 + 1)q/2$ , as illustrated in Fig. N.5.

We can exactly calculate the moments of the non-quantized and of the quantized variables. The 2<sup>nd</sup> and 4<sup>th</sup> moments of  $x$  are:

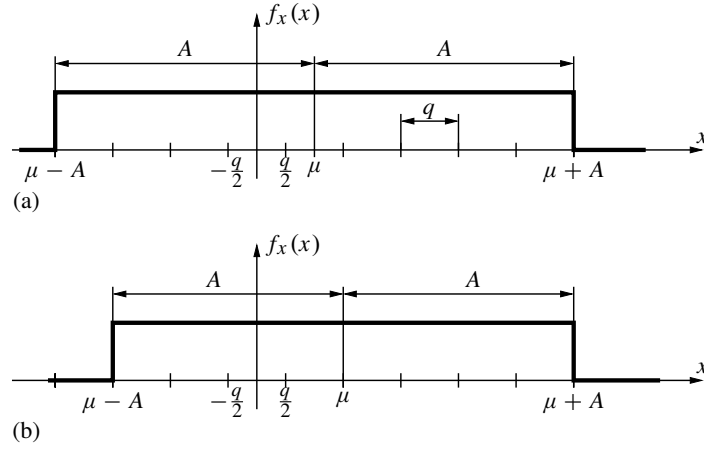


**Figure N.5** Uniform distributions for which Sheppard's corrections are wrong: (a)  $2A/q$  odd; (b)  $2A/q$  even.

$$E\{x^2\} = \frac{A^2}{3} + \mu^2, \quad E\{x^4\} = \frac{A^4}{5} + 2A^2\mu^2 + \mu^4. \quad (\text{N.24})$$

The centralized moments are

$$E\{\tilde{x}^2\} = \frac{A^2}{3}, \quad E\{\tilde{x}^4\} = \frac{A^4}{5}. \quad (\text{N.25})$$

In order to calculate the moments of the quantized variables, we need a few sum formulas (Gradshteyn and Ryzhik, 1994):

$$\sum_{k=1}^n k^2 = \frac{n(n+1)(2n+1)}{6}. \quad (\text{N.26})$$

$$\sum_{k=1}^n (2k-1)^2 = \frac{n(4n^2-1)}{3}. \quad (\text{N.27})$$

$$\sum_{k=1}^n k^4 = \frac{n(n+1)(2n+1)(3n^2+3n-1)}{30}. \quad (\text{N.28})$$

$$\sum_{k=1}^n (2k-1)^4 = \frac{n(4n^2-1)(12n^2-7)}{15}. \quad (\text{N.29})$$

Because of the symmetry,  $\mu_{x'} = E\{x'\} = E\{x\} = \mu$ , therefore the same expressions hold between the centralized and non-centralized moments of  $x'$  as between those of  $x$ , see Eq. (N.24).

$$E\{(x')^2\} = E\{(\tilde{x}')^2\} + \mu^2, \quad E\{(x')^4\} = E\{(\tilde{x}')^4\} + 6E\{(\tilde{x}')^2\}\mu^2 + \mu^4. \quad (\text{N.30})$$

We will calculate the centralized moments. The non-centralized ones can be determined from these.

a)  $s = 2A/q$  odd

$$\begin{aligned} E\{(\tilde{x}')^2\} &= \sum_{k=-\frac{s-1}{2}}^{\frac{s-1}{2}} \frac{1}{s} (kq)^2 \\ &= 2q^2 \cdot \frac{1}{s} \cdot \frac{(s-1)(s+1)s}{4 \cdot 6} = q^2 \frac{s^2-1}{12} = \frac{A^2}{3} - \frac{q^2}{12} \\ &= E\{\tilde{x}^2\} - \frac{q^2}{12}. \end{aligned} \quad (\text{N.31})$$

$$\begin{aligned} E\{(\tilde{x}')^4\} &= \sum_{k=-\frac{s-1}{2}}^{\frac{s-1}{2}} \frac{1}{s} (kq)^4 = 2q^4 \cdot \frac{1}{s} \cdot \frac{(s-1)(s+1)s(3s^2-13)}{16 \cdot 30} \\ &= \frac{q^4}{240} (s^2-1)(3s^2-7) = \frac{q^4 s^4}{80} - \frac{q^4 s^2}{24} + \frac{7q^4}{240} \\ &= \frac{A^4}{5} - \frac{A^2 q^2}{6} + \frac{7q^4}{240} = E\{\tilde{x}^4\} - E\{\tilde{x}^2\} \frac{q^2}{2} + \frac{7q^4}{240} \\ &= E\{\tilde{x}^4\} - E\{(\tilde{x}')^2\} \frac{q^2}{2} - \frac{q^4}{80}. \end{aligned} \quad (\text{N.32})$$

b)  $s = 2A/q$  even

$$\begin{aligned} E\{(\tilde{x}')^2\} &= \sum_{k=-s/2}^{s/2} \frac{1}{s} \left( (2|k|-1) \frac{q}{2} \right)^2 \\ &= \frac{q^2 s (s^2-1)}{2s \cdot 2 \cdot 3} = \frac{q^2}{12} (s^2-1) \\ &= E\{\tilde{x}^2\} - \frac{q^2}{12}. \end{aligned} \quad (\text{N.33})$$

$$\begin{aligned} E\{(\tilde{x}')^4\} &= \sum_{k=-s/2}^{s/2} \frac{1}{2} \left( (2|k|-1) \frac{q}{2} \right)^4 \\ &= \frac{q^4 s (s^2-1)(3s^2-7)}{8s \cdot 2 \cdot 15} = \frac{q^4 s^4}{80} - \frac{q^4 s^2}{24} + \frac{7q^4}{240} \end{aligned}$$



$$\begin{aligned}
&= \frac{A^4}{5} - \frac{A^2 q^2}{6} + \frac{7q^4}{240} = E\{\tilde{x}^4\} - E\{\tilde{x}^2\} \frac{q^2}{2} + \frac{7q^4}{240} \\
&= E\{\tilde{x}^4\} - E\{(\tilde{x}')^2\} \frac{q^2}{2} - \frac{q^4}{80}. \tag{N.34}
\end{aligned}$$

From Eq. (N.31) and Eq. (N.33), it follows that

$$E\{\tilde{x}^2\} = E\{(\tilde{x}')^2\} + \frac{q^2}{12} \quad \text{and} \quad E\{x^2\} = E\{(x')^2\} + \frac{q^2}{12}. \tag{N.35}$$

By rearranging Eq. (N.32) and Eq. (N.34), we obtain

$$E\{\tilde{x}^4\} = E\{(\tilde{x}')^4\} + E\{(\tilde{x}')^2\} \frac{q^2}{2} + \frac{q^4}{80}, \tag{N.36}$$

and

$$\begin{aligned}
E\{x^4\} &= E\{\tilde{x}^4\} + 6E\{\tilde{x}^2\}\mu^2 + \mu^4 \\
&= E\{(\tilde{x}')^4\} + E\{(\tilde{x}')^2\} \frac{q^2}{2} + \frac{q^4}{80} + 6 \left( E\{(\tilde{x}')^2\} + \frac{q^2}{12} \right) \mu^2 + \mu^4 \\
&= E\{(x')^4\} + 6E\{(x')^2\} \frac{q^2}{2} + \frac{q^4}{80}. \tag{N.37}
\end{aligned}$$

Indeed, Eq. (N.35) indicates a necessary correction equal in value to Sheppard's correction, but *opposite in sign*. Eq. (N.36) and Eq. (N.37) exhibit a similar aberration for small enough  $q$  values, when the second term dominates over the third one.

This is a rather surprising example and is worthy of more consideration. First of all, note that neither Sheppard's conditions are met (there are jumps at the edges), nor is the CF bandlimited (it is a sinc function which has a very slow decay). Therefore, Sheppard's corrections cannot be expected to work. Let us have a closer look at Sheppard's conditions, in order to see what breaks down. Let us define for the second moment

$$g(x) = x^2 \int_{-q/2}^{q/2} \frac{1}{2A} d\zeta = \frac{qx^2}{2A}. \tag{N.38}$$

This definition allows the use of the Euler-Maclaurin formula. For  $k = 1$ , the sum (N.13) gives an error term:

$$\frac{B_2(0.5)}{2!} q (\dot{g}(a) - \dot{g}(b)) = \frac{q^2 (2a - 2b)}{24 \cdot 2A} = -\frac{q^2}{12}. \tag{N.39}$$

The third and higher derivatives of  $g(x)$  disappear, so the other terms of the sum and the remainder are equal to zero when  $K \geq 2$ .

The approximation of the integral causes an additional error.

$$\begin{aligned}
 E_b = E_1 - E_3 &= \frac{1}{q} \iint_{T_1} (y - \zeta)^2 f_x(y) d\zeta dy - \frac{1}{q} \iint_{T_3} (y - \zeta)^2 f_x(y) d\zeta dy \\
 &= -\frac{1}{q} \int_{b-q/2}^{b+q/2} \int_0^{y-b} (y - \zeta)^2 \frac{1}{2A} d\zeta dy \\
 &= \frac{1}{2Aq} \int_{b-q/2}^{b+q/2} \frac{b^3 - y^3}{3} dy \\
 &= \frac{1}{2Aq} \left( q \frac{b^3}{3} + \frac{(b - q/2)^4 - (b + q/2)^4}{12} \right) \\
 &= \frac{-bq^2}{24A}. \tag{N.40}
 \end{aligned}$$

By performing a similar calculation for  $E_a$ , and using  $2A = b - q$ ,

$$E_a + E_b = \frac{-bq^2}{24A} + \frac{aq^2}{24A} = -\frac{q^2}{12}. \tag{N.41}$$

The sum of the two calculated error terms (N.39) and Eq. (N.41) is the total error,  $-2q^2/12$ , which corresponds to the deviation of Eq. (N.35) from Sheppard's second correction. The calculation was rather lengthy, which is typical for the evaluation of Sheppard's approximation errors.

One may wonder if under such circumstances, quantized data can be used at all. The answer is of course yes. For small enough  $q$  values the correction terms become negligible compared to the moments themselves, therefore the corrections become unimportant. They do not improve the moments, but they do no harm either.

We will see in Chapter 5 that for a uniformly distributed input, with  $2A/q$  integer, the quantization noise is uniformly distributed, so its variance is  $q^2/12$ . Where does then the change of the sign come from?

By comparing

$$E\{(x')^2\} = E\{(x + v)^2\} = E\{x^2\} + E\{2xv\} + E\{v^2\} = E\{x^2\} + 2E\{xv\} + \frac{q^2}{12} \tag{N.42}$$

to (N.35), we conclude that the only way to have both equations true is if

$$E\{xv\} = -\frac{q^2}{12}, \quad (\text{N.43})$$

that is, the input signal and the quantization noise are negatively correlated. This correlation has the same absolute value as the noise variance, even for very small values of  $q$ . This does not mean however that the signal and the noise were not less coupled for smaller  $q$  values. The correlation coefficient does decrease with  $q$ :

$$\rho_{xv} = \frac{E\{xv\}}{\sqrt{\text{var}\{x\} \text{var}\{v\}}} = \frac{\frac{q^2}{12}}{\sigma_x \sqrt{\frac{q^2}{12}}} = \frac{q}{\sigma_x} \frac{1}{\sqrt{12}}. \quad (\text{N.44})$$

Finally, we will show that the choice of the values of  $\mu$  and  $A$  is very special, and by changing them the situation significantly improves. Figures N.6-N.7 illustrate the behavior of the residual errors of Sheppard's record and fourth corrections, respectively, as functions of  $\mu$  and  $A$ . The plots are normalized to Sheppard's corrections, so that the value  $R_r/S_r = -2$  corresponds to our cases. We can observe that the anomalous behavior appears for selected parameter values only.

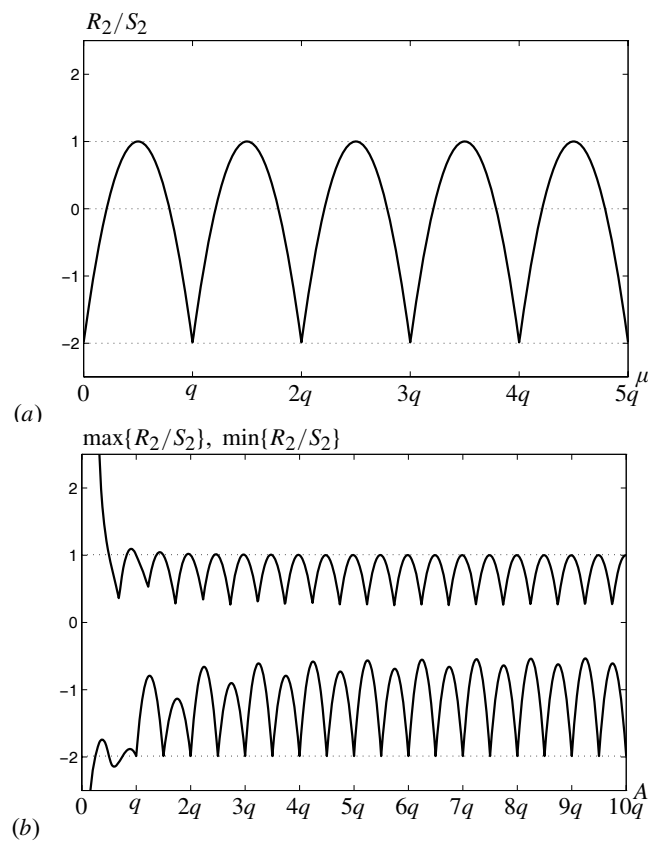


**Figure N.6** Behavior of the residual error of Sheppard's second correction, normalized by the value of the correction  $S_2$ , for uniform distribution: (a) relative error as a function of  $\mu$ , for the amplitude of  $x$  equal to  $A = 3.5q$ ; (b) Maximum and minimum errors. For each value of  $A$ , the minimum and maximum are determined by running  $\mu$  through  $[0, q]$ .

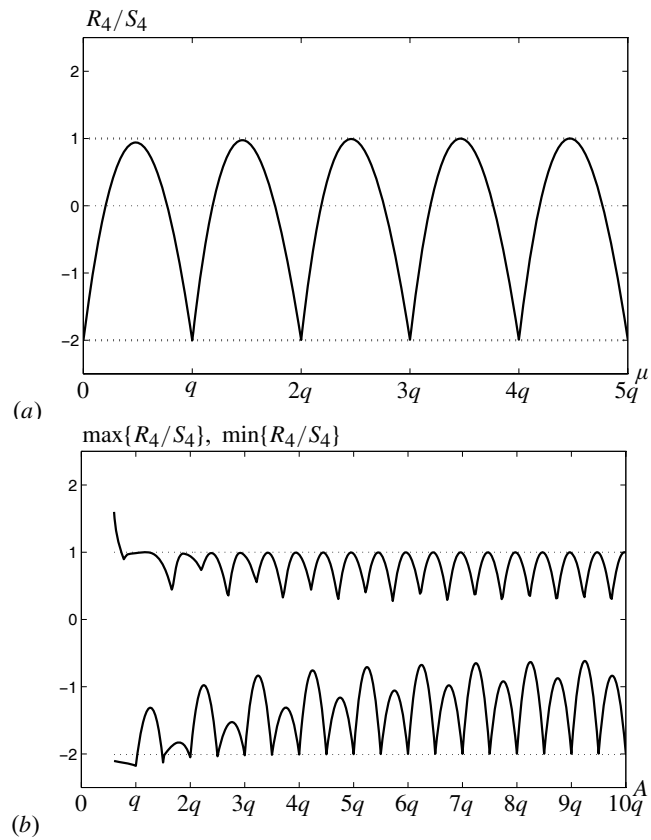


**Figure N.7** Behavior of the residual error of Shepard's fourth correction, normalized by the value of the correction  $S_4$ , for uniform distribution: (a) relative error as a function of  $\mu$ , for the amplitude of  $x$  equal to  $A = 3.5q$ ; (b) Maximum and minimum errors. For each value of  $A$ , the minimum and maximum are determined by running  $\mu$  through  $[0, q]$ .



## Addendum O

---

---

# ***Interpolation of the Cumulative Distribution Function from the Histogram and Numerical Reconstruction of the Input PDF***

In Sect. 4.4, samples of the input cumulative distribution function (CDF) were obtained from the output probabilities by summation, and these samples were used for interpolating the CDF. The CDF was defined by Eq. (4.9). The input PDF was obtained by numerical differentiation (see Fig. 4.10). This procedure was explained in heuristic terms, and it leads to seemingly correct results. However, precise justification needs additional arguments. The difficulty arises from the fact that the CDF cannot be Fourier transformed in a strict sense, since

$$\int_{-\infty}^{\infty} F_x(x) dx = \infty \quad \text{and} \quad \int_{-\infty}^{\infty} F_x^2(x) dx = \infty. \quad (\text{O.1})$$

Therefore, the conventional sampling theorem cannot be applied. We cannot state bandlimitedness in the usual way, and the interpolation formula is not guaranteed to converge. The goal here is to provide a rigorous justification for the procedure of Section 4.4.

### **O.1 SAMPLING THEOREMS FOR CUMULATIVE DISTRIBUTION FUNCTIONS**

A quite simple generalized sampling theorem was formulated by (Zakai, 1965), as follows.

**Zakai's sampling theorem (reformulated for CDF's)**

If

$$\int_{-\infty}^{\infty} \frac{|F_x(x)|^2}{1+x^2} dx < \infty, \quad (\text{O.2})$$

and  $F_x(x)$  is bandlimited in the sense that

$$F_x(x) = F_x(x) \star \text{sinc}(\pi x/q) = \int_{-\infty}^{\infty} F_x(x - \zeta) \text{sinc}(\pi \zeta/q) d\zeta, \quad (\text{O.3})$$

then

$$\sum_{m=-\infty}^{\infty} F_x(mq) \text{sinc}(\pi(x - mq)/q) \quad (\text{O.4})$$

uniformly converges to  $F_x(x)$  in any bounded interval.

It is heuristically straightforward, though difficult to strictly prove that this theorem applies indeed to CDF's whose PDF is bandlimited. We will illustrate this for continuous distributions. Condition (O.2) is obviously fulfilled. For bandlimited PDFs Eq. (O.3) also holds, since

$$\begin{aligned} \int_{-\infty}^{\infty} F_x(x - \zeta) \text{sinc}(\pi \zeta/q) d\zeta &= \int_{-\infty}^{\infty} \int_{-\infty}^{x-\zeta} f_x(y) dy \text{sinc}(\pi \zeta/q) d\zeta \\ &= \int_{-\infty}^{\infty} \int_{-\infty}^{x-\zeta} f_x(y) \text{sinc}(\pi \zeta/q) dy d\zeta && \text{note: } y = \eta - \zeta \\ &= \int_{-\infty}^{\infty} \int_{-\infty}^x f_x(\eta - \zeta) \text{sinc}(\pi \zeta/q) d\eta d\zeta \\ &= \int_{-\infty}^x \int_{-\infty}^{\infty} f_x(\eta - \zeta) \text{sinc}(\pi \zeta/q) d\zeta d\eta \\ &= \int_{-\infty}^x f_x(\eta) d\eta \\ &= F_x(x). \end{aligned} \quad (\text{O.5})$$



We think that changing the order of integration (lines 3-4) is allowable here, but the general validity is not yet proven. Fubini's theorem may not be directly applied here, since its condition (absolute integrability of the integrand) is not fulfilled.

In the before last step (lines 4-5) we made use of the bandlimitedness of the PDF, which yielded

$$f_x(\eta) \star \text{sinc}(\pi \eta/q) = f_x(\eta). \quad (\text{O.6})$$

Zakai's theorem ensures that the CDF can be interpolated from its samples. However, condition (O.3) is an implicit formulation of bandlimitedness, and it is not easy to see its relation to the usual formulation of the sampling theorem. Therefore, we will also formulate a suitable theorem that is more similar to the classical one. For this, we will need to obtain the *generalized* Fourier transform of  $F_x(x)$ . This is a so-called distribution (Arsac, 1966; Bremermann, 1965; Lighthill, 1958; Zemanian, 1965), and its form is given by many books as the *integration property* of the Fourier transform (Oppenheim, Willsky and Young, 1983). For the CDF this yields

$$\int_{-\infty}^{\infty} F_x(x) e^{jux} dx = \int_{-\infty}^{\infty} \int_{-\infty}^x f_x(\zeta) d\zeta dx = \frac{-1}{ju} \Phi_x(u) + \pi \Phi_x(0) \delta(u). \quad (\text{O.7})$$

If  $\Phi_x(u)$  is bandlimited, then the distribution at the right side of Eq. (O.7) is different from zero obviously in a finite interval only. For such distributions, Campbell (1968) proved a useful theorem. We state here a simplified version of it.

**Campbell's generalized sampling theorem (formulated for CDF's)**

*If  $F_x(x)$  is the inverse Fourier transform of a distribution which is identically zero outside  $(-\pi/q + \alpha, \pi/q - \alpha)$ , and  $W(u)$  is a function which is differentiable infinite times, and*

$$W(u) = \begin{cases} 1 & \text{for } |u| < \pi/q - \alpha, \\ \text{arbitrary} & \text{for } \pi/q - \alpha \geq |u| < \pi/q, \\ 0 & \text{for } |u| \geq \pi/q, \end{cases} \quad (\text{O.8})$$

*then*

$$F_x(x) = \sum_{m=-\infty}^{\infty} F_x(mq) w(x - mq), \quad (\text{O.9})$$

*with*

$$w(x) = \frac{1}{2\pi} \int_{-\infty}^{\infty} W(u) e^{-jxu} du. \quad (\text{O.10})$$

An example for such a function  $W(u)$  will be given later.

Eq. (O.9) is a modified version of the interpolation formula. Campbell proved that if Eq. (O.9) uniformly converges for given  $x$  and  $0 \leq \alpha < \alpha_0$ , then  $\alpha \rightarrow 0$  can be taken, and Eq. (O.9) yields the familiar interpolation formula. This can be proved for the case of CDF's.

## O.2 CONVERGENCE OF THE INTERPOLATION FORMULA

We have seen that special theorems are required to assure the convergence of the interpolation series. We may notice that while this series converges, it is not absolutely convergent, because the sinc function disappears as  $\mathcal{O}(1/m)$  for large values of  $m$ . It can also be noticed that for large positive values of  $m$ , where  $F_x(mq) \approx 1$ , the interpolating series converges very slowly. The convergence is similar to that of the sum

$$\sum_{m=1}^{\infty} \frac{(-1)^{m+1}}{m} = \ln 2 \approx 0.693. \quad (\text{O.11})$$

The convergence can be monitored in a simple way by noticing that for  $x = (k + 0.25)q$ ,  $x = (k + 0.5)q$ , and  $x = (k + 0.75)q$ , the interpolation formula can be explicitly summed for large enough values of  $m$ , for which  $F_x(x) \approx 1$ . Another possibility is to calculate in advance an auxiliary sum for large enough values of  $m$ :

$$\begin{aligned} & \sum_{m=m_0}^{\infty} F_x(mq) \operatorname{sinc}(\pi(x - mq)/q) \\ &= \sum_{m=m_0}^{\infty} \operatorname{sinc}(\pi(x - mq)/q) - \sum_{m=m_0}^{\infty} (1 - F_x(mq)) \operatorname{sinc}(\pi(x - mq)/q) \\ &= S(x) - \sum_{m=m_0}^{\infty} (1 - F_x(mq)) \operatorname{sinc}(\pi(x - mq)/q). \end{aligned} \quad (\text{O.12})$$

The first sum is independent of  $F_x(x)$ . The second sum is usually small and can be approximated well enough by a finite number of its terms.

However, it is even more desirable to *accelerate* the convergence. A possibility is to modify the interpolation formula as follows.

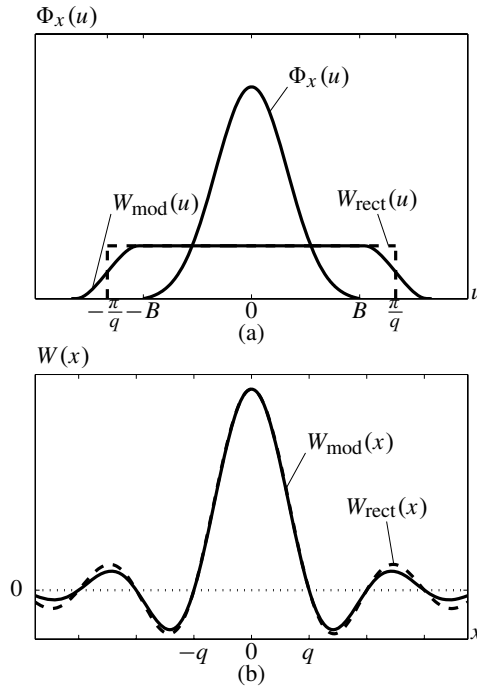


**Figure O.1** Window functions for interpolation: (a) in the CF domain; (b) in the PDF domain.

The sinc function arises as the inverse Fourier transform of the window function which selects the central replica of the spectrum. The slow decay of the sinc function is the consequence of the jumps in the window function at both edges. When the bandlimit is lower than  $\pi/q$ , we can modify the window function in order to have smooth edges, and thus have a quick rolloff in the PDF domain, as illustrated in Fig. O.1.

Campbell (1968) suggested the following function. Let  $\Phi_x(u)$  be bandlimited in  $(-\pi/q + \alpha, \pi/q - \alpha)$ . Define the function

$$\Lambda(u) = \begin{cases} K e^{\frac{\alpha^2}{u^2 - \alpha^2}} & \text{for } |u| < \alpha, \\ 0 & \text{elsewhere,} \end{cases} \quad (\text{O.13})$$

with  $K$  chosen so that

$$\int_{-\infty}^{\infty} \Lambda(u) du = 1. \quad (\text{O.14})$$

This corresponds in the PDF domain to

$$\lambda(x) = \frac{1}{2\pi} \int_{-\infty}^{\infty} \Lambda(u) e^{-jux} du. \quad (\text{O.15})$$

$\lambda(x)$  has a rapid decay. Using the modified window function

$$W_{\text{mod}}(u) = W_{\text{rect}}(u) \star \Lambda(u), \quad (\text{O.16})$$

the following modified, quickly converging interpolation formula can be obtained:

$$F_x(x) = \sum_{m=-\infty}^{\infty} F_x(mq) \text{sinc}(\pi(x - mq)/q) \lambda(x - mq). \quad (\text{O.17})$$

It can be seen that Eq. (O.16) is differentiable infinite times, so it is a suitable function for use in Eqs. (O.8)–(O.10).

The same technique can be applied for the interpolation using the modified window function, given in Exercise 4.22.

### O.3 NUMERICAL DIFFERENTIATION

The PDF can be obtained from  $F_x(x)$  by differentiation. Since  $F_x(x)$  is interpolated by using a digital computer, differentiation can only be done numerically from the samples of  $F_x(x)$ .

However,  $f_x(x)$  can also be directly obtained from the samples of  $F_x(x)$ , as follows.

$$\begin{aligned} f_x(x) &= \frac{d}{dx} F_x(x) = \frac{d}{dx} \sum_{m=-\infty}^{\infty} F_x(mq) w(x - mq) \\ &= \sum_{m=-\infty}^{\infty} F_x(mq) \frac{dw(x - mq)}{dx}. \end{aligned} \quad (\text{O.18})$$

The differentiation and summation can be interchanged if both sums converge and the functions are all differentiable (Korn and Korn, 1968, Sect. 4.84). For bandlimited PDFs this is fulfilled. Eq. (O.18) is the direct interpolation formula for the PDF.

## Addendum P

---

# Small Bit-Number Correlation

In this book, we investigate the conditions for being able to restore the input moments (e.g. the covariance) from the output moments, independently of the concrete form of the input PDF. We have determined the conditions for this, requiring that the quantum size be small enough compared to the standard deviation of the input signal. If the quantized variables represent the signal values on at least a few bits,  $E\{x'_1 x'_2\}$  well approximates the correlation,  $R_{x_1, x_2} = E\{x_1 x_2\}$ .

When quantization is very rough, significant deviations from the true correlation values will occur. However, *if we know* that the input PDF is *Gaussian*, the input covariance can be perfectly *restored* from the small-bit output covariance, even if no dither is applied. Such cases are briefly discussed in this section.

### P.1 HYBRID SIGN CORRELATOR

If one of the input quantizers is realized with a comparator (one-bit quantizer), and the mean of its input is removed, we obtain the so-called hybrid sign correlator (or ring or relay correlator, see Fig. P.1).

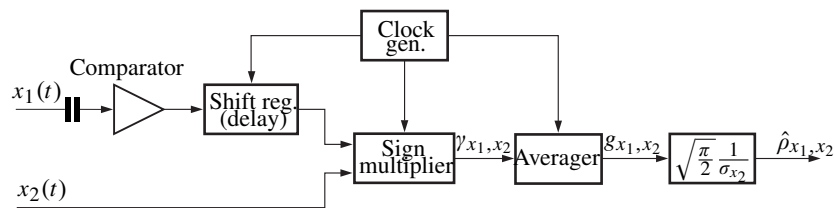


**Figure P.1** Signal processing in the hybrid sign correlator

It can be proven (Hagen and Farley, 1973) that the expected value of the output of the averager equals

$$E\{g_{x_1, x_2}\} = E\{\gamma_{x_1, x_2}\} = E\{\text{sign}(\tilde{x}_1)x_2\} = \sqrt{\frac{2}{\pi}} \sigma_{x_2} \rho_{x_1, x_2}. \quad (\text{P.1})$$

The comparator which produces  $\text{sign}(\tilde{x}_1)$  can produce a large set of differently delayed “samples” at high rate. The evaluation of  $E\{\text{sign}(\tilde{x}_1)x_2\}$  is also very quick, since it needs no digital multiplier, because only the changing of the sign of  $\tilde{x}_2$  is necessary when  $\text{sign}(\tilde{x}_1)$  is negative. This high rate assures that the hybrid sign correlator can process signals of very high bandwidth.

The unbiased estimate of the covariance can be obtained by correcting for the multiplying terms in Eq. (P.1):

$$\hat{\rho}_{x_1, x_2} = \sqrt{\frac{\pi}{2}} \frac{1}{\sigma_{x_2}} g_{x_1, x_2}. \quad (\text{P.2})$$

Averaging is needed to reduce the variance of the estimate. The variance of a single product ( $N = 1$ , that is,  $g_{x_1, x_2} = \text{sign}(\tilde{x}_1(k))x_2(k)$ ) can be determined as:

$$\begin{aligned} \text{var}\{\hat{\rho}_{x_1, x_2}\} &= \text{var}\left\{\sqrt{\frac{\pi}{2}} \frac{1}{\sigma_{x_2}} g_{x_1, x_2}^{(1)}\right\} \\ &= E\left\{\left(\sqrt{\frac{\pi}{2}} \frac{1}{\sigma_{x_2}} \gamma_{x_1, x_2}\right)^2\right\} - \left(E\left\{\sqrt{\frac{\pi}{2}} \frac{1}{\sigma_{x_2}} \gamma_{x_1, x_2}\right\}\right)^2 \\ &= \frac{\pi}{2} \frac{1}{\sigma_{x_2}^2} E\{\text{sign}^2(\tilde{x}_1)x_2^2\} - \rho_{x_1, x_2}^2 \\ &= \frac{\pi}{2} - \rho_{x_1, x_2}^2. \end{aligned} \quad (\text{P.3})$$

It may be surprising that this variance is not significantly larger than the variance of the product of two finely quantized samples, which is equal to

$$\text{var}\{\hat{\rho}_{x_1, x_2}^{(1)}\} = \text{var}\left\{\frac{x_1 x_2}{\sigma_{x_1} \sigma_{x_2}}\right\} = 1 + \rho_{x_1, x_2}^2 \quad (\text{P.4})$$

(see Exercise 11.11).

## P.2 POLARITY COINCIDENCE CORRELATOR

Another interesting arrangement is the one where both channels contain a comparator each (see Fig. P.2).

The multiplication is realized by a simple coincidence gate which returns high-level value if the inputs are equal, and low-level value when they differ (hence the name of the correlator). The averager is an up/down counter. The delay is controlled by the clock frequency of the shift register.

The expected value of the product of the comparator outputs is a nonlinear function of the correlation coefficient (Hagen and Farley, 1973):

$$E\{\beta_{x_1, x_2}\} = E\{\text{sign}(\tilde{x}_1) \text{sign}(\tilde{x}_2)\} = \frac{2}{\pi} \arcsin(\rho_{x_1, x_2}). \quad (\text{P.5})$$

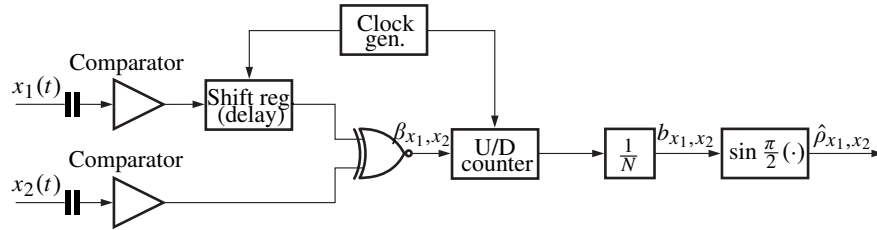


**Figure P.2** Polarity coincidence correlator for Gaussian signals

Therefore, in order to obtain the true correlation coefficient function, a nonlinear restoration block is applied at the right in Fig. P.2. If the variance after the  $1/N$  multiplier is small, the output is approximately unbiased after the nonlinear reconstruction:

$$E\{\hat{\rho}_{x_1, x_2}\} = E\left\{\sin\left(\frac{\pi}{2}\beta_{x_1, x_2}^{(N)}\right)\right\} \approx \sin\left(\frac{\pi}{2}E\{\beta_{x_1, x_2}\}\right) = \rho_{x_1, x_2}. \quad (\text{P.6})$$

It can be shown (Kollár, 1988) that the variance of one single product is equal to

$$\begin{aligned} \text{var}\{\hat{\rho}_{x_1, x_2}^{(1)}\} &\approx \left(\frac{d\hat{\rho}_{x_1, x_2}}{d\beta_{x_1, x_2}^{(N)}}\right)^2 \text{var}\{\beta_{x_1, x_2}\} \\ &= \left(\frac{\pi}{2}\right)^2 \cos^2\left(\frac{\pi}{2}E\{\beta_{x_1, x_2}\}\right) \text{var}\{\beta_{x_1, x_2}\} \\ &= \left(1 - \sin^2\left(\frac{\pi}{2}E\{\beta_{x_1, x_2}\}\right)\right) \left(\frac{\pi}{2}\right)^2 \left(E\{\beta_{x_1, x_2}^2\} - (E\{\beta_{x_1, x_2}\})^2\right) \\ &\approx \left(1 - \rho_{x_1, x_2}^2\right) \left(\left(\frac{\pi}{2}\right)^2 - \arcsin^2(\rho_{x_1, x_2})\right), \end{aligned} \quad (\text{P.7})$$

since  $\beta_{x_1, x_2}^2 \equiv 1$ .

This variance is decreased by a factor  $1/N$  when  $N$  independent samples are averaged by the counter.

The variances of the above mentioned three different correlators can be compared. These variances, based on Eqs. (P.3), (P.4), and (P.7), are shown in Fig. P.3.

These three variances are comparable. Moreover, the polarity coincidence correlator has the smallest variance for  $|\rho_{x_1, x_2}| > 0.65$ . This fact, and speed and low price are the reasons for the popularity of the polarity coincidence correlator in high frequency applications, like in radio astronomy.

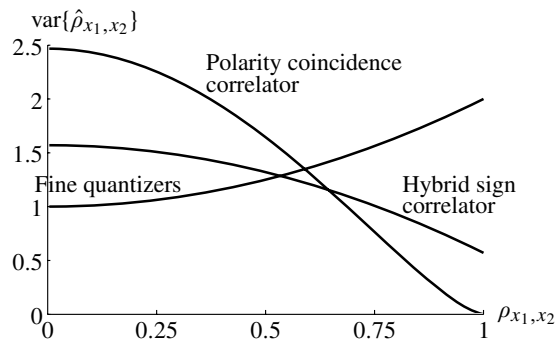


**Figure P.3** Comparison of the variance of different correlators for zero mean Gaussian signals, when measuring the correlation coefficient from  $N$  samples



## Addendum Q

---

# Noise Shaping and Sigma-delta Modulation

In Chapter 20, we have investigated the conditions to have a white quantization noise sequence. This would distribute the noise power uniformly in the frequency band up to the Nyquist frequency, and the noise power which disturbs us would be proportional to the width of the frequency band of interest.

However, by proper feedback, the spectrum of the noise can be altered beneficially. As we will see, instead of making the spectrum constant, we can push the major part of the noise power to high frequencies, and by lowpass filtering we can remove most of it. This is the basic idea of sigma-delta modulation, first described by Inose, Yasuda and Murakami (1962). This has acquired an important role with the development of VLSI technology which made possible its full integration on a single chip.

We show here how to describe its working by simply assuming PQN at the output of the comparator, which is a very coarse quantizer. The basic idea is illustrated in Fig. Q.1. The feedback loop strives to make the feedback signal equal the

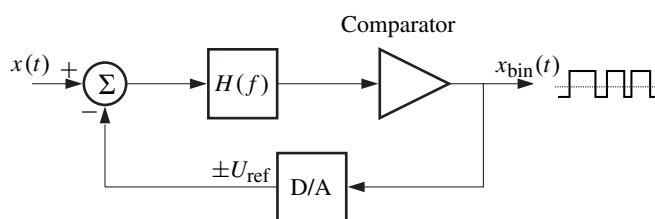


**Figure Q.1** Principle of sigma-delta modulation

input signal. However, since the difference signal is lowpass filtered by  $H(f)$ , this balancing is made only for the low frequency part of the feedback signal.

The filtered difference is led to the comparator. The resulting two-level signal is set to appropriate levels by the one-bit “D/A converter”, and is applied as the

feedback signal. The allowable range of the input signal is smaller than the output range of this D/A converter, so that the two different output values of the DAC can yield positive or negative signals at the input of the comparator, respectively.

Thus, the mean value of the oscillating binary output of the D/A converter is forced to be equal with the slowly varying input signal  $x$ . We can obtain the corresponding information by measuring the mean value of the digital  $x_{\text{bin}}(t)$ . This mean value can be easily obtained by applying a digital lowpass filter to  $x_{\text{bin}}(t)$ . Therefore, by extending the arrangement in Fig. Q.1 with a digital lowpass filter, we can realize an A/D converter. Since no precise elements are needed (except the output voltage setting of the one/bit DAC), this ADC has high accuracy. In fact, most modern audio converters work basically like this.

For a simple but mathematical analysis of the properties of the sigma-delta modulator, let us analyze the closed loop in Fig. Q.1. Let us use the PQN model for the comparator, and determine the output signal in terms of the input signal and the noise. Introducing an “equivalent gain” ( $g_e$ ) for the comparator,

$$X_{\text{bin}}(f) = (X(f) - X_{\text{bin}}(f)) H(f) g_e + N(f), \quad (\text{Q.1})$$

where  $X(f)$  and  $X_{\text{bin}}(f)$  are the Fourier transforms of the sampled input and output signals, respectively, and  $N(f)$  is the Fourier transform of the sampled quantization error. After some rearrangement,

$$X_{\text{bin}}(f) = \frac{H(f) g_e}{1 + H(f) g_e} X(f) + \frac{1}{1 + H(f) g_e} N(f). \quad (\text{Q.2})$$

It is obvious that the power of the useful signal is concentrated at low frequencies, where  $H(f) g_e$  is large: here the coefficient of the signal is approximately 1. The noise is practically suppressed at these frequencies; it is large only where the low-pass filter already significantly attenuates. Thus, signal and noise are *separated* in the frequency domain (noise shaping), and a consecutive digital lowpass filter can suppress the high frequency noise, while keeping the low-frequency input signal.

#### Example Q.1 Output noise spectrum of a sigma-delta converter

Let us investigate a sigma-delta converter using an integrator as a built-in filter:

$H(f) = 1/(j2\pi f T_i)$ . The transfer function of noise shaping is from (Q.2):

$$H_{\text{effn}}(f) = \frac{j2\pi f T_i}{j2\pi f T_i + g_e}. \quad (\text{Q.3})$$

At low frequencies, where  $f \ll 1/(2\pi T_i)$ , the power spectral density function of the noise is multiplied by the square of the absolute value of the transfer function:

$$|H_{\text{effn}}(f)|^2 \approx \left( \frac{2\pi f T_i}{g_e} \right)^2. \quad (\text{Q.4})$$

The quadratic behavior as a function of frequency shows that for small frequencies the quantization noise can be very well suppressed.

The sigma-delta modulator has several different implementations, since the shape of the transfer function of  $H(f)$  can be chosen in different ways, the comparator can be replaced by a small bit-number ADC, etc., see e. g. (Norsworthy, Schreier and Temes, 1997; Schreier and Temes, 2005). Even A/D converters with 18-24 bit resolution can be built using the sigma-delta modulation principle, especially if a high-order filter is used in the loop.



## Addendum R

---

---

# ***Second-order Statistical Properties of a Triangle-Wave Signal***

A triangle wave is less likely to appear at the input of a quantizer than a sinusoidal wave, unless the system designer deliberately puts it there. Such is the case when the triangle wave is used as a dither signal. The properties of the triangle wave that make it suitable as a dither signal can be obtained from the mathematics of this appendix. A more advanced application would be to use the sum of two independent triangle waves (generating by this a triangularly *distributed* dither). Dither is discussed in Chapter 19.

Samples of a triangle wave can be investigated in a similar manner as samples of a sine wave. Although the mathematical details and expressions will be different since the triangle wave has uniform distribution, we may expect similar results because of the similarities of the two waveforms.

### **R.1 THE SIGNAL MODEL**

Let us consider a randomly timed, symmetrical, zero mean triangle wave with amplitude  $A$  and period length  $T$  (see Fig. R.1). The time shift  $t_0$  is uniformly distributed in  $[0, 2\pi)$ .

Let us denote the ( $A = 1, T = 1, t_0 = 0$ ) triangle wave by  $\text{trw}(t)$  (in order to emphasize similarity to the cosine function), see Fig. R.2. With this notation,

$$x(t) = A \text{trw} \left( \frac{t - t_0}{T} \right). \quad (\text{R.1})$$

This function can be analytically defined as:

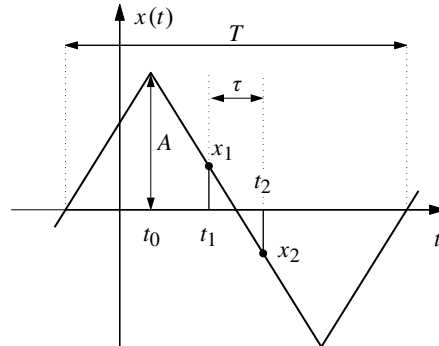


**Figure R.1** Sampling of a randomly timed symmetrical triangle wave.

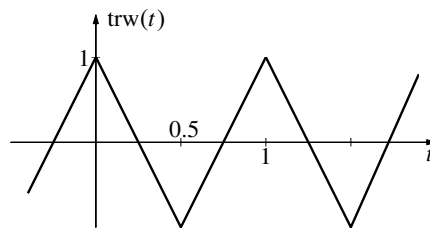


**Figure R.2** The standardized triangle function  $\text{trw}(t)$ .

$$\text{trw}\left(\frac{\tau}{T}\right) = \begin{cases} 1 - \frac{4|\tau|}{T} & \text{for } -\frac{T}{2} \leq \tau \leq \frac{T}{2} \\ \text{repeated with period } T & \text{elsewhere} \end{cases} . \quad (\text{R.2})$$

## R.2 DERIVATION OF THE JOINT PDF

Each sample has a uniform distribution with PDF

$$f(x) = \begin{cases} \frac{1}{2A} & \text{for } |x| \leq A \\ 0 & \text{elsewhere} \end{cases} . \quad (\text{R.3})$$

The joint PDF can be determined as

$$f(x_1, x_2) = f(x_2|x_1)f(x_1) . \quad (\text{R.4})$$

The conditional PDF is discrete for given  $A, T$  and  $\tau$ . Given  $x_1$ , there are two possibilities for the value  $x_2$ .

For a given value of  $x_1$ , the positions can be  $t'_1$  and  $t''_1$ . Since the absolute values of the slopes are equal, each case has equal probability  $p = 0.5$ . The possible positions of  $x_2$  can be determined as  $t'_2 = t'_1 + \tau, t''_2 = t''_1 + \tau$ . Therefore,  $f(x_2|x_1)$  is a discrete PDF:

$$f(x_2|x_1) = 0.5\delta(x_2 - x(t'_2)) + 0.5\delta(x_2 - x(t''_2)). \tag{R.5}$$

The explicit expression of  $x_2(x_1, \tau)$  is somewhat complex, but as we will see, it will not be needed. Instead, it is quite simple to determine the possible  $(x_1, x_2)$  points of the  $x_1$ - $x_2$  plane (see Fig. R.3).

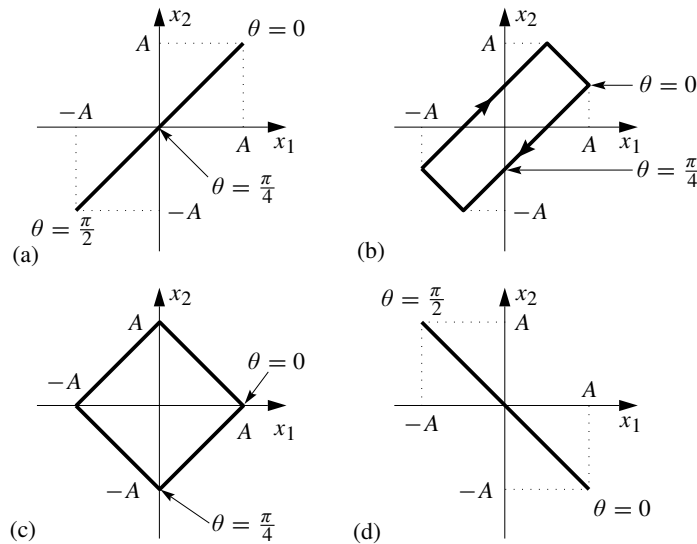


**Figure R.3** Possible Combinations of  $x_1, x_2$ , for selected values of  $\tau$ : (a)  $\tau = 0, T, 2T, \dots$ ; (b)  $\tau = T/8, 9T/8, \dots$ ; (c)  $\tau = T/4, 5T/4, \dots$ ; (d)  $\tau = T/2, 3T/2, \dots$

The parametric expression of the rectangles is, in accord with Eq. (R.1),

$$x_1 = A \operatorname{trw} \left( \frac{\theta}{T} \right), \quad x_2 = A \operatorname{trw} \left( \frac{\theta + \tau}{T} \right), \quad -\frac{T}{2} \leq \theta < \frac{T}{2}. \tag{R.6}$$

An implicit equation for the rectangles, similar to Eq. (G.17), can be obtained as follows. A rectangle, like the one in Fig. R.3(b), can be represented as

$$|x_1 - mx_2| + |mx_1 - x_2| = c, \tag{R.7}$$

where  $m$  and  $c$  are appropriately chosen constants. These constants can be determined by examining Fig. R.4 in light of Eq. (R.7).

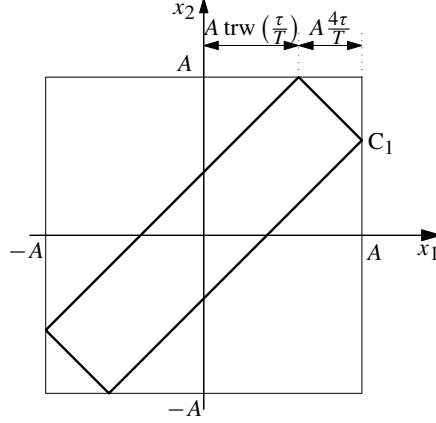


**Figure R.4** The contour of  $(x_1, x_2)$  for  $0 \leq \tau \leq T/2$ .

It is easy to see that the corner points of the rectangle correspond to sign-changing of one of the absolute value functions in Eq. (R.7). That is, for  $-1 \leq m \leq 1$ ,

$$x_1 = A \quad \text{and} \quad mx_1 - x_2 = 0 \quad \Rightarrow \quad x_2 = mA. \quad (\text{R.8})$$

By substituting  $x_1$  and  $x_2$  back to the equation, the left-hand side gives

$$|x_1 - mx_2| + |0| = A(1 - m^2) \quad \Rightarrow \quad c = A(1 - m^2). \quad (\text{R.9})$$

Comparing Eq. (R.8) and Eq. (R.6),

$$x_1 = A \quad \Rightarrow \quad \theta = 0 + kT \quad \Rightarrow \quad x_2 = A \operatorname{trw}\left(\frac{\tau}{T}\right) \quad \Rightarrow \quad m = \operatorname{trw}\left(\frac{\tau}{T}\right). \quad (\text{R.10})$$

With these values, Eq. (R.7) becomes

$$\left| x_1 - \operatorname{trw}\left(\frac{\tau}{T}\right) x_2 \right| + \left| \operatorname{trw}\left(\frac{\tau}{T}\right) x_1 - x_2 \right| = A \left( 1 - \operatorname{trw}^2\left(\frac{\tau}{T}\right) \right). \quad (\text{R.11})$$

This is the general implicit formula we were seeking. The joint PDF consists of impulse sheets over the above contours, as illustrated in Fig. R.5.

The joint PDF is thus

$$f(x_1, x_2) = \frac{1}{2A} \left( 0.5\delta(x_2 - x_2'(x_1)) + 0.5\delta(x_2 - x_2''(x_1)) \right). \quad (\text{R.12})$$



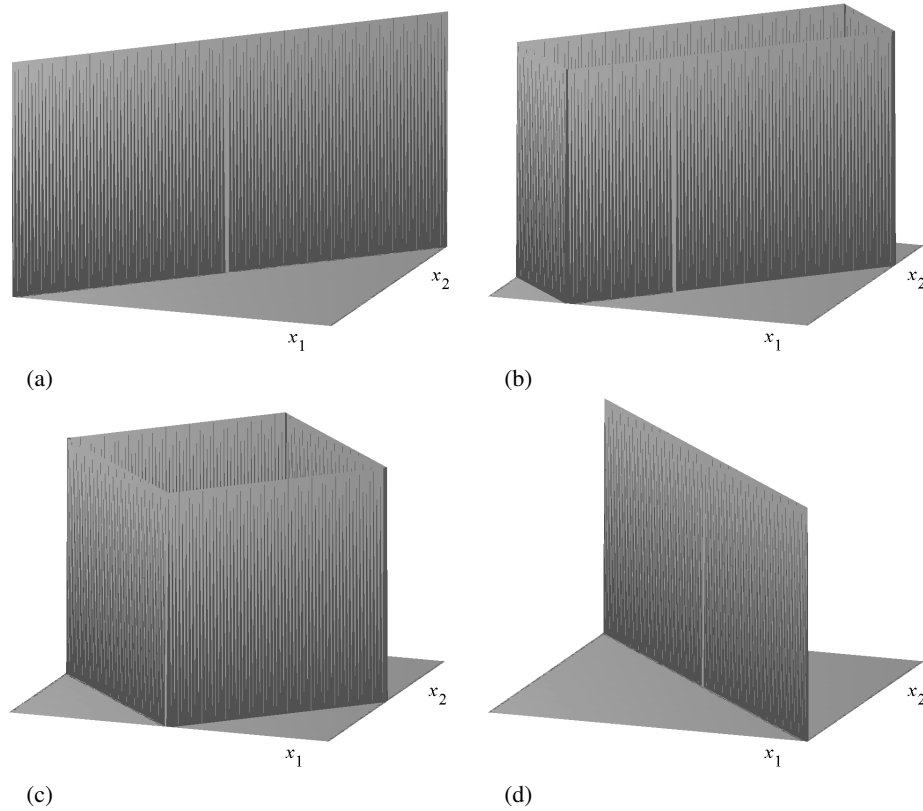


**Figure R.5** Joint PDF of two samples of a symmetric triangle wave: (a)  $\tau = 0, T, \dots$ ; (b)  $\tau = T/8, 9T/8, \dots$  (c)  $\tau = T/4, 5T/4, \dots$  (d)  $\tau = T/2, 3T/2, \dots$

### R.3 DERIVATION OF THE JOINT CF

The one-dimensional CF is the Fourier transform of Eq. (R.3).

$$\begin{aligned}
 \Phi(u) &= \mathcal{F}\{f(x)\} = \int_{-A}^A \frac{1}{2A} e^{jux} dx \\
 &= \left[ \frac{1}{ju2A} e^{jux} \right]_{-A}^A \\
 &= \frac{1}{uA} \frac{e^{juA} - e^{-juA}}{2j} = \frac{\sin uA}{uA} = \text{sinc}(uA). \quad (\text{R.13})
 \end{aligned}$$

The joint CF is the two-dimensional Fourier transform of the joint PDF:

$$\begin{aligned}\Phi(u_1, u_2) &= \mathcal{F}\{f(x_1, x_2)\} \\ &= \int_{-\infty}^{\infty} \int_{-\infty}^{\infty} f(x_1, x_2) e^{j(u_1 x_1 + u_2 x_2)} dx_2 dx_1.\end{aligned}\quad (\text{R.14})$$

Because of the Dirac delta functions in  $f(x_1, x_2)$  (see (Eq. (R.12))), the integral with respect to  $x_2$  just selects the points on the contour, and thus

$$\Phi(u_1, u_2) = \int_{-A}^A \frac{1}{2A} 0.5 e^{j(u_1 x_1 + u_2 x_2(x_1))} dx_1.\quad (\text{R.15})$$

The integral needs to be evaluated for both values of  $x_2(x_1)$ .

Let us calculate the two-dimensional CF by evaluating Eq. (R.15). The  $x_2(x_1)$  function has two values for  $-A < x_1 < A$  (see Fig. R.6), so that  $x_2(x_1)$  can be put

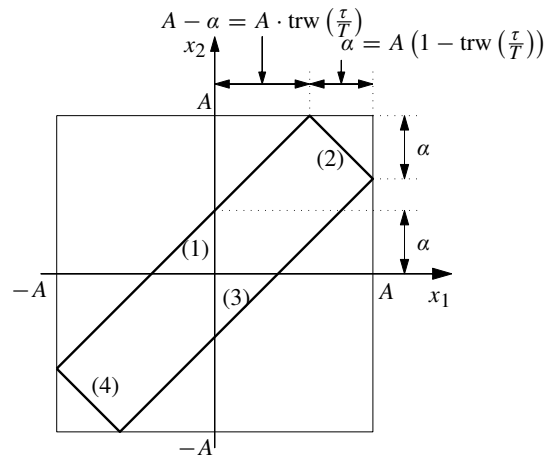


**Figure R.6** Integration contour on the  $x_1$ - $x_2$  plane.

together from four sections. With  $\alpha = A(1 - \text{trw}(\tau/T))$ ,

- 1) for  $-A \leq x_1 \leq A - \alpha$ ,  $x_2(x_1) = x_1 + \alpha$
- 2) for  $A - \alpha \leq x_1 \leq A$ ,  $x_2(x_1) = 2A - \alpha - x_1$
- 3) for  $-(A - \alpha) \leq x_1 \leq A$ ,  $x_2(x_1) = x_1 - \alpha$
- 4) for  $-A \leq x_1 \leq -(A - \alpha)$ ,  $x_2(x_1) = \alpha - 2A - x_1$

The following indefinite integral applies to all sections:

$$\begin{aligned} I &= \frac{1}{4A} \frac{1}{j(u_1 \pm u_2)} e^{j(u_1 x_1 + u_2 x_2(x_1))} + C \\ &= \frac{1}{2A(u_1 \pm u_2)} \frac{e^{j(u_1 x_1 + u_2 x_2(x_1))}}{2j} + C. \end{aligned} \quad (\text{R.16})$$

The positive sign applies for sections 1 and 3, and the negative sign for sections 2 and 4.

$$\begin{aligned} I_1 &= \left[ \frac{1}{2A(u_1 + u_2)} \frac{e^{j(u_1 x_1 + u_2(x_1 + a))}}{2j} \right]_{-A}^{A-\alpha} \\ &= \frac{e^{ju_2 a}}{2A(u_1 + u_2)} \left( \frac{e^{j(u_1 + u_2)(A-\alpha)} - e^{-j(u_1 + u_2)A}}{2j} \right) \\ &= \frac{e^{ju_2 a - j\frac{u_1 + u_2}{2}a}}{2A(u_1 + u_2)} \sin\left(\frac{u_1 + u_2}{2}(2A - \alpha)\right) \\ &= \frac{e^{-j\frac{u_1 - u_2}{2}a}}{2} \frac{2A - \alpha}{2A} \operatorname{sinc}\left(\frac{u_1 + u_2}{2}(2A - \alpha)\right). \end{aligned} \quad (\text{R.17})$$

$$\begin{aligned} I_3 &= \left[ \frac{1}{2A(u_1 + u_2)} \frac{e^{j(u_1 x_1 + u_2(x_1 - a))}}{2j} \right]_{-(A-\alpha)}^A \\ &= \frac{e^{-ju_2 a}}{2A(u_1 + u_2)} \left( \frac{e^{j(u_1 + u_2)A} - e^{-j(u_1 + u_2)(A-\alpha)}}{2j} \right) \\ &= \frac{e^{-ju_2 a + j\frac{u_1 + u_2}{2}a}}{2A(u_1 + u_2)} \sin\left(\frac{u_1 + u_2}{2}(2A - \alpha)\right) \\ &= \frac{e^{j\frac{u_1 - u_2}{2}a}}{2} \frac{2A - \alpha}{2A} \operatorname{sinc}\left(\frac{u_1 + u_2}{2}(2A - \alpha)\right). \end{aligned} \quad (\text{R.18})$$

$$\begin{aligned} I_2 &= \left[ \frac{1}{2A(u_1 - u_2)} \frac{e^{j(u_1 x_1 + u_2(2A - \alpha - x_1))}}{2j} \right]_{A-\alpha}^A \\ &= \frac{e^{ju_2(2A - \alpha)}}{2A(u_1 - u_2)} \left( \frac{e^{j(u_1 - u_2)A} - e^{j(u_1 - u_2)(A-\alpha)}}{2j} \right) \\ &= \frac{e^{ju_2(2A - \alpha) + j\frac{u_1 - u_2}{2}(2A - \alpha)}}{2A(u_1 - u_2)} \sin\left(\frac{u_1 - u_2}{2}\alpha\right) \end{aligned}$$

$$= \frac{e^{j\frac{u_1+u_2}{2}(2A-\alpha)}}{2} \frac{\alpha}{2A} \operatorname{sinc}\left(\frac{u_1-u_2}{2}\alpha\right). \quad (\text{R.19})$$

$$\begin{aligned} I_4 &= \left[ \frac{1}{2A(u_1-u_2)} \frac{e^{j(u_1x_1+u_2(\alpha-2A-x_1))}}{2j} \right]_{-A}^{-(A-\alpha)} \\ &= \frac{e^{-ju_2(2A-\alpha)}}{2A(u_1-u_2)} \left( \frac{e^{-j(u_1-u_2)(A-\alpha)} - e^{-j(u_1-u_2)A}}{2j} \right) \\ &= \frac{e^{-ju_2(2A-\alpha)-j\frac{u_1-u_2}{2}(2A-\alpha)}}{2A(u_1-u_2)} \sin\left(\frac{u_1-u_2}{2}\alpha\right) \\ &= \frac{e^{-j\frac{u_1+u_2}{2}(2A-\alpha)}}{2} \frac{\alpha}{2A} \operatorname{sinc}\left(\frac{u_1-u_2}{2}\alpha\right). \quad (\text{R.20}) \end{aligned}$$

It can be noticed that  $I_1$  and  $I_3$  are complex conjugates of each other, and  $I_2$  and  $I_4$  are also complex conjugates. This allows a simplification in  $\Phi(u_1, u_2)$ .

$$\begin{aligned} \Phi(u_1, u_2) &= I_1 + I_2 + I_3 + I_4 \\ &= \cos\left(\frac{u_1-u_2}{2}\alpha\right) \frac{2A-\alpha}{2A} \operatorname{sinc}\left(\frac{u_1+u_2}{2}(2A-\alpha)\right) \\ &\quad + \cos\left(\frac{u_1+u_2}{2}(2A-\alpha)\right) \frac{\alpha}{2A} \operatorname{sinc}\left(\frac{u_1-u_2}{2}\alpha\right). \quad (\text{R.21}) \end{aligned}$$

The behavior of this function is illustrated in Fig. R.7.

By using  $\alpha = A(1 - \operatorname{trw}(\tau/T))$ , this expression can be easily evaluated.

A check of expression Eq. (R.21) shows that for  $u_1 = 0$  or  $u_2 = 0$ , the one-dimensional CFs are obtained. In order to prove this, we put Eq. (R.21) into a more convenient form. By using

$$\cos a \sin b = \frac{\sin(b+a) + \sin(b-a)}{2}, \quad (\text{R.22})$$

$$\begin{aligned} \Phi(u_1, u_2) &= \frac{1}{2A} \cos\left(\frac{u_1-u_2}{2}\alpha\right) \frac{2}{u_1+u_2} \sin\left(\frac{u_1+u_2}{2}(2A-\alpha)\right) \\ &\quad + \frac{1}{2A} \cos\left(\frac{u_1+u_2}{2}(2A-\alpha)\right) \frac{2}{u_1-u_2} \sin\left(\frac{u_1-u_2}{2}\alpha\right) \\ &= \frac{1}{2A(u_1+u_2)} (\sin(u_1A + u_2(A-\alpha)) + \sin(u_1(A-\alpha) + u_2A)) \\ &\quad + \frac{1}{2A(u_1-u_2)} (\sin(u_1A + u_2(A-\alpha)) - \sin(u_1(A-\alpha) + u_2A)) \\ &= \frac{\sin(u_1A + u_2(A-\alpha))}{A} \frac{1}{2} \left( \frac{1}{u_1+u_2} + \frac{1}{u_1-u_2} \right) \end{aligned}$$

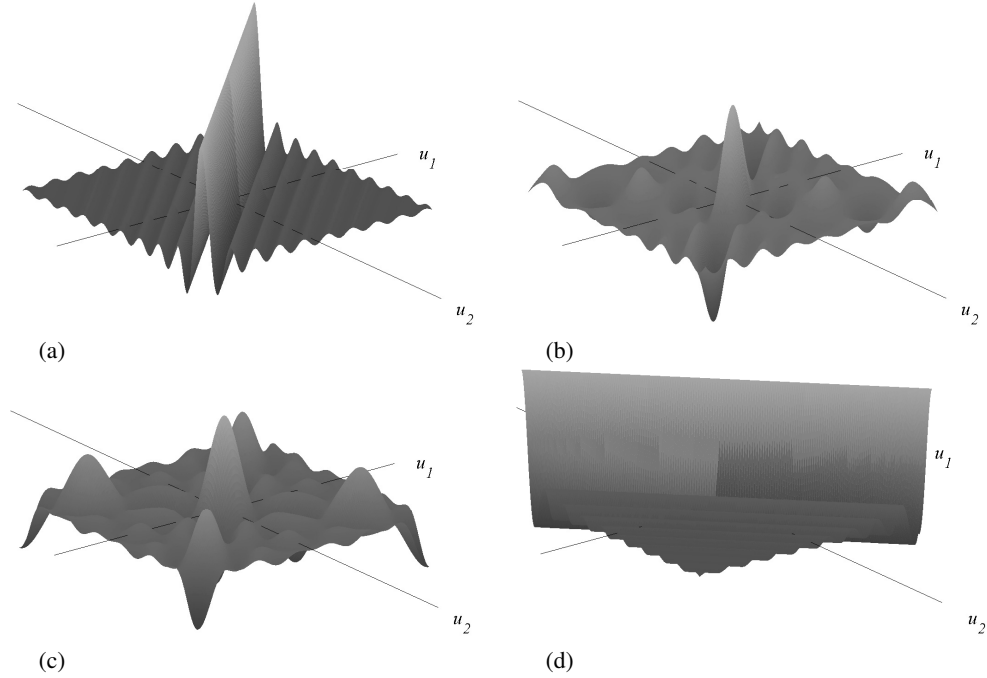


**Figure R.7** Joint characteristic function of two samples of a randomly timed symmetrical triangle wave: (a)  $\tau = 0$ ; (b)  $\tau = T/8$ ; (c)  $\tau = T/4$ ; (d)  $\tau = T/2$ .

$$+ \frac{\sin(u_1(A - \alpha) + u_2A)}{A} \frac{1}{2} \left( \frac{1}{u_1 + u_2} - \frac{1}{u_1 - u_2} \right). \quad (\text{R.23})$$

From this it follows that, indeed,

$$\Phi_{x_1, x_2}(u_1, 0) = \Phi_{x_1}(u_1) = \frac{\sin(u_1 A)}{u_1 A}. \quad (\text{R.24})$$

and

$$\Phi_{x_1, x_2}(0, u_2) = \Phi_{x_2}(u_2) = \frac{\sin(u_2 A)}{u_2 A}. \quad (\text{R.25})$$

For the determination of correlations and covariances, the derivatives of the joint CF are necessary. From Eq. (R.23),

$$\frac{\partial \Phi(u_1, u_2)}{\partial u_1} = \frac{-1}{2A(u_1 + u_2)^2} \left( \sin(u_1 A + u_2(A - \alpha)) + \sin(u_1(A - \alpha) + u_2 A) \right)$$

$$\begin{aligned}
& + \frac{1}{2(u_1 + u_2)} \left( \cos(u_1 A + u_2(A - \alpha)) + \frac{A - \alpha}{A} \cos(u_1(A - \alpha) + u_2 A) \right) \\
& - \frac{1}{2A(u_1 - u_2)^2} \left( \sin(u_1 A + u_2(A - \alpha)) - \sin(u_1(A - \alpha) + u_2 A) \right) \\
& + \frac{1}{2(u_1 - u_2)} \left( \cos(u_1 A + u_2(A - \alpha)) - \frac{A - \alpha}{A} \cos(u_1(A - \alpha) + u_2 A) \right) \\
& = \cos(u_1 A + u_2(A - \alpha)) \frac{1}{2} \left( \frac{1}{u_1 + u_2} + \frac{1}{u_1 - u_2} \right) \\
& \quad - \frac{\sin(u_1 A + u_2(A - \alpha))}{A} \frac{1}{2} \left( \frac{1}{(u_1 + u_2)^2} + \frac{1}{(u_1 - u_2)^2} \right) \\
& \quad + \cos(u_1(A - \alpha) + u_2 A) \frac{A - \alpha}{A} \frac{1}{2} \left( \frac{1}{u_1 + u_2} - \frac{1}{u_1 - u_2} \right) \\
& \quad - \frac{\sin(u_1(A - \alpha) + u_2 A)}{A} \frac{1}{2} \left( \frac{1}{(u_1 + u_2)^2} - \frac{1}{(u_1 - u_2)^2} \right). \tag{R.26}
\end{aligned}$$

$$\begin{aligned}
\frac{\partial \Phi(u_1, u_2)}{\partial u_2} & = \frac{-1}{2A(u_1 + u_2)^2} \left( \sin(u_1 A + u_2(A - \alpha)) + \sin(u_1(A - \alpha) + u_2 A) \right) \\
& \quad + \frac{1}{2(u_1 + u_2)} \left( \frac{A - \alpha}{A} \cos(u_1 A + u_2(A - \alpha)) + \cos(u_1(A - \alpha) + u_2 A) \right) \\
& \quad + \frac{1}{2A(u_1 - u_2)^2} \left( \sin(u_1 A + u_2(A - \alpha)) - \sin(u_1(A - \alpha) + u_2 A) \right) \\
& \quad + \frac{1}{2(u_1 - u_2)} \left( \frac{A - \alpha}{A} \cos(u_1 A + u_2(A - \alpha)) - \cos(u_1(A - \alpha) + u_2 A) \right) \\
& = \cos(u_1 A + u_2(A - \alpha)) \frac{A - \alpha}{A} \frac{1}{2} \left( \frac{1}{u_1 + u_2} + \frac{1}{u_1 - u_2} \right) \\
& \quad - \frac{\sin(u_1 A + u_2(A - \alpha))}{A} \frac{1}{2} \left( \frac{1}{(u_1 + u_2)^2} - \frac{1}{(u_1 - u_2)^2} \right) \\
& \quad + \cos(u_1(A - \alpha) + u_2 A) \frac{1}{2} \left( \frac{1}{u_1 + u_2} - \frac{1}{u_1 - u_2} \right) \\
& \quad - \frac{\sin(u_1(A - \alpha) + u_2 A)}{A} \frac{1}{2} \left( \frac{1}{(u_1 + u_2)^2} + \frac{1}{(u_1 - u_2)^2} \right). \tag{R.27}
\end{aligned}$$

$$\begin{aligned}
\frac{\partial^2 \Phi(u_1, u_2)}{\partial u_1 \partial u_2} & = \frac{1}{A(u_1 + u_2)^3} \left( \sin(u_1 A + u_2(A - \alpha)) + \sin(u_1(A - \alpha) + u_2 A) \right) \\
& \quad - \frac{1}{2(u_1 + u_2)^2} \frac{2A - \alpha}{A} \left( \cos(u_1 A + u_2(A - \alpha)) + \cos(u_1(A - \alpha) + u_2 A) \right) \\
& \quad - \frac{A - \alpha}{2(u_1 + u_2)} \left( \sin(u_1 A + u_2(A - \alpha)) + \sin(u_1(A - \alpha) + u_2 A) \right)
\end{aligned}$$

$$\begin{aligned}
& - \frac{1}{A(u_1 - u_2)^3} \left( \sin(u_1 A + u_2(A - \alpha)) - \sin(u_1(A - \alpha) + u_2 A) \right) \\
& + \frac{1}{2(u_1 - u_2)^2} \frac{\alpha}{A} \left( \cos(u_1 A + u_2(A - \alpha)) + \cos(u_1(A - \alpha) + u_2 A) \right) \\
& - \frac{A - \alpha}{2(u_1 - u_2)} \left( \sin(u_1 A + u_2(A - \alpha)) - \sin(u_1(A - \alpha) + u_2 A) \right) \\
= & - \sin(u_1 A + u_2(A - \alpha)) \\
& \times \left( \frac{A - \alpha}{2(u_1 + u_2)} + \frac{A - \alpha}{2(u_1 - u_2)} - \frac{1}{A(u_1 + u_2)^3} + \frac{1}{A(u_1 - u_2)^3} \right) \\
& - \cos(u_1 A + u_2(A - \alpha)) \left( \frac{2A - \alpha}{2A(u_1 + u_2)^2} - \frac{\alpha}{2A(u_1 - u_2)^2} \right) \\
& - \sin(u_1(A - \alpha) + u_2 A) \\
& \times \left( \frac{A - \alpha}{2(u_1 + u_2)} - \frac{A - \alpha}{2(u_1 - u_2)} - \frac{1}{A(u_1 + u_2)^3} - \frac{1}{A(u_1 - u_2)^3} \right) \\
& - \cos(u_1(A - \alpha) + u_2 A) \left( \frac{2A - \alpha}{2A(u_1 + u_2)^2} - \frac{\alpha}{2A(u_1 - u_2)^2} \right). \quad (\text{R.28})
\end{aligned}$$

These derivatives are difficult to evaluate at  $(u_1, u_2) = (0, 0)$ , because of the zero denominators. It can be shown, however, that the limiting values of Eqs. (R.26) and (R.27) are both zero, as it should be, because these give the expected value of the zero mean triangular wave:

$$\left. \frac{\partial \Phi(u_1, u_2)}{\partial u_1} \right|_{u_1=0, u_2=0} = \left. \frac{\partial \Phi(u_1, u_2)}{\partial u_2} \right|_{u_1=0, u_2=0} = E\{x\} = 0. \quad (\text{R.29})$$

The second partial derivative, Eq. (R.28), gives the autocorrelation function for  $(u_1, u_2) = (0, 0)$ . For  $u_2 = 0$ , taking the first few terms from the Taylor expansions of the trigonometric functions,

$$\begin{aligned}
\left. \frac{\partial^2 \Phi(u_1, u_2)}{\partial u_1 \partial u_2} \right|_{u_2=0} & = - \sin(u_1 A) \frac{A - \alpha}{u_1} - \cos(u_1 A) \frac{A - \alpha}{A u_1^2} \\
& + \sin(u_1(A - \alpha)) \frac{2}{A u_1^3} - \cos(u_1(A - \alpha)) \frac{A - \alpha}{A u_1^2} \\
& \approx - u_1 A \frac{A - \alpha}{u_1} - \left( 1 - \frac{u_1^2 A^2}{2} \right) \frac{A - \alpha}{A u_1^2} \\
& + \left( u_1(A - \alpha) - \frac{u_1^3 (A - \alpha)^3}{6} \right) \frac{2}{A u_1^3} - \left( 1 - \frac{u_1^2 (A - \alpha)^2}{2} \right) \frac{A - \alpha}{A u_1^2} \\
& = - A(A - \alpha) - \frac{A - \alpha}{A u_1^2} + \frac{A(A - \alpha)}{2}
\end{aligned}$$

$$\begin{aligned}
& + \frac{2(A - \alpha)}{Au_1^2} - \frac{(A - \alpha)^3}{3A} - \frac{A - \alpha}{Au_1^2} + \frac{(A - \alpha)^3}{2A} \\
& = - \frac{(A - \alpha)(6A^2 - 3A^2 - A^2 + 2A\alpha - \alpha^2)}{6A} \\
& = - \frac{(A - \alpha)(2A^2 + 2A\alpha - \alpha^2)}{6A}. \tag{R.30}
\end{aligned}$$

This is the correlation of the samples of the triangle wave.

Substituting  $\alpha = A(1 - \text{trw}(\tau/T))$ , in accord with Eq. (R.2), the autocorrelation function is obtained in the form

$$R(\tau) = \frac{A^2}{3} \left( \frac{\text{trw}(\tau/T)(3 - \text{trw}^2(\tau/T))}{2} \right). \tag{R.31}$$

The autocorrelation function is illustrated in Fig. R.8. The shape is very close to a cosine. This is understandable if we consider the Fourier series of the triangle wave: it contains odd harmonics only, with amplitudes decreasing as  $1/n^2$ ,  $n$  being the harmonic number. The spectrum can be obtained as the absolute square of the Fourier amplitudes, so the Fourier coefficients of the autocorrelation function disappear as  $n^4$ .

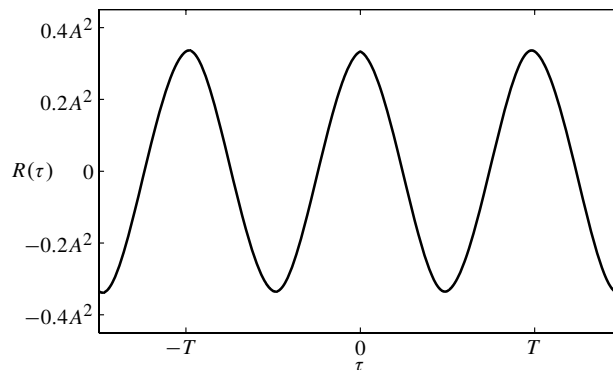


**Figure R.8** Autocorrelation function of the symmetrical triangle wave

For  $\tau = 0$  the equation  $\text{trw}(\tau/T) = 1$  holds, and Eq. (R.31) gives  $A^2/3$  which is indeed the variance of the uniform PDF.

## R.4 EXERCISES

**R.1** Derive (R.21) using variable transformation of (R.15) into a straight standing rectangle.



# **Characteristic Functions of Quantities Involved when Using Dither**

### S.1 CALCULATION OF THE JOINT CHARACTERISTIC FUNCTIONS OF $\zeta$ , $x$ AND $(x + d)'$

The CF of the total quantization noise  $\zeta$  is not easy to calculate because the dither and the input both can be stochastically related to  $v$ . Therefore, a special way is selected, following the thoughts of Wannamaker (1994). First the joint PDF of  $\zeta$ ,  $x$  and  $d$  will be determined, then, after three-dimensional Fourier transformation,  $u_x$  and  $u_d$  will be set to zero to obtain the PDF of  $\zeta$ , and variable transformations are performed to obtain the joint CF.

Making use of the fact that  $\zeta = (x + d)' - x = v + d$ , the joint PDF can be directly written as

$$\begin{aligned}
 f_{\zeta,x,d}(\zeta, x, d) &= f_{\zeta|x,d}(\zeta, x, d) \cdot f_{x,d}(x, d) \\
 &= \text{rect}\left(\frac{v}{q}\right) \cdot \sum_{m=-\infty}^{\infty} \delta((x + d)' + mq) \cdot f_x(x) f_d(d) \\
 &= \text{rect}\left(\frac{\zeta - d}{q}\right) \cdot \sum_{m=-\infty}^{\infty} \delta(x + \zeta + mq) \cdot f_x(x) f_d(d) \\
 &= t_1(\zeta, x, d) \cdot t_2(\zeta, x, d) \cdot t_3(\zeta, x, d). \tag{S.1}
 \end{aligned}$$

The three terms can be Fourier transformed individually:

$$T_1(u_\zeta, u_x, u_d) = \int_{-\infty}^{\infty} \int_{-\infty}^{\infty} \int_{-\infty}^{\infty} \text{rect}\left(\frac{\zeta - d}{q}\right) e^{j(\zeta u_\zeta + x u_x + d u_d)} d\zeta dx dd$$

$$\begin{aligned}
&= \int_{-\infty}^{\infty} \int_{-\infty}^{\infty} \int_{-\infty}^{\infty} \text{rect}\left(\frac{y}{q}\right) e^{j((y+d)u_{\xi}+xu_x+du_d)} dy dx dd \\
&= \text{sinc}\left(\frac{qu_{\xi}}{2}\right) \delta(u_x) \delta(u_d + u_{\xi}), \tag{S.2}
\end{aligned}$$

$$\begin{aligned}
T_2(u_{\xi}, u_x, u_d) &= \int_{-\infty}^{\infty} \int_{-\infty}^{\infty} \int_{-\infty}^{\infty} \sum_{m=-\infty}^{\infty} \delta(x + \xi + mq) e^{j(\xi u_{\xi} + xu_x + du_d)} d\xi dx dd \\
&= \int_{-\infty}^{\infty} \int_{-\infty}^{\infty} \int_{-\infty}^{\infty} \sum_{m=-\infty}^{\infty} \delta(z + mq) e^{j((z-x)u_{\xi} + xu_x + du_d)} dz dx dd \\
&= \sum_{l=-\infty}^{\infty} \delta(u_{\xi} + l\Psi) \delta(u_x - u_{\xi}) \delta(u_d) \\
&= \sum_{l=-\infty}^{\infty} \delta(u_{\xi} + l\Psi) \delta(u_x + l\Psi) \delta(u_d), \tag{S.3}
\end{aligned}$$

$$\begin{aligned}
T_3(u_{\xi}, u_x, u_d) &= \int_{-\infty}^{\infty} \int_{-\infty}^{\infty} \int_{-\infty}^{\infty} f_x(x) f_d(d) e^{j(\xi u_{\xi} + xu_x + du_d)} d\xi dx dd \\
&= \delta(u_{\xi}) \Phi_x(u_x) \Phi_d(u_d). \tag{S.4}
\end{aligned}$$

The joint CF is the three-dimensional convolution of the three quantities. The convolutions can be evaluated the easiest by making use of the convolutions with the Dirac delta functions.

$$\begin{aligned}
\Phi_{\xi,x,d}(u_{\xi}, u_x, u_d) &= T_1(u_{\xi}, u_x, u_d) \star T_2(u_{\xi}, u_x, u_d) \star T_3(u_{\xi}, u_x, u_d) \\
&= \text{sinc}\left(\frac{qu_{\xi}}{2}\right) \delta(u_x) \delta(u_d + u_{\xi}) \star \sum_{l=-\infty}^{\infty} \delta(u_{\xi} + l\Psi) \delta(u_x + l\Psi) \delta(u_d) \\
&\quad \star \delta(u_{\xi}) \Phi_x(u_x) \Phi_d(u_d) \\
&= \sum_{l=-\infty}^{\infty} \text{sinc}\left(\frac{q(u_{\xi} + l\Psi)}{2}\right) \delta(u_x + l\Psi) \delta(u_d + u_{\xi} + l\Psi) \\
&\quad \star \delta(u_{\xi}) \Phi_x(u_x) \Phi_d(u_d) \\
&= \sum_{l=-\infty}^{\infty} \text{sinc}\left(\frac{q(u_{\xi} + l\Psi)}{2}\right) \Phi_x(u_x + l\Psi) \Phi_d(u_d + u_{\xi} + l\Psi). \tag{S.5}
\end{aligned}$$

The one-dimensional CF of the quantization error can be obtained by setting  $u_x = 0$  and  $u_d = 0$  in Eq. (S.5):

$$\Phi_{\zeta}(u_{\zeta}) = \sum_{l=-\infty}^{\infty} \operatorname{sinc}\left(\frac{q(u_{\zeta} + l\Psi)}{2}\right) \Phi_x(l\Psi) \Phi_d(u_{\zeta} + l\Psi). \quad (\text{S.6})$$

The joint CF of  $\zeta$  and  $x$  is obtained by setting  $u_d = 0$  in Eq. (S.5):

$$\Phi_{\zeta,x}(u_{\zeta}, u_x) = \sum_{l=-\infty}^{\infty} \operatorname{sinc}\left(\frac{q(u_{\zeta} + l\Psi)}{2}\right) \Phi_x(u_x + l\Psi) \Phi_d(u_{\zeta} + l\Psi). \quad (\text{S.7})$$

The joint CF of  $\zeta$ ,  $x$  and  $(x+d)'$  is obtained now by using the relation  $(x+d)' = x + \zeta$ , applying similar argumentation as was applied for Eq. (3.36):

$$\begin{aligned} \Phi_{\zeta,x,(x+d)'}(u_{\zeta}, u_x, u_{(x+d)'}) &= \Phi_{\zeta,x}(u_{\zeta} + u_{(x+d)'}, u_x + u_{(x+d)'}) \\ &= \sum_{l=-\infty}^{\infty} \operatorname{sinc}\left(\frac{q(u_{\zeta} + u_{(x+d)'}) + l\Psi}{2}\right) \\ &\quad \times \Phi_x(u_x + u_{(x+d)'}) \Phi_d(u_{\zeta} + u_{(x+d)'}) . \end{aligned} \quad (\text{S.8})$$

## S.2 CALCULATION OF THE JOINT CHARACTERISTIC FUNCTIONS OF INPUT/OUTPUT QUANTITIES, DITHER, AND QUANTIZATION ERRORS

To determine the moments and joint moments between  $x$ ,  $d$ ,  $(x+d)$ ,  $v$ , and  $(x+d)'$ , we can make use of the ideas developed in Chapter 7 which are embodied in Eq. (7.82), page 161. In accord with it, we have

$$\begin{aligned} \Phi_{(x+d),v,(x+d)'}(u_{(x+d)}, u_v, u_{(x+d)'}) \\ = \sum_{l=-\infty}^{\infty} \Phi_{(x+d),n,(x+d+n)}(u_{(x+d)}, u_v, u_{(x+d)'}) + l\Psi . \end{aligned} \quad (\text{S.9})$$

This equation can be generalized to encompass all of the variables of dithered quantization, represented in Fig. 19.3b:

$$\begin{aligned} \Phi_{x,d,(x+d),v,(x+d)',\zeta}(u_x, u_d, u_{(x+d)}, u_v, u_{(x+d)'}, u_{\zeta}) \\ = \sum_{l=-\infty}^{\infty} \Phi_{x,d,(x+d),n,(x+d+n),(d+n)}(u_x, u_d, u_{(x+d)}, u_v, u_{(x+d)'}) + l\Psi, u_{\zeta} \end{aligned} \quad (\text{S.10})$$

To evaluate this, we need the joint PQN CF. This can be obtained from the simple CF  $\Phi_{x,d,n}(u_x, u_d, u_n) = \Phi_x(u_x) \Phi_d(u_d) \Phi_n(u_n)$ , by applying Eq. (3.36):

$$\begin{aligned} \Phi_{x,d,(x+d),n,(x+d+n),(d+n)}(u_x, u_d, u_{(x+d)}, u_n, u_{(x+d+n)}, u_{(d+n)}) \\ = \Phi_x(u_x + u_{x+d} + u_{x+d+n}) \Phi_d(u_d + u_{x+d} + u_{x+d+n} + u_{d+n}) \\ \times \Phi_n(u_n + u_{x+d+n} + u_{d+n}). \end{aligned} \quad (\text{S.11})$$

Substituting this into Eq. (S.10), we obtain

$$\begin{aligned}
& \Phi_{x,d,(x+d),v,(x+d)',\zeta}(u_x, u_d, u_{(x+d)}, u_v, u_{(x+d)', u_\zeta}) \\
&= \sum_{l=-\infty}^{\infty} \Phi_x(u_x + u_{x+d} + u_{(x+d)'} + l\Psi) \Phi_d(u_d + u_{x+d} + u_{(x+d)'} + l\Psi + u_\zeta) \\
&\quad \times \Phi_n(u_v + u_{(x+d)'} + l\Psi + u_\zeta) \\
&= \sum_{l=-\infty}^{\infty} \Phi_x(u_x + u_{x+d} + u_{(x+d)'} + l\Psi) \Phi_d(u_d + u_{x+d} + u_{(x+d)'} + l\Psi + u_\zeta) \\
&\quad \times \operatorname{sinc}\left(\frac{q(u_v + u_{(x+d)'} + l\Psi + u_\zeta)}{2}\right). \tag{S.12}
\end{aligned}$$

From this joint CF, several different CFs can be derived by setting the unwanted variables to zero (see Eq. (3.37)):

$$\begin{aligned}
& \Phi_{x,d,v}(u_x, u_d, u_v) \\
&= \sum_{l=-\infty}^{\infty} \Phi_x(u_x + l\Psi) \Phi_d(u_d + l\Psi) \Phi_n(u_v + l\Psi) \\
&= \sum_{l=-\infty}^{\infty} \Phi_x(u_x + l\Psi) \Phi_d(u_d + l\Psi) \operatorname{sinc}\left(\frac{q(u_v + l\Psi)}{2}\right). \tag{S.13}
\end{aligned}$$

The marginal PDF of this is

$$\begin{aligned}
\Phi_{x,v}(u_x, u_v) &= \sum_{l=-\infty}^{\infty} \Phi_x(u_x + l\Psi) \Phi_d(l\Psi) \Phi_n(u_v + l\Psi) \\
&= \sum_{l=-\infty}^{\infty} \Phi_x(u_x + l\Psi) \Phi_d(l\Psi) \operatorname{sinc}\left(\frac{q(u_v + l\Psi)}{2}\right). \tag{S.14}
\end{aligned}$$

The variable  $v$  can be changed to  $\zeta$  with a simple transformation:

$$\Phi_{x,d,\zeta}(u_x, u_d, u_\zeta) = \sum_{l=-\infty}^{\infty} \Phi_x(u_x + l\Psi) \Phi_d(u_d + u_\zeta + l\Psi) \operatorname{sinc}\left(\frac{q(u_\zeta + l\Psi)}{2}\right). \tag{S.15}$$

The joint CF of  $x$  and  $\zeta$  is

$$\begin{aligned}
\Phi_{x,\zeta}(u_x, u_\zeta) &= \sum_{l=-\infty}^{\infty} \Phi_x(u_x + l\Psi) \Phi_d(u_\zeta + l\Psi) \Phi_n(u_\zeta + l\Psi) \\
&= \sum_{l=-\infty}^{\infty} \Phi_x(u_x + l\Psi) \Phi_d(u_\zeta + l\Psi) \operatorname{sinc}\left(\frac{q(u_\zeta + l\Psi)}{2}\right). \tag{S.16}
\end{aligned}$$

The joint CF of  $x$  and  $d$  is from (S.15)

$$\begin{aligned}\Phi_{d,\xi}(u_d, u_\xi) &= \sum_{l=-\infty}^{\infty} \Phi_x(l\Psi) \Phi_d(u_d + u_\xi + l\Psi) \Phi_n(u_\xi + l\Psi) \\ &= \sum_{l=-\infty}^{\infty} \Phi_x(l\Psi) \Phi_d(u_d + u_\xi + l\Psi) \operatorname{sinc}\left(\frac{q(u_\xi + l\Psi)}{2}\right).\end{aligned}\quad (\text{S.17})$$

The CF of  $\xi$  is

$$\begin{aligned}\Phi_\xi(u_\xi) &= \sum_{l=-\infty}^{\infty} \Phi_x(l\Psi) \Phi_d(u_\xi + l\Psi) \Phi_n(u_\xi + l\Psi) \\ &= \sum_{l=-\infty}^{\infty} \Phi_x(l\Psi) \Phi_d(u_\xi + l\Psi) \operatorname{sinc}\left(\frac{q(u_\xi + l\Psi)}{2}\right) \\ &= \Phi_d(u_\xi) \operatorname{sinc}\left(\frac{qu_\xi}{2}\right) \\ &\quad + \sum_{\substack{l=-\infty \\ l \neq 0}}^{\infty} \Phi_x(l\Psi) \Phi_d(u_\xi + l\Psi) \operatorname{sinc}\left(\frac{q(u_\xi + l\Psi)}{2}\right).\end{aligned}\quad (\text{S.18})$$

The study of the interrelation of  $x$  and the quantization errors  $v$  or  $\xi$  can be based on the so-called *conditional CFs* of the quantization noise:

$$\begin{aligned}\Phi_{v|x}(u_v) &= \sum_{l=-\infty}^{\infty} \Phi_d(l\Psi) e^{jl\Psi x} \operatorname{sinc}\left(\frac{q(u_v + l\Psi)}{2}\right) \\ &= \operatorname{sinc}\left(\frac{qu_v}{2}\right) \\ &\quad + \sum_{\substack{l=-\infty \\ l \neq 0}}^{\infty} \Phi_d(l\Psi) e^{jl\Psi x} \operatorname{sinc}\left(\frac{q(u_v + l\Psi)}{2}\right).\end{aligned}\quad (\text{S.19})$$

This function can be derived in the same way as (5.10), taking into account that a fixed value of  $x$  acts just as a constant value that changes the mean of the dither signal.

It can be seen that, since

$$\mathbb{E}_x \left\{ e^{ju_x} \right\} = \Phi_x(u), \quad (\text{S.20})$$

$$\begin{aligned}\mathbb{E}_x \{ \Phi_{v|x}(u_v) \} &= \int_{-\infty}^{\infty} \Phi_{v|x}(u_v) f_x(x) dx \\ &= \Phi_v(u_v),\end{aligned}\quad (\text{S.21})$$

which is the same as (5.10).

Similarly, the conditional CF of  $\zeta$  is:

$$\begin{aligned}\Phi_{\zeta|x}(u_\zeta) &= \sum_{l=-\infty}^{\infty} \Phi_d(u_\zeta + l\Psi) e^{jl\Psi x} \operatorname{sinc}\left(\frac{q(u_\zeta + l\Psi)}{2}\right) \\ &= \Phi_d(u_\zeta) \operatorname{sinc}\left(\frac{qu_\zeta}{2}\right) \\ &\quad + \sum_{\substack{l=-\infty \\ l \neq 0}}^{\infty} \Phi_d(u_\zeta + l\Psi) e^{jl\Psi x} \operatorname{sinc}\left(\frac{q(u_\zeta + l\Psi)}{2}\right).\end{aligned}\quad (\text{S.22})$$

It can be seen that

$$\begin{aligned}\mathbb{E}_x\{\Phi_{\zeta|x}(u_\zeta)\} &= \int_{-\infty}^{\infty} \Phi_{\zeta|x}(u_\zeta) f_x(x) dx \\ &= \Phi_d(u_\zeta) \operatorname{sinc}\left(\frac{qu_\zeta}{2}\right) \\ &\quad + \sum_{\substack{l=-\infty \\ l \neq 0}}^{\infty} \Phi_d(u_\zeta + l\Psi) \Phi_x(l\Psi) \operatorname{sinc}\left(\frac{q(u_\zeta + l\Psi)}{2}\right),\end{aligned}\quad (\text{S.23})$$

which is the same as (S.18), that is,  $\Phi_\zeta(u_\zeta)$ .

We can also express the conditional two-dimensional CF of the quantization noises as follows:

$$\begin{aligned}\Phi_{v_1 v_2|x_1, x_2}(u_1, u_2) &= \sum_{l_1=-\infty}^{\infty} \sum_{l_2=-\infty}^{\infty} \Phi_{d_1, d_2}(l_1\Psi_1, l_2\Psi_2) e^{jl_1\Psi_1 x_1} e^{jl_2\Psi_2 x_2} \\ &\quad \times \operatorname{sinc}\left(\frac{q_1(u_1 + l_1\Psi_1)}{2}\right) \operatorname{sinc}\left(\frac{q_2(u_2 + l_2\Psi_2)}{2}\right).\end{aligned}\quad (\text{S.24})$$

Similarly, the conditional two-dimensional CF for non-subtractive dither is

$$\begin{aligned}\Phi_{\xi_1 \xi_2|x_1, x_2}(u_1, u_2) &= \sum_{l_1=-\infty}^{\infty} \sum_{l_2=-\infty}^{\infty} \Phi_{d_1, d_2}(u_1 + l_1\Psi_1, u_2 + l_2\Psi_2) e^{jl_1\Psi_1 x_1} e^{jl_2\Psi_2 x_2} \\ &\quad \times \operatorname{sinc}\left(\frac{q_1(u_1 + l_1\Psi_1)}{2}\right) \operatorname{sinc}\left(\frac{q_2(u_2 + l_2\Psi_2)}{2}\right).\end{aligned}\quad (\text{S.25})$$

### S.3 A GENERAL THEOREM CONCERNING SUBRACTIVE DITHER

The interdependence of  $\nu$  and  $d$  can be investigated by studying the derivatives of Eq. (S.13). The following general theorem can be formulated:

#### General Quantizing Theorem for Subtractive Dither (GQTSD)

*If in dithered quantization*

$$\left. \frac{d^m \Phi_d(u_d)}{du_d^m} \right|_{u_d=l\Psi} = 0 \quad (\text{S.26})$$

*for  $m$  being a nonnegative integer, and  $l = \pm 1, \pm 2, \dots$ , then*

$$E\{x^{t_x} d^m \nu^{t_\nu}\} = E\{x^{t_x} d^m n^{t_\nu}\}$$

*for  $t_x = 0, 1, \dots$ , and  $t_\nu = 0, 1, \dots$*

QTSD (page 508) is a special case of this, with  $m = 0$ .

If (S.26) is fulfilled for  $m = 0, 1, \dots, r$ , we say that the dither is  $r$ th-order.





## Addendum T

---

---

# ***Fluctuations about the Mean, and Their Moments — The Kind Corrections***

Sheppard's corrections allow us to compute the moments of  $x$  from the moments of  $x'$ , based on the PQN model. When  $\mu$ , the mean of  $x$ , is large, the moments of  $x'$  and  $x$  become large and Sheppard's corrections also become large. When the PQN model does not perfectly apply, the residual errors of Sheppard's corrections also become large and the accuracy of the PQN approximation becomes unclear. This will be illustrated in the following section.

### **T.1 NUMERICAL EVALUATION OF THE RESIDUAL ERRORS OF SHEPPARD'S CORRECTIONS FOR A GAUSSIAN INPUT**

When the input  $x$  is Gaussian but  $\mu$  is not zero, relations (B.9), (B.11), (B.15), and (B.18) can be used to calculate the relative corrections for Sheppard's corrections. This has been done, and the results are plotted in Figs. T.1(a)–(b), and Figs. T.2(a)–(b).

The relative corrections for Sheppard's second and fourth corrections are negligible for  $q = \sigma$ . This would also be the case for even smaller  $q$ . The plots are drawn for ratios of  $\mu/q$  having values of 10 or less. This ratio could be made much larger, with the relative corrections still remaining negligible. The situation is not as nice when  $q = 2\sigma$ . Now the relative corrections are significant, especially when  $\mu$  becomes large. With  $\mu/\sigma$  less than 10, the relative error in Sheppard's second correction could be as large as 50%, and the relative error in Sheppard's fourth correction could be as large as 17%. Sheppard's corrections are still usable for such cases, although they would not be highly accurate. With  $\mu$  not equal to zero, there will be a nonzero correction to the Sheppard's first correction (which itself is zero).

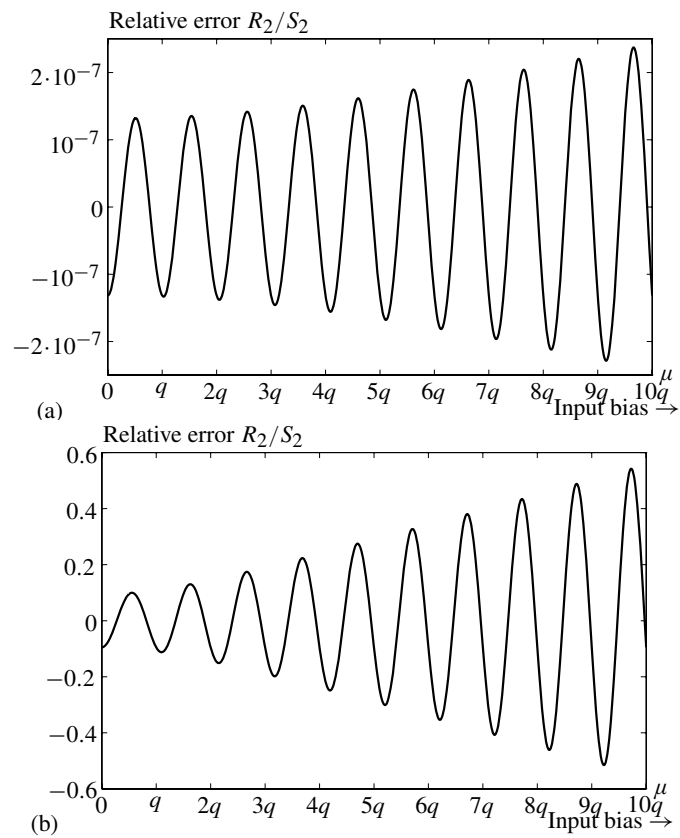


**Figure T.1** Relative error in Sheppard's second correction for Gaussian input signal with nonzero mean: (a)  $q = \sigma$ ; (b)  $q = 2\sigma$ .

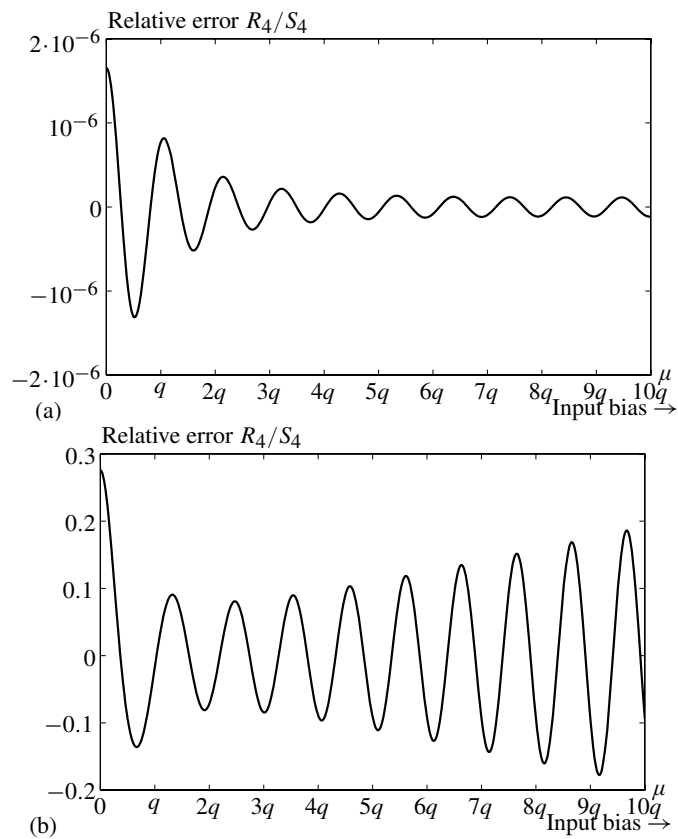


**Figure T.2** Relative error in Sheppard's fourth correction for Gaussian input signal with nonzero mean: (a)  $q = \sigma$ ; (b)  $q = 2\sigma$ .

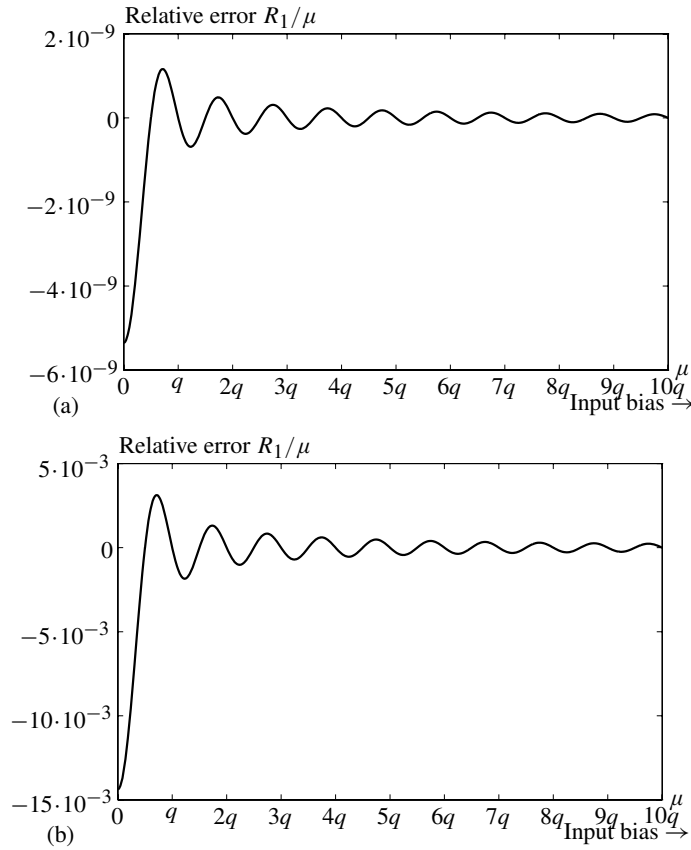


**Figure T.3** Relative error in Sheppard's first correction for Gaussian input signal with nonzero mean: (a)  $q = \sigma$ ; (b)  $q = 2\sigma$ .

The relative correction would be infinite and meaningless. One could consider the correction itself, given by Eq. (B.9). We have chosen to normalize this with respect to  $\mu$ , and plots are given in Figs. T.3(a)–(b). The corrections for Sheppard's first correction are small even when  $q = 2\sigma$ . This is not the case for Sheppard's third correction. Plots are given in Figs. T.4(a)–(b), derived from Eqs. (B.15). The relative errors of Sheppard's third correction are negligible for  $q = \sigma$ , but become significant for  $q = 2\sigma$ . However, Sheppard's third correction is still useful although it is not highly accurate when  $q = 2\sigma$  with  $\mu/q$  less than 10.

When  $\mu$  is large, it may be preferable to make use of an alternative to Sheppard's classic corrections by relating the centralized moments of  $x$  and  $x'$ , that is, the moments of  $\tilde{x}$  and  $\tilde{x}'$  to each other.

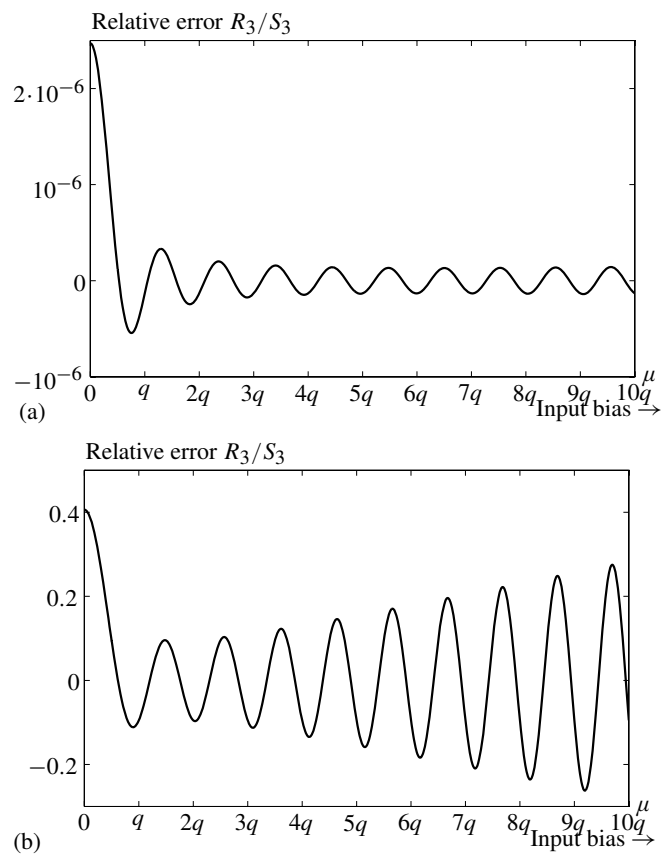


**Figure T.4** Relative error in Sheppard's third correction for Gaussian input signal with nonzero mean: (a)  $q = \sigma$ ; (b)  $q = 2\sigma$ .

## T.2 KIND CORRECTIONS FOR ONE VARIABLE

In Chapter 3, we have defined the fluctuation of quantizer input  $x$  about its mean  $\mu$  as

$$\tilde{x} = x - \mu. \quad (3.13)$$

We now define the fluctuation of the quantizer output  $x'$  about its mean as

$$\tilde{x}' = x' - E\{x'\} = x' - \mu'. \quad (T.1)$$

Since  $x' = x + v$ , it is clear that  $\mu' = \mu + E\{v\} = \mu + \mu_v$ , and

$$\tilde{x}' = \tilde{x} + \mu + v - \mu' = \tilde{x} + (v - \mu_v). \quad (T.2)$$

Our purpose is to obtain expressions of the moments of  $\tilde{x}$  in terms of the moments of  $\tilde{x}'$ . First we will obtain the moments of  $\tilde{x}'$ .

When the PQN model is applicable, i.e., when conditions for QT I, QT II, or QT III with  $r = 0, 1, \dots, \infty$  are satisfied, the quantization noise is uniformly distributed and its joint moments with  $x$  are as if  $v$  was independent of  $x$ . Recognizing that  $\mu = \mu'$  is also true, we can determine the following relationships, similarly to Eqs. (4.22-4.26),

$$\begin{aligned} E\{\tilde{x}'\} &= 0, \\ E\{(\tilde{x}')^2\} &= E\{(\tilde{x} + n)^2\} \\ &= E\{\tilde{x}^2 + 2\tilde{x}n + n^2\} \\ &= E\{\tilde{x}^2\} + q^2/12, \\ E\{(\tilde{x}')^3\} &= E\{(\tilde{x} + n)^3\} \\ &= E\{\tilde{x}^3 + 3\tilde{x}^2n + 3\tilde{x}n^2 + n^3\}, \\ E\{(\tilde{x}')^4\} &= E\{(\tilde{x} + n)^4\} \\ &= E\{\tilde{x}^4 + 4\tilde{x}^3n + 6\tilde{x}^2n^2 + 4\tilde{x}n^3 + n^4\} \\ &= E\{\tilde{x}^4\} + \frac{q^2}{2}E\{\tilde{x}^2\} + \frac{q^4}{80}, \\ E\{(\tilde{x}')^5\} &= E\{(\tilde{x} + n)^5\} \\ &= E\{\tilde{x}^5 + 5\tilde{x}^4n + 10\tilde{x}^3n^2 + 10\tilde{x}^2n^3 + 5\tilde{x}n^4 + n^5\} \\ &= E\{\tilde{x}^5\} + \frac{5}{6}q^2E\{\tilde{x}^3\}, \\ &\vdots \end{aligned} \quad (T.3)$$

The above expressions have the common form

$$E\{(\tilde{x}')^r\} = E\{\tilde{x}^r\} + \tilde{M}_r, \quad (T.4)$$

where  $\tilde{M}_r$  is the *centralized moment difference*. It depends on  $q$ , and the lower moments of  $\tilde{x}$  for  $r = 1, 2, \dots, r - 2$ .

$$\begin{aligned}
 \tilde{M}_1 &= 0 \\
 \tilde{M}_2 &= \frac{q^2}{12} \\
 \tilde{M}_3 &= 0 \\
 \tilde{M}_4 &= \frac{1}{2}q^2E\{x^2\} + \frac{1}{80}q^4 \\
 \tilde{M}_5 &= \frac{5}{6}E\{x^3\}q^2 \\
 &\vdots
 \end{aligned} \tag{T.5}$$

Equations (T.3) may be rearranged to yield the following results (see also Eq. (4.30):

$$\begin{aligned}
 E\{\tilde{x}\} &= E\{\tilde{x}'\} = 0, \\
 E\{\tilde{x}^2\} &= E\{(\tilde{x}')^2\} - \left(\frac{q^2}{12}\right), \\
 E\{\tilde{x}^3\} &= E\{(\tilde{x}')^3\} - (0), \\
 E\{\tilde{x}^4\} &= E\{(\tilde{x}')^4\} - \left(\frac{q^2}{2}E\{(\tilde{x}')^2\} - \frac{7q^4}{240}\right), \\
 E\{\tilde{x}^5\} &= E\{(\tilde{x}')^5\} - \left(\frac{5q^2}{6}E\{(\tilde{x}')^3\}\right), \\
 &\vdots
 \end{aligned} \tag{T.6}$$

The corrections shown in the parentheses of Eq. (T.6) are somewhat simpler than Sheppard's corrections.

$$\begin{aligned}
 \tilde{S}_1 &= 0 \\
 \tilde{S}_2 &= \frac{q^2}{12} \\
 \tilde{S}_3 &= 0 \\
 \tilde{S}_4 &= \frac{1}{2}q^2E\{(\tilde{x}')^2\} - \frac{7}{240}q^4 \\
 \tilde{S}_5 &= \frac{5}{6}E\{(\tilde{x}')^3\}q^2 \\
 &\vdots
 \end{aligned} \tag{T.7}$$

Corrections  $\tilde{S}_1 \dots \tilde{S}_5$  were given in Sheppard's original paper. We call them the "Kind" corrections<sup>1</sup>. They are unaffected by the value of  $\mu$ , since they deal only with moments of fluctuations about  $\mu$ . Sheppard's corrections are strongly affected by the value of  $\mu$ . The advantages of the Kind corrections will become apparent when we study the moments of  $x$  and  $x'$ , and  $\tilde{x}$  and  $\tilde{x}'$  for specific input PDFs such as the Gaussian.

### T.2.1 General Expressions for the Centralized Moments of the Quantizer Output, and for the Errors of the Kind Corrections

When the PQN model does not apply perfectly, we will need expressions of the residual errors of the Kind corrections. In order to derive these, the CF of  $\tilde{x}'$  will be used.

The CF of  $x'$  was obtained in (4.11) as

$$\Phi_{x'}(u) = \sum_{l=-\infty}^{\infty} \Phi_x(u + l\Psi) \operatorname{sinc}\left(\frac{q(u + l\Psi)}{2}\right). \quad (4.11)$$

Substituting  $\Phi_x(u) = e^{ju\mu} \Phi_{\tilde{x}}(u)$ , we can write

$$\begin{aligned} \Phi_{\tilde{x}'}(u) &= e^{-ju\mu'} \Phi_{\tilde{x}'}(u) \\ &= e^{-ju\mu'} \sum_{l=-\infty}^{\infty} e^{j(u+l\Psi)\mu} \Phi_{\tilde{x}}(u + l\Psi) \operatorname{sinc}\left(\frac{q(u + l\Psi)}{2}\right) \\ &= e^{-ju\mu'} \sum_{l=-\infty}^{\infty} e^{jl\Psi\mu} \Phi_{\tilde{x}}(u + l\Psi) \operatorname{sinc}\left(\frac{q(u + l\Psi)}{2}\right). \end{aligned} \quad (T.8)$$

This expression is quite similar to the one that can be derived from (4.11) for the CF of  $x'$ :

$$\begin{aligned} \Phi_{x'}(u) &= \sum_{l=-\infty}^{\infty} \Phi_x(u + l\Psi) \operatorname{sinc}\left(\frac{q(u + l\Psi)}{2}\right) \\ &= \sum_{l=-\infty}^{\infty} e^{j(u+l\Psi)\mu} \Phi_{\tilde{x}}(u + l\Psi) \operatorname{sinc}\left(\frac{q(u + l\Psi)}{2}\right) \\ &= e^{ju\mu} \sum_{l=-\infty}^{\infty} e^{jl\Psi\mu} \Phi_{\tilde{x}}(u + l\Psi) \operatorname{sinc}\left(\frac{q(u + l\Psi)}{2}\right). \end{aligned} \quad (T.9)$$

<sup>1</sup>If there were only two kinds of people in the world, mean and kind, removing the mean leaves us with the kind. And so it goes with corrections.



Therefore, the derivation of the general expressions of the residual errors of the Kind corrections may follow the same pattern as those of Sheppard's corrections, examined in Section B.

### T.2.2 General Expressions for the Centralized Moments of the Quantizer Output

For each moment, we will determine the expressions of the moments of the quantized variables in the form of

$$E\{(\tilde{x}')^r\} = E\{\tilde{x}^r\} + \tilde{M}_r + \tilde{N}_r, \quad (\text{T.10})$$

where  $\tilde{M}_r$  denotes the terms that depend on moments of  $\tilde{x}$  (see Eq. (T.4)), and do not generally vanish when QT II is satisfied, and  $\tilde{N}_r$  denotes the deviation from the ideal case when QT II is not satisfied.

We will repeatedly use the general expression of the mean of the quantization noise, calculated from Eq. (B.3):

$$\begin{aligned} \mu_v = E\{v\} = E\{x' - x\} &= \frac{q}{\pi} \sum_{l=1}^{\infty} \text{Im}\{\Phi_x(l\Psi)\} \frac{(-1)^l}{l} \\ &= \frac{q}{\pi} \sum_{l=1}^{\infty} \text{Im}\{e^{jl\Psi\mu} \Phi_{\tilde{x}}(l\Psi)\} \frac{(-1)^l}{l}. \end{aligned} \quad (\text{T.11})$$

The first moment of  $\tilde{x}'$  is

$$E\{\tilde{x}'\} = E\{\tilde{x}\} + E\{v - \mu_v\} = 0. \quad (\text{T.12})$$

The residue of the expression is also zero:  $\tilde{N}_1 = 0$ .

The second moment of  $\tilde{x}'$  is as follows:

$$\begin{aligned} E\{(\tilde{x}')^2\} &= \frac{1}{j^2} \left. \frac{d^2 \Phi_{\tilde{x}'}(u)}{du^2} \right|_{u=0} \\ &= - \left[ \frac{d^2}{du^2} e^{-ju\mu_v} \sum_{l=-\infty}^{\infty} e^{jl\Psi\mu} \Phi_{\tilde{x}}(u + l\Psi) \text{sinc}\left(\frac{q(u + l\Psi)}{2}\right) \right]_{u=0} \\ &= \mu_v^2 \sum_{l=-\infty}^{\infty} e^{jl\Psi\mu} \Phi_{\tilde{x}}(l\Psi) \text{sinc}(l\pi) \\ &\quad - \sum_{l=-\infty}^{\infty} e^{jl\Psi\mu} \ddot{\Phi}_{\tilde{x}}(l\Psi) \text{sinc}(l\pi) \end{aligned}$$

$$\begin{aligned}
& - \sum_{l=-\infty}^{\infty} e^{jl\Psi\mu} \Phi_{\tilde{x}}(l\Psi) \frac{d^2 \operatorname{sinc}(\frac{qu}{2} + l\pi)}{du^2} \Big|_{u=0} \\
& + 2j\mu_v \sum_{l=-\infty}^{\infty} e^{jl\Psi\mu} \dot{\Phi}_{\tilde{x}}(l\Psi) \operatorname{sinc}(l\pi) \\
& + 2j\mu_v \sum_{l=-\infty}^{\infty} e^{jl\Psi\mu} \Phi_{\tilde{x}}(l\Psi) \frac{d \operatorname{sinc}(\frac{qu}{2} + l\pi)}{du} \Big|_{u=0} \\
& - 2 \sum_{l=-\infty}^{\infty} e^{jl\Psi\mu} \dot{\Phi}_{\tilde{x}}(l\Psi) \frac{d \operatorname{sinc}(\frac{qu}{2} + l\pi)}{du} \Big|_{u=0} \\
= & \mu_v^2 \\
& + E\{\tilde{x}^2\} \\
& + \frac{q^2}{12} - \sum_{\substack{l=-\infty \\ l \neq 0}}^{\infty} e^{jl\Psi\mu} \Phi_{\tilde{x}}(l\Psi) \frac{q^2}{2\pi^2} \frac{(-1)^{l+1}}{l^2} \\
& + 2j\mu_v \cdot 0 \\
& - 2\mu_v \sum_{\substack{l=-\infty \\ l \neq 0}}^{\infty} \frac{e^{jl\Psi\mu}}{j} \Phi_{\tilde{x}}(l\Psi) \frac{q}{2} \frac{(-1)^l}{l\pi} \\
& - 2 \sum_{\substack{l=-\infty \\ l \neq 0}}^{\infty} e^{jl\Psi\mu} \dot{\Phi}_{\tilde{x}}(l\Psi) \frac{q}{2} \frac{(-1)^l}{l\pi} \\
= & E\{\tilde{x}^2\} + \frac{q^2}{12} \\
& + \mu_v^2 \\
& - \frac{q^2}{\pi^2} \sum_{l=1}^{\infty} \operatorname{Re}\{e^{jl\Psi\mu} \Phi_{\tilde{x}}(l\Psi)\} \frac{(-1)^{l+1}}{l^2} \\
& + 2\mu_v\mu_v \\
& - 2\frac{q}{\pi} \sum_{l=1}^{\infty} \operatorname{Re}\{e^{jl\Psi\mu} \dot{\Phi}_{\tilde{x}}(l\Psi)\} \frac{(-1)^l}{l} \\
= & E\{\tilde{x}^2\} + \frac{q^2}{12} \\
& + \left( -\frac{q^2}{\pi^2} \sum_{l=1}^{\infty} \operatorname{Re}\{e^{jl\Psi\mu} \Phi_{\tilde{x}}(l\Psi)\} \frac{(-1)^{l+1}}{l^2} \right. \\
& \left. - \mu_v^2 \right)
\end{aligned}$$

$$\begin{aligned}
& -2\frac{q}{\pi} \sum_{l=1}^{\infty} \operatorname{Re}\{e^{jl\Psi\mu} \dot{\Phi}_{\tilde{x}}(l\Psi)\} \frac{(-1)^l}{l} \\
& = E\{\tilde{x}^2\} + \tilde{M}_2 + \tilde{N}_2,
\end{aligned} \tag{T.13}$$

with  $\tilde{N}_2$  defined by the preceding line of (T.13).

The third moment of  $\tilde{x}'$  is as follows.

$$\begin{aligned}
E\{(\tilde{x}')^3\} &= \frac{1}{j^3} \frac{d^3}{du^3} \left[ e^{-ju\mu_v} \sum_{l=-\infty}^{\infty} e^{jl\Psi\mu} \Phi_{\tilde{x}}(u+l\Psi) \operatorname{sinc}\left(\frac{q(u+l\Psi)}{2}\right) \right]_{u=0} \\
&= -\mu_v^3 \sum_{l=-\infty}^{\infty} e^{jl\Psi\mu} \Phi_{\tilde{x}}(l\Psi) \operatorname{sinc}(l\pi) \\
&\quad + 3\frac{1}{j}\mu_v^2 \sum_{l=-\infty}^{\infty} e^{jl\Psi\mu} \dot{\Phi}_{\tilde{x}}(l\Psi) \operatorname{sinc}(l\pi) \\
&\quad + 3\frac{1}{j}\mu_v^2 \sum_{l=-\infty}^{\infty} e^{jl\Psi\mu} \Phi_{\tilde{x}}(l\Psi) \left. \frac{d \operatorname{sinc}\left(\frac{qu}{2} + l\pi\right)}{du} \right|_{u=0} \\
&\quad + 3\mu_v \sum_{l=-\infty}^{\infty} e^{jl\Psi\mu} \ddot{\Phi}_{\tilde{x}}(l\Psi) \operatorname{sinc}(l\pi) \\
&\quad + 6\mu_v \sum_{l=-\infty}^{\infty} e^{jl\Psi\mu} \dot{\Phi}_{\tilde{x}}(l\Psi) \left. \frac{d \operatorname{sinc}\left(\frac{qu}{2} + l\pi\right)}{du} \right|_{u=0} \\
&\quad + 3\mu_v \sum_{l=-\infty}^{\infty} e^{jl\Psi\mu} \Phi_{\tilde{x}}(l\Psi) \left. \frac{d^2 \operatorname{sinc}\left(\frac{qu}{2} + l\pi\right)}{du^2} \right|_{u=0} \\
&\quad - \frac{1}{j} \sum_{l=-\infty}^{\infty} e^{jl\Psi\mu} \ddot{\Phi}_{\tilde{x}}(l\Psi) \operatorname{sinc}(l\pi) \\
&\quad - 3\frac{1}{j} \sum_{l=-\infty}^{\infty} e^{jl\Psi\mu} \ddot{\Phi}_{\tilde{x}}(l\Psi) \left. \frac{d \operatorname{sinc}\left(\frac{qu}{2} + l\pi\right)}{du} \right|_{u=0} \\
&\quad - 3\frac{1}{j} \sum_{l=-\infty}^{\infty} e^{jl\Psi\mu} \dot{\Phi}_{\tilde{x}}(l\Psi) \left. \frac{d^2 \operatorname{sinc}\left(\frac{qu}{2} + l\pi\right)}{du^2} \right|_{u=0} \\
&\quad - \frac{1}{j} \sum_{l=-\infty}^{\infty} e^{jl\Psi\mu} \Phi_{\tilde{x}}(l\Psi) \left. \frac{d^3 \operatorname{sinc}\left(\frac{qu}{2} + l\pi\right)}{du^3} \right|_{u=0} \\
&= -\mu_v^3 \\
&\quad + 3\frac{1}{j}\mu_v^2 \cdot 0
\end{aligned}$$

$$\begin{aligned}
& + 3\mu_v^2\mu_v \\
& - 3\mu_v\mathbb{E}\{\tilde{x}^2\} \\
& + 6\mu_v \sum_{\substack{l=-\infty \\ l \neq 0}}^{\infty} e^{jl\Psi\mu} \dot{\Phi}_{\tilde{x}}(l\Psi) \frac{q}{2\pi} \frac{(-1)^l}{l} \\
& - 3\mu_v \frac{q^2}{12} + 3\mu_v \sum_{\substack{l=-\infty \\ l \neq 0}}^{\infty} e^{jl\Psi\mu} \Phi_{\tilde{x}}(l\Psi) \frac{q^2}{2\pi^2} \frac{(-1)^{l+1}}{l^2} \\
& + \mathbb{E}\{\tilde{x}^3\} \\
& - 3 \sum_{\substack{l=-\infty \\ l \neq 0}}^{\infty} \frac{e^{jl\Psi\mu}}{j} \ddot{\Phi}_{\tilde{x}}(l\Psi) \frac{q}{2\pi} \frac{(-1)^l}{l} \\
& - 3 \sum_{\substack{l=-\infty \\ l \neq 0}}^{\infty} \frac{e^{jl\Psi\mu}}{j} \dot{\Phi}_{\tilde{x}}(l\Psi) \frac{q^2}{2\pi^2} \frac{(-1)^{l+1}}{l^2} \\
& - \sum_{\substack{l=-\infty \\ l \neq 0}}^{\infty} \frac{e^{jl\Psi\mu}}{j} \Phi_{\tilde{x}}(l\Psi) \left(\frac{q}{2}\right)^3 \left(\frac{(-1)^{l+1}}{l\pi} + 6\frac{(-1)^l}{(l\pi)^3}\right) \\
= & \mathbb{E}\{\tilde{x}^3\} \\
& + \left( 2\mu_v^3 \right. \\
& \quad - 3\mu_v\mathbb{E}\{\tilde{x}^2\} \\
& \quad + 6\mu_v \frac{q}{\pi} \sum_{l=1}^{\infty} \operatorname{Re}\{e^{jl\Psi\mu} \dot{\Phi}_{\tilde{x}}(l\Psi)\} \frac{(-1)^l}{l} \\
& \quad - 3\mu_v \frac{q^2}{12} + 3\mu_v \frac{q^2}{\pi^2} \sum_{l=1}^{\infty} \operatorname{Re}\{e^{jl\Psi\mu} \Phi_{\tilde{x}}(l\Psi)\} \frac{(-1)^{l+1}}{l^2} \\
& \quad - 3\frac{q}{\pi} \sum_{l=1}^{\infty} \operatorname{Im}\{e^{jl\Psi\mu} \ddot{\Phi}_{\tilde{x}}(l\Psi)\} \frac{(-1)^l}{l} \\
& \quad - 3\frac{q^2}{\pi^2} \sum_{l=1}^{\infty} \operatorname{Im}\{e^{jl\Psi\mu} \dot{\Phi}_{\tilde{x}}(l\Psi)\} \frac{(-1)^{l+1}}{l^2} \\
& \quad \left. - \frac{q^3}{4} \sum_{l=1}^{\infty} \operatorname{Im}\{e^{jl\Psi\mu} \Phi_{\tilde{x}}(l\Psi)\} \left(\frac{(-1)^{l+1}}{l\pi} + 6\frac{(-1)^l}{(l\pi)^3}\right) \right) \\
= & \mathbb{E}\{\tilde{x}^3\} + \tilde{N}_3, \tag{T.14}
\end{aligned}$$

with  $\tilde{M}_3$  being 0 (see Eq. (T.5), and  $\tilde{N}_3$  defined by the preceding line of (T.14).  
The fourth moment is as follows.

$$\begin{aligned}
E\{(\tilde{x}')^4\} &= \frac{1}{j^4} \frac{d^4}{du^4} \left[ e^{-ju\mu_v} \sum_{l=-\infty}^{\infty} e^{jl\Psi\mu} \Phi_{\tilde{x}}(u+l\Psi) \operatorname{sinc}\left(\frac{q(u+l\Psi)}{2}\right) \right]_{u=0} \\
&= \mu_v^4 \sum_{l=-\infty}^{\infty} e^{jl\Psi\mu} \Phi_{\tilde{x}}(l\Psi) \operatorname{sinc}(l\pi) \\
&\quad - 4j^3 \mu_v^3 \sum_{l=-\infty}^{\infty} e^{jl\Psi\mu} \dot{\Phi}_{\tilde{x}}(l\Psi) \operatorname{sinc}(l\pi) \\
&\quad - 4j^3 \mu_v^3 \sum_{l=-\infty}^{\infty} e^{jl\Psi\mu} \Phi_{\tilde{x}}(l\Psi) \frac{d \operatorname{sinc}\left(\frac{qu}{2} + l\pi\right)}{du} \Big|_{u=0} \\
&\quad + 6j^2 \mu_v^2 \sum_{l=-\infty}^{\infty} e^{jl\Psi\mu} \ddot{\Phi}_{\tilde{x}}(l\Psi) \operatorname{sinc}(l\pi) \\
&\quad + 12j^2 \mu_v^2 \sum_{l=-\infty}^{\infty} e^{jl\Psi\mu} \dot{\Phi}_{\tilde{x}}(l\Psi) \frac{d \operatorname{sinc}\left(\frac{qu}{2} + l\pi\right)}{du} \Big|_{u=0} \\
&\quad + 6j^2 \mu_v^2 \sum_{l=-\infty}^{\infty} e^{jl\Psi\mu} \Phi_{\tilde{x}}(l\Psi) \frac{d^2 \operatorname{sinc}\left(\frac{qu}{2} + l\pi\right)}{du^2} \Big|_{u=0} \\
&\quad - 4j \mu_v \sum_{l=-\infty}^{\infty} e^{jl\Psi\mu} \ddot{\Phi}_{\tilde{x}}(l\Psi) \operatorname{sinc}(l\pi) \\
&\quad - 12j \mu_v \sum_{l=-\infty}^{\infty} e^{jl\Psi\mu} \ddot{\Phi}_{\tilde{x}}(l\Psi) \frac{d \operatorname{sinc}\left(\frac{qu}{2} + l\pi\right)}{du} \Big|_{u=0} \\
&\quad - 12j \mu_v \sum_{l=-\infty}^{\infty} e^{jl\Psi\mu} \dot{\Phi}_{\tilde{x}}(l\Psi) \frac{d^2 \operatorname{sinc}\left(\frac{qu}{2} + l\pi\right)}{du^2} \Big|_{u=0} \\
&\quad - 4j \mu_v \sum_{l=-\infty}^{\infty} e^{jl\Psi\mu} \Phi_{\tilde{x}}(l\Psi) \frac{d^3 \operatorname{sinc}\left(\frac{qu}{2} + l\pi\right)}{du^3} \Big|_{u=0} \\
&\quad + \sum_{l=-\infty}^{\infty} e^{jl\Psi\mu} \ddot{\Phi}_{\tilde{x}}(l\Psi) \operatorname{sinc}(l\pi) \\
&\quad + 4 \sum_{l=-\infty}^{\infty} e^{jl\Psi\mu} \ddot{\Phi}_{\tilde{x}}(l\Psi) \frac{d \operatorname{sinc}\left(\frac{qu}{2} + l\pi\right)}{du} \Big|_{u=0}
\end{aligned}$$

$$\begin{aligned}
& + 6 \sum_{l=-\infty}^{\infty} e^{jl\Psi\mu} \ddot{\Phi}_{\tilde{x}}(l\Psi) \frac{d^2 \operatorname{sinc}(\frac{qu}{2} + l\pi)}{du^2} \Big|_{u=0} \\
& + 4 \sum_{l=-\infty}^{\infty} e^{jl\Psi\mu} \dot{\Phi}_{\tilde{x}}(l\Psi) \frac{d^3 \operatorname{sinc}(\frac{qu}{2} + l\pi)}{du^3} \Big|_{u=0} \\
& + \sum_{l=-\infty}^{\infty} e^{jl\Psi\mu} \Phi_{\tilde{x}}(l\Psi) \frac{d^4 \operatorname{sinc}(\frac{qu}{2} + l\pi)}{du^4} \Big|_{u=0} \\
= & \mu_v^4 \\
& - 4j^3 \mu_v^3 \cdot 0 \\
& - 4\mu_v^3 \mu_v \\
& + 6\mu_v^2 E\{\tilde{x}^2\} \\
& - 12\mu_v^2 \sum_{\substack{l=-\infty \\ l \neq 0}}^{\infty} e^{jl\Psi\mu} \dot{\Phi}_{\tilde{x}}(l\Psi) \frac{q}{2\pi} \frac{(-1)^l}{l} \\
& + 6\mu_v^2 \frac{q^2}{12} - 6\mu_v^2 \sum_{\substack{l=-\infty \\ l \neq 0}}^{\infty} e^{jl\Psi\mu} \Phi_{\tilde{x}}(l\Psi) \frac{q^2}{2\pi^2} \frac{(-1)^{l+1}}{l^2} \\
& - 4\mu_v E\{\tilde{x}^3\} \\
& + 12\mu_v \sum_{\substack{l=-\infty \\ l \neq 0}}^{\infty} \frac{e^{jl\Psi\mu}}{j} \ddot{\Phi}_{\tilde{x}}(l\Psi) \frac{q}{2\pi} \frac{(-1)^l}{l} \\
& + 12\mu_v \sum_{\substack{l=-\infty \\ l \neq 0}}^{\infty} \frac{e^{jl\Psi\mu}}{j} \dot{\Phi}_{\tilde{x}}(l\Psi) \frac{q^2}{2\pi^2} \frac{(-1)^{l+1}}{l^2} \\
& + 4\mu_v \sum_{\substack{l=-\infty \\ l \neq 0}}^{\infty} \frac{e^{jl\Psi\mu}}{j} \Phi_{\tilde{x}}(l\Psi) \left(\frac{q}{2}\right)^3 \left(\frac{(-1)^{l+1}}{l\pi} + 6\frac{(-1)^l}{(l\pi)^3}\right) \\
& + E\{\tilde{x}^4\} \\
& + 4 \sum_{\substack{l=-\infty \\ l \neq 0}}^{\infty} e^{jl\Psi\mu} \ddot{\Phi}_{\tilde{x}}(l\Psi) \frac{q}{2\pi} \frac{(-1)^l}{l} \\
& + 6E\{\tilde{x}^2\} \frac{q^2}{12} + 6 \sum_{\substack{l=-\infty \\ l \neq 0}}^{\infty} e^{jl\Psi\mu} \ddot{\Phi}_{\tilde{x}}(l\Psi) \frac{q^2}{2\pi^2} \frac{(-1)^{l+1}}{l^2}
\end{aligned}$$

$$\begin{aligned}
& + 4 \sum_{\substack{l=-\infty \\ l \neq 0}}^{\infty} e^{jl\Psi\mu} \dot{\Phi}_{\tilde{x}}(l\Psi) \left(\frac{q}{2}\right)^3 \left(\frac{(-1)^{l+1}}{l\pi} + 6\frac{(-1)^l}{(l\pi)^3}\right) \\
& + \frac{q^4}{80} + \sum_{\substack{l=-\infty \\ l \neq 0}}^{\infty} e^{jl\Psi\mu} \Phi_{\tilde{x}}(l\Psi) \frac{q^4}{4} \left(\frac{(-1)^l}{(l\pi)^2} + 6\frac{(-1)^{l+1}}{(l\pi)^4}\right) \\
= & \text{E}\{\tilde{x}^4\} + 6\text{E}\{\tilde{x}^2\} \frac{q^2}{12} + \frac{q^4}{80} \\
& + \left( -3\mu_v^4 \right. \\
& \quad + 6\mu_v^2 \text{E}\{\tilde{x}^2\} \\
& \quad - 12\mu_v^2 \frac{q}{\pi} \sum_{l=1}^{\infty} \text{Re}\{e^{jl\Psi\mu} \dot{\Phi}_{\tilde{x}}(l\Psi)\} \frac{(-1)^l}{l} \\
& \quad + 6\mu_v^2 \frac{q^2}{12} - 6\mu_v^2 \frac{q^2}{\pi^2} \sum_{l=1}^{\infty} \text{Re}\{e^{jl\Psi\mu} \Phi_{\tilde{x}}(l\Psi)\} \frac{(-1)^{l+1}}{l^2} \\
& \quad - 4\mu_v \text{E}\{\tilde{x}^3\} \\
& \quad + 12\mu_v \frac{q}{\pi} \sum_{l=1}^{\infty} \text{Im}\{e^{jl\Psi\mu} \ddot{\Phi}_{\tilde{x}}(l\Psi)\} \frac{(-1)^l}{l} \\
& \quad + 12\mu_v \frac{q^2}{\pi^2} \sum_{l=1}^{\infty} \text{Im}\{e^{jl\Psi\mu} \dot{\Phi}_{\tilde{x}}(l\Psi)\} \frac{(-1)^{l+1}}{l^2} \\
& \quad + \mu_v q^3 \sum_{l=1}^{\infty} \text{Im}\{e^{jl\Psi\mu} \Phi_{\tilde{x}}(l\Psi)\} \left(\frac{(-1)^{l+1}}{l\pi} + 6\frac{(-1)^l}{(l\pi)^3}\right) \\
& \quad + 4\frac{q}{\pi} \sum_{l=1}^{\infty} \text{Re}\{e^{jl\Psi\mu} \ddot{\Phi}_{\tilde{x}}(l\Psi)\} \frac{(-1)^l}{l} \\
& \quad + 6\frac{q^2}{\pi^2} \sum_{l=1}^{\infty} \text{Re}\{e^{jl\Psi\mu} \ddot{\Phi}_{\tilde{x}}(l\Psi)\} \frac{(-1)^{l+1}}{l^2} \\
& \quad + q^3 \sum_{l=1}^{\infty} \text{Re}\{e^{jl\Psi\mu} \dot{\Phi}_{\tilde{x}}(l\Psi)\} \left(\frac{(-1)^{l+1}}{l\pi} + 6\frac{(-1)^l}{(l\pi)^3}\right) \\
& \quad \left. + \frac{q^4}{2} \sum_{l=1}^{\infty} \text{Re}\{e^{jl\Psi\mu} \dot{\Phi}_{\tilde{x}}(l\Psi)\} \left(\frac{(-1)^l}{(l\pi)^2} + 6\frac{(-1)^{l+1}}{(l\pi)^4}\right) \right) \\
= & \text{E}\{\tilde{x}^4\} + \tilde{M}_4 + \tilde{N}_4, \tag{T.15}
\end{aligned}$$

with  $\tilde{M}_4$  given by Eq. (T.5), and  $\tilde{N}_4$  defined by the preceding line of (T.15).

### T.2.3 General Expressions for the Errors of the Kind Corrections

When neither QT I nor QT II are satisfied, the Kind corrections may be applied only approximately. Our purpose here is to derive expressions for the errors in the Kind corrections. We will use the general expressions of the moments of  $\tilde{x}'$ , determined in the previous subsection, and rearrange them in order to obtain formulas that directly correspond to the Kind corrections:

$$E\{\tilde{x}^r\} = E\{(\tilde{x}')^r\} - \tilde{S}_r - \tilde{R}_r, \quad (\text{T.16})$$

where  $\tilde{S}_r$  is the  $r$ th Kind correction (see Eq. (T.7)), and  $\tilde{R}_r$  is the residual error that cannot be corrected for in general. Our aim will be then to provide reasonable upper bounds of  $\tilde{R}_r$ .

Note that  $\tilde{S}_r$  is expressed with moments of  $\tilde{x}'$ , while  $\tilde{M}_r$  is expressed with moments of  $\tilde{x}$ . When PQN applies,  $\tilde{S}_r = \tilde{M}_r$ , but otherwise they may be slightly different, so the errors in the Kind corrections,  $\tilde{R}_r$ , are not equal to  $\tilde{N}_r$ .

From Eq. (T.12) it is obvious that  $\tilde{R}_1 = 0$ .

The exact expression of the second moment of  $\tilde{x}$  can be expressed from Eq. (T.13) as

$$\begin{aligned} E\{\tilde{x}^2\} &= E\{(\tilde{x}')^2\} - \frac{q^2}{12} \\ &\quad - \left( -\frac{q^2}{\pi^2} \sum_{l=1}^{\infty} \text{Re}\{e^{jl\Psi\mu} \Phi_{\tilde{x}}(l\Psi)\} \frac{(-1)^{l+1}}{l^2} \right. \\ &\quad \quad \left. - \mu_v^2 \right. \\ &\quad \quad \left. - 2\frac{q}{\pi} \sum_{l=1}^{\infty} \text{Re}\{e^{jl\Psi\mu} \dot{\Phi}_{\tilde{x}}(l\Psi)\} \frac{(-1)^l}{l} \right) \\ &= E\{(\tilde{x}')^2\} - \tilde{S}_2 - \tilde{R}_2. \end{aligned} \quad (\text{T.17})$$

For PDFs symmetrical about their mean values,

$$\begin{aligned} \tilde{R}_2 &= -\frac{q^2}{\pi^2} \sum_{l=1}^{\infty} \Phi_{\tilde{x}}(l\Psi) \frac{(-1)^{l+1}}{l^2} \cos(l\Psi\mu) \\ &\quad - \left( \frac{q}{\pi} \sum_{l=1}^{\infty} \Phi_{\tilde{x}}(l\Psi) \frac{(-1)^l}{l} \sin(l\Psi\mu) \right)^2 \\ &\quad - 2\frac{q}{\pi} \sum_{l=1}^{\infty} \dot{\Phi}_{\tilde{x}}(l\Psi) \frac{(-1)^l}{l} \cos(l\Psi\mu). \end{aligned} \quad (\text{T.18})$$



The exact expression of the third moment of  $\tilde{x}$  can be expressed from Eq. (T.14), using the general expression of  $E\{\tilde{x}^2\}$  (Eq. (T.17)), as

$$\begin{aligned}
E\{\tilde{x}^3\} &= E\{(\tilde{x}')^3\} \\
&\quad - \left( 2\mu_v^3 \right. \\
&\quad - 3\mu_v E\{\tilde{x}^2\} \\
&\quad + 6\mu_v \frac{q}{\pi} \sum_{l=1}^{\infty} \operatorname{Re}\{e^{jl\Psi\mu} \dot{\Phi}_{\tilde{x}}(l\Psi)\} \frac{(-1)^l}{l} \\
&\quad - 3\mu_v \frac{q^2}{12} + 3\mu_v \frac{q^2}{\pi^2} \sum_{l=1}^{\infty} \operatorname{Re}\{e^{jl\Psi\mu} \Phi_{\tilde{x}}(l\Psi)\} \frac{(-1)^{l+1}}{l^2} \\
&\quad - 3 \frac{q}{\pi} \sum_{l=1}^{\infty} \operatorname{Im}\{e^{jl\Psi\mu} \ddot{\Phi}_{\tilde{x}}(l\Psi)\} \frac{(-1)^l}{l} \\
&\quad - 3 \frac{q^2}{\pi^2} \sum_{l=1}^{\infty} \operatorname{Im}\{e^{jl\Psi\mu} \dot{\Phi}_{\tilde{x}}(l\Psi)\} \frac{(-1)^{l+1}}{l^2} \\
&\quad \left. - \frac{q^3}{4} \sum_{l=1}^{\infty} \operatorname{Im}\{e^{jl\Psi\mu} \Phi_{\tilde{x}}(l\Psi)\} \left( \frac{(-1)^{l+1}}{l\pi} + 6 \frac{(-1)^l}{(l\pi)^3} \right) \right) \\
&= E\{(\tilde{x}')^3\} - \tilde{S}_3 - \tilde{R}_3. \tag{T.19}
\end{aligned}$$

It can be seen that  $\tilde{R}_3$  is equal to  $\tilde{N}_3$ .

For PDFs symmetrical about their mean values,

$$\begin{aligned}
\tilde{R}_3 &= 2 \left( \frac{q}{\pi} \sum_{l=1}^{\infty} \Phi_{\tilde{x}}(l\Psi) \frac{(-1)^l}{l} \sin(l\Psi\mu) \right)^3 \\
&\quad - 3 \left( \frac{q}{\pi} \sum_{l=1}^{\infty} \Phi_{\tilde{x}}(l\Psi) \frac{(-1)^l}{l} \sin(l\Psi\mu) \right) E\{(\tilde{x})^2\} \\
&\quad + 6 \left( \frac{q}{\pi} \sum_{l=1}^{\infty} \Phi_{\tilde{x}}(l\Psi) \frac{(-1)^l}{l} \sin(l\Psi\mu) \right) \frac{q}{\pi} \sum_{l=1}^{\infty} \dot{\Phi}_{\tilde{x}}(l\Psi) \frac{(-1)^l}{l} \cos(l\Psi\mu) \\
&\quad - 3 \left( \frac{q}{\pi} \sum_{l=1}^{\infty} \Phi_{\tilde{x}}(l\Psi) \frac{(-1)^l}{l} \sin(l\Psi\mu) \right) \frac{q^2}{12} \\
&\quad + 3 \left( \frac{q}{\pi} \sum_{l=1}^{\infty} \Phi_{\tilde{x}}(l\Psi) \frac{(-1)^l}{l} \sin(l\Psi\mu) \right) \frac{q^2}{\pi^2} \sum_{l=1}^{\infty} \Phi_{\tilde{x}}(l\Psi) \frac{(-1)^{l+1}}{l^2} \cos(l\Psi\mu)
\end{aligned}$$

$$\begin{aligned}
& - 3 \frac{q}{\pi} \sum_{l=1}^{\infty} \ddot{\Phi}_{\tilde{x}}(l\Psi) \frac{(-1)^l}{l} \sin(l\Psi\mu) \\
& - 3 \frac{q^2}{\pi^2} \sum_{l=1}^{\infty} \dot{\Phi}_{\tilde{x}}(l\Psi) \frac{(-1)^{l+1}}{l^2} \sin(l\Psi\mu) \\
& - \frac{q^3}{4} \sum_{l=1}^{\infty} \Phi_{\tilde{x}}(l\Psi) \left( \frac{(-1)^{l+1}}{l\pi} + 6 \frac{(-1)^l}{(l\pi)^3} \right) \sin(l\Psi\mu) . \tag{T.20}
\end{aligned}$$

The exact expression of the fourth moment of  $\tilde{x}$  can be expressed from Eq. (T.15) as

$$\begin{aligned}
\mathbb{E}\{\tilde{x}^4\} = & \mathbb{E}\{(\tilde{x}')^4\} - \left( 6\mathbb{E}\{\tilde{x}'^2\} \frac{q^2}{12} - \frac{7q^4}{240} \right) \\
& - \left( \frac{q^2}{2} \left( \frac{q^2}{\pi^2} \sum_{l=1}^{\infty} \operatorname{Re}\{e^{jl\Psi\mu} \Phi_{\tilde{x}}(l\Psi)\} \frac{(-1)^{l+1}}{l^2} \right. \right. \\
& \quad \left. \left. + \mu_v^2 \right. \right. \\
& \quad \left. \left. + 2 \frac{q}{\pi} \sum_{l=1}^{\infty} \operatorname{Re}\{e^{jl\Psi\mu} \dot{\Phi}_{\tilde{x}}(l\Psi)\} \frac{(-1)^l}{l} \right) \right) \\
& - 3\mu_v^4 \\
& + 6\mu_v^2 \mathbb{E}\{\tilde{x}^2\} \\
& - 12\mu_v^2 \frac{q}{\pi} \sum_{l=1}^{\infty} \operatorname{Re}\{e^{jl\Psi\mu} \dot{\Phi}_{\tilde{x}}(l\Psi)\} \frac{(-1)^l}{l} \\
& + 6\mu_v^2 \frac{q^2}{12} - 6\mu_v^2 \frac{q^2}{\pi^2} \sum_{l=1}^{\infty} \operatorname{Re}\{e^{jl\Psi\mu} \Phi_{\tilde{x}}(l\Psi)\} \frac{(-1)^{l+1}}{l^2} \\
& - 4\mu_v \mathbb{E}\{\tilde{x}^3\} \\
& + 12\mu_v \frac{q}{\pi} \sum_{l=1}^{\infty} \operatorname{Im}\{e^{jl\Psi\mu} \ddot{\Phi}_{\tilde{x}}(l\Psi)\} \frac{(-1)^l}{l} \\
& + 12\mu_v \frac{q^2}{\pi^2} \sum_{l=1}^{\infty} \operatorname{Im}\{e^{jl\Psi\mu} \dot{\Phi}_{\tilde{x}}(l\Psi)\} \frac{(-1)^{l+1}}{l^2} \\
& + \mu_v q^3 \sum_{l=1}^{\infty} \operatorname{Im}\{e^{jl\Psi\mu} \Phi_{\tilde{x}}(l\Psi)\} \left( \frac{(-1)^{l+1}}{l\pi} + 6 \frac{(-1)^l}{(l\pi)^3} \right) \\
& + 4 \frac{q}{\pi} \sum_{l=1}^{\infty} \operatorname{Re}\{e^{jl\Psi\mu} \ddot{\Phi}_{\tilde{x}}(l\Psi)\} \frac{(-1)^l}{l}
\end{aligned}$$

$$\begin{aligned}
& + 6 \frac{q^2}{\pi^2} \sum_{l=1}^{\infty} \operatorname{Re}\{e^{jl\Psi\mu} \ddot{\Phi}_{\tilde{x}}(l\Psi)\} \frac{(-1)^{l+1}}{l^2} \\
& + q^3 \sum_{l=1}^{\infty} \operatorname{Re}\{e^{jl\Psi\mu} \dot{\Phi}_{\tilde{x}}(l\Psi)\} \left( \frac{(-1)^{l+1}}{l\pi} + 6 \frac{(-1)^l}{(l\pi)^3} \right) \\
& + \frac{q^4}{2} \sum_{l=1}^{\infty} \operatorname{Re}\{e^{jl\Psi\mu} \Phi_{\tilde{x}}(l\Psi)\} \left( \frac{(-1)^l}{(l\pi)^2} + 6 \frac{(-1)^{l+1}}{(l\pi)^4} \right) \\
& = E\{(\tilde{x}')^4\} - \tilde{S}_4 - \tilde{R}_4.
\end{aligned} \tag{T.21}$$

It can be seen that  $\tilde{R}_4$  can be expressed by the  $\tilde{N}$ -terms as

$$\tilde{R}_4 = \tilde{N}_4 - \tilde{N}_2 \frac{q^2}{2}. \tag{T.22}$$

For PDFs symmetrical about their mean values,

$$\begin{aligned}
\tilde{R}_4 &= \frac{q^2}{2} \left( \frac{q^2}{\pi^2} \sum_{l=1}^{\infty} \Phi_{\tilde{x}}(l\Psi) \frac{(-1)^{l+1}}{l^2} \cos(l\Psi\mu) \right. \\
& \quad + \left. \left( \frac{q}{\pi} \sum_{l=1}^{\infty} \Phi_{\tilde{x}}(l\Psi) \frac{(-1)^l}{l} \sin(l\Psi\mu) \right)^2 \right. \\
& \quad + \left. 2 \frac{q}{\pi} \sum_{l=1}^{\infty} \dot{\Phi}_{\tilde{x}}(l\Psi) \frac{(-1)^l}{l} \cos(l\Psi\mu) \right) \\
& - 3 \left( \frac{q}{\pi} \sum_{l=1}^{\infty} \Phi_{\tilde{x}}(l\Psi) \frac{(-1)^l}{l} \sin(l\Psi\mu) \right)^4 \\
& + 6 \left( \frac{q}{\pi} \sum_{l=1}^{\infty} \Phi_{\tilde{x}}(l\Psi) \frac{(-1)^l}{l} \sin(l\Psi\mu) \right)^2 E\{\tilde{x}^2\} \\
& - 12 \left( \frac{q}{\pi} \sum_{l=1}^{\infty} \Phi_{\tilde{x}}(l\Psi) \frac{(-1)^l}{l} \sin(l\Psi\mu) \right)^2 \frac{q}{\pi} \sum_{l=1}^{\infty} \dot{\Phi}_{\tilde{x}}(l\Psi) \frac{(-1)^l}{l} \cos(l\Psi\mu) \\
& + 6 \left( \frac{q}{\pi} \sum_{l=1}^{\infty} \Phi_{\tilde{x}}(l\Psi) \frac{(-1)^l}{l} \sin(l\Psi\mu) \right)^2 \frac{q^2}{12} \\
& - 6 \left( \frac{q}{\pi} \sum_{l=1}^{\infty} \Phi_{\tilde{x}}(l\Psi) \frac{(-1)^l}{l} \sin(l\Psi\mu) \right)^2 \frac{q^2}{\pi^2} \sum_{l=1}^{\infty} \Phi_{\tilde{x}}(l\Psi) \frac{(-1)^{l+1}}{l^2} \cos(l\Psi\mu)
\end{aligned}$$

$$\begin{aligned}
& -4 \left( \frac{q}{\pi} \sum_{l=1}^{\infty} \Phi_{\tilde{x}}(l\Psi) \frac{(-1)^l}{l} \sin(l\Psi\mu) \right) E\{\tilde{x}^3\} \\
& + 12 \left( \frac{q}{\pi} \sum_{l=1}^{\infty} \Phi_{\tilde{x}}(l\Psi) \frac{(-1)^l}{l} \sin(l\Psi\mu) \right) \frac{q}{\pi} \sum_{l=1}^{\infty} \ddot{\Phi}_{\tilde{x}}(l\Psi) \frac{(-1)^l}{l} \sin(l\Psi\mu) \\
& + 12 \left( \frac{q}{\pi} \sum_{l=1}^{\infty} \Phi_{\tilde{x}}(l\Psi) \frac{(-1)^l}{l} \sin(l\Psi\mu) \right) \frac{q^2}{\pi^2} \sum_{l=1}^{\infty} \dot{\Phi}_{\tilde{x}}(l\Psi) \frac{(-1)^{l+1}}{l^2} \sin(l\Psi\mu) \\
& + \left( \frac{q}{\pi} \sum_{l=1}^{\infty} \Phi_{\tilde{x}}(l\Psi) \frac{(-1)^l}{l} \sin(l\Psi\mu) \right) \\
& \quad \times q^3 \sum_{l=1}^{\infty} \Phi_{\tilde{x}}(l\Psi) \left( \frac{(-1)^{l+1}}{l\pi} + 6 \frac{(-1)^l}{(l\pi)^3} \right) \sin(l\Psi\mu) \\
& + 4 \frac{q}{\pi} \sum_{l=1}^{\infty} \ddot{\Phi}_{\tilde{x}}(l\Psi) \frac{(-1)^l}{l} \cos(l\Psi\mu) \\
& + 6 \frac{q^2}{\pi^2} \sum_{l=1}^{\infty} \ddot{\Phi}_{\tilde{x}}(l\Psi) \frac{(-1)^{l+1}}{l^2} \cos(l\Psi\mu) \\
& + q^3 \sum_{l=1}^{\infty} \dot{\Phi}_{\tilde{x}}(l\Psi) \left( \frac{(-1)^{l+1}}{l\pi} + 6 \frac{(-1)^l}{(l\pi)^3} \right) \cos(l\Psi\mu) \\
& + \frac{q^4}{2} \sum_{l=1}^{\infty} \Phi_{\tilde{x}}(l\Psi) \left( \frac{(-1)^l}{(l\pi)^2} + 6 \frac{(-1)^{l+1}}{(l\pi)^4} \right) \cos(l\Psi\mu) . \tag{T.23}
\end{aligned}$$

### T.3 CENTRALIZED MOMENTS OF THE QUANTIZER OUTPUT FOR GAUSSIAN INPUT

When the quantizer input has a large mean value, the moments of the quantizer input and output become large, and Sheppard's corrections become large. The moments of the quantization noise itself do not become large, and are usually affected only slightly by the input mean.

The Kind corrections, like Sheppard's corrections, are based on PQN. The Kind corrections are given by (T.6). Unlike Sheppard's corrections, they are affected only in a limited way by the input mean  $\mu$ . The Kind corrections are easily calculated and, as we shall see, apply very well with Gaussian inputs even when  $q$  is as big as  $2\sigma$  or somewhat more. We will demonstrate this by finding the residual errors of the Kind corrections for the Gaussian case, using Eqs. (T.18), (T.20) and (T.23).

The residual errors are rather complicated. Significant simplifications can be achieved by noticing that the terms  $e^{-2\pi^2 l^2 \frac{\sigma^2}{q^2}}$  quickly disappear with increasing values of  $l$ , so that such terms with  $l \geq 2$  can be neglected beside the terms  $l = 1$ , furthermore the products of such terms are also negligible. By using these approximations, we can determine the approximate expressions of the residual errors of the first Kind corrections:

$$\tilde{R}_1 = 0. \quad (\text{T.24})$$

$$\begin{aligned} \tilde{R}_2 &= -\frac{q^2}{\pi^2} \sum_{l=1}^{\infty} e^{-2\pi^2 l^2 \frac{\sigma^2}{q^2}} \frac{(-1)^{l+1}}{l^2} \cos\left(2\pi l \frac{\mu}{q}\right) \\ &\quad - \left( \frac{q}{\pi} \sum_{l=1}^{\infty} e^{-2\pi^2 l^2 \frac{\sigma^2}{q^2}} \frac{(-1)^l}{l} \sin\left(2\pi l \frac{\mu}{q}\right) \right)^2 \\ &\quad - 2\frac{q}{\pi} \sum_{l=1}^{\infty} -\sigma^2 \frac{2\pi}{q} l e^{-2\pi^2 l^2 \frac{\sigma^2}{q^2}} \frac{(-1)^l}{l} \cos\left(2\pi l \frac{\mu}{q}\right) \\ &\approx -\frac{q^2}{\pi^2} e^{-2\pi^2 \frac{\sigma^2}{q^2}} \cos\left(2\pi \frac{\mu}{q}\right) \\ &\quad - 4\sigma^2 e^{-2\pi^2 \frac{\sigma^2}{q^2}} \cos\left(2\pi \frac{\mu}{q}\right) \\ &= \left( -\frac{q^2}{\pi^2} - 4\sigma^2 \right) e^{-2\pi^2 \frac{\sigma^2}{q^2}} \cos\left(2\pi \frac{\mu}{q}\right). \end{aligned} \quad (\text{T.25})$$

The behavior of  $\tilde{R}_2$  is illustrated in Figs. T.5 and T.6.

$$\begin{aligned} \tilde{R}_3 &\approx 3\sigma^2 \frac{q}{\pi} e^{-2\pi^2 \frac{\sigma^2}{q^2}} \sin\left(2\pi \frac{\mu}{q}\right) \\ &\quad + 3\frac{q^2}{12\pi} e^{-2\pi^2 \frac{\sigma^2}{q^2}} \sin\left(2\pi \frac{\mu}{q}\right) \\ &\quad + 3\frac{q}{\pi} \left( -\sigma^2 + \sigma^4 \left( \frac{2\pi}{q} \right)^2 \right) e^{-2\pi^2 \frac{\sigma^2}{q^2}} \sin\left(2\pi \frac{\mu}{q}\right) \\ &\quad - 3\frac{q^2}{\pi^2} \left( -\sigma^2 \frac{2\pi}{q} \right) e^{-2\pi^2 \frac{\sigma^2}{q^2}} \sin\left(2\pi \frac{\mu}{q}\right) \\ &\quad - \frac{q^3}{4} e^{-2\pi^2 \frac{\sigma^2}{q^2}} \left( \frac{1}{\pi} - \frac{6}{\pi^3} \right) \sin\left(2\pi \frac{\mu}{q}\right) \end{aligned}$$

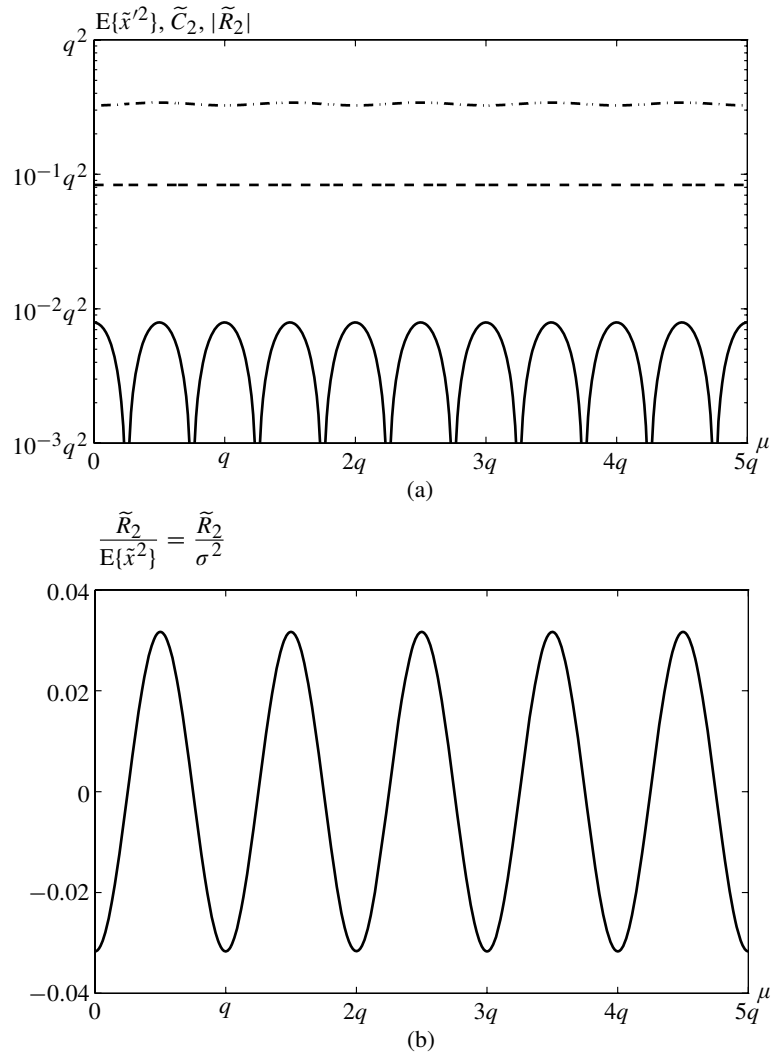


**Figure T.5** The second centralized moment of the quantizer output, the second Kind correction, and its error for Gaussian input,  $q = 2$ ,  $\sigma = 1$ : (a) the second centralized moment of the output (dash-dot), Kind correction (dashed), residual error of the correction (continuous line); (b) relative error of the second centralized moment.

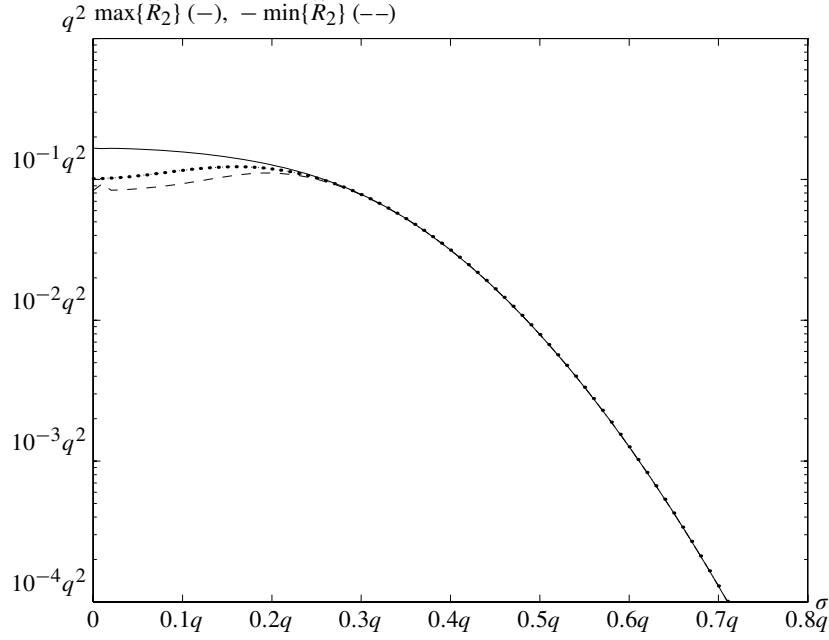


**Figure T.6** Maximum and minimum values of the residual error of the second Kind correction for Gaussian input, as a function of  $\sigma$ . The continuous line illustrates the exact value of the maximal residual error, the dashed line shows (-1) times the minimum error. The dotted line is calculated from the approximation by the  $l = 1$  terms of (T.25).

$$= \left( 12\pi \sigma^3 \frac{\sigma}{q} + \frac{6}{\pi} \sigma^2 q + \frac{3}{2\pi^3} q^3 \right) e^{-2\pi^2 \frac{\sigma^2}{q^2}} \sin \left( 2\pi \frac{\mu}{q} \right). \quad (\text{T.26})$$

The behavior of  $\tilde{R}_3$  is illustrated in Figs. T.7 and T.8.

$$\begin{aligned} \tilde{R}_4 \approx & \frac{q^2}{2} \frac{q^2}{\pi^2} e^{-2\pi^2 \frac{\sigma^2}{q^2}} \cos \left( 2\pi \frac{\mu}{q} \right) + \frac{q^2}{2} 4\sigma^2 e^{-2\pi^2 \frac{\sigma^2}{q^2}} \cos \left( 2\pi \frac{\mu}{q} \right) \\ & - 4 \frac{q}{\pi} \left( 3\sigma^4 \frac{2\pi}{q} - \sigma^6 \left( \frac{2\pi}{q} \right)^3 \right) e^{-2\pi^2 \frac{\sigma^2}{q^2}} \cos \left( 2\pi \frac{\mu}{q} \right) \\ & + 6 \frac{q^2}{\pi^2} \left( -\sigma^2 + \sigma^4 \left( \frac{2\pi}{q} \right)^2 \right) e^{-2\pi^2 \frac{\sigma^2}{q^2}} \cos \left( 2\pi \frac{\mu}{q} \right) \\ & + q^3 \left( -\sigma^2 \frac{2\pi}{q} \right) \left( \frac{1}{\pi} - \frac{6}{\pi^3} \right) e^{-2\pi^2 \frac{\sigma^2}{q^2}} \cos \left( 2\pi \frac{\mu}{q} \right) \end{aligned}$$

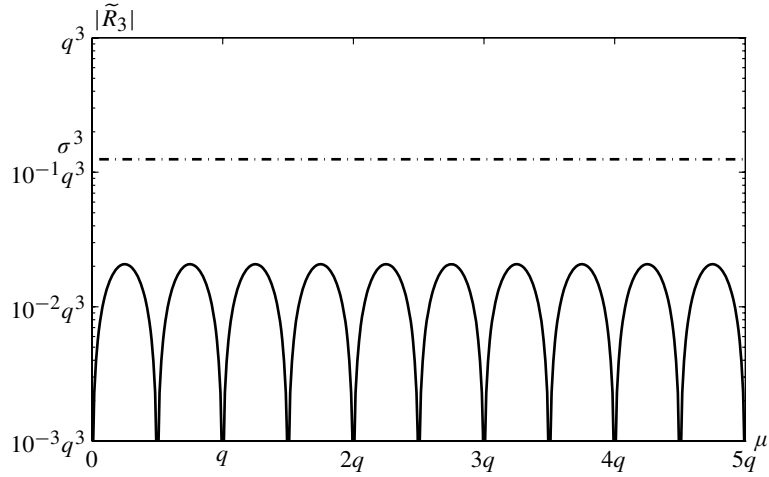


**Figure T.7** The error of the (Kind-)corrected third centralized moment of the quantizer input for Gaussian input,  $q = 2$ ,  $\sigma = 1$ . Because of the symmetry of the Gaussian distribution, the third moment and the Kind correction are both zero, so the error is equal to the third moment of the centralized quantizer output.

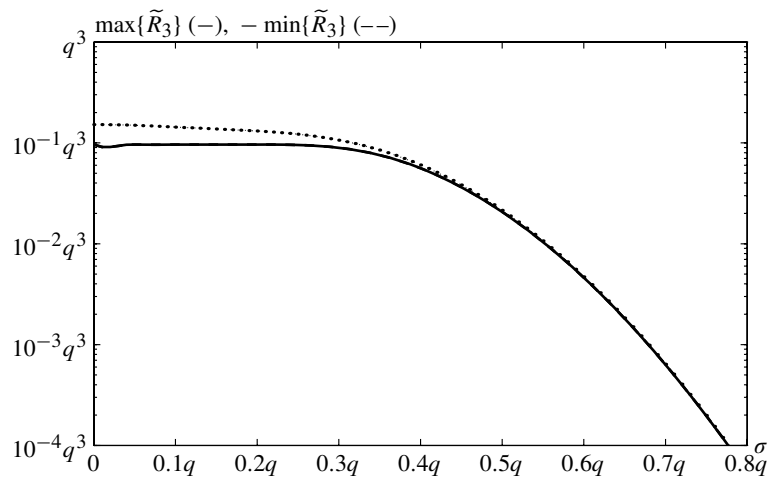


**Figure T.8** Maximum and minimum values of the residual error of the third Kind correction for Gaussian input, as a function of  $\sigma$ . The continuous line illustrates the exact value of the maximal residual error, the dashed line shows  $(-1)$  times the minimum error. The dotted line is calculated from the approximation by the  $l = 1$  terms (T.26).



$$\begin{aligned}
& -\frac{q^4}{2} \left( \frac{1}{\pi^2} - 6\frac{1}{\pi^4} \right) e^{-2\pi^2 \frac{\sigma^2}{q^2}} \cos \left( 2\pi \frac{\mu}{q} \right) \\
& = \left( 32\pi^2 \sigma^4 \frac{\sigma^2}{q^2} + \frac{6}{\pi^2} \sigma^2 q^2 + \frac{3q^4}{\pi^4} \right) e^{-2\pi^2 \frac{\sigma^2}{q^2}} \cos \left( 2\pi \frac{\mu}{q} \right). \quad (\text{T.27})
\end{aligned}$$

The behavior of  $\tilde{R}_4$  is illustrated in Figs. T.9 and T.10.

#### T.4 KIND CORRECTIONS FOR TWO VARIABLES

Similarly to the one-dimensional case, the moments of the fluctuations about the mean value can also be studied for the two-dimensional case. We give the first few two-dimensional Kind corrections which can be obtained from Sheppard's corrections, taking into account the zero mean of  $\tilde{x}$  and  $\tilde{x}'$ :

$$\begin{aligned}
E\{\tilde{x}_1 \tilde{x}_2\} &= E\{\tilde{x}'_1 \tilde{x}'_2\} \\
E\{\tilde{x}_1^2 \tilde{x}_2\} &= E\{(\tilde{x}'_1)^2 \tilde{x}'_2\} - (0) \\
E\{\tilde{x}_1 \tilde{x}_2^2\} &= E\{\tilde{x}'_1 (\tilde{x}'_2)^2\} - (0) \\
E\{\tilde{x}_1^2 \tilde{x}_2^2\} &= E\{(\tilde{x}'_1)^2 (\tilde{x}'_2)^2\} - \left( \frac{q_1^2}{12} E\{(\tilde{x}'_2)^2\} + \frac{q_2^2}{12} E\{(\tilde{x}'_1)^2\} - \frac{q_1^2 q_2^2}{144} \right) \\
&\vdots \quad \quad \quad (\text{T.28})
\end{aligned}$$

#### T.5 EXERCISES

- T.1** Derive the general formula of the  $r$ th moment of  $\tilde{x}'$  as a function of  $q$  and the moments of  $\tilde{x}$ . Hint: see Exercise 4.24.
- T.2** Express  $E\{\tilde{x}'^r\}$  with the moments  $E\{\tilde{x}''^r\}$ , using the so-called Bernoulli numbers (see T.2.FN1).  
Hint: Prove the following formula:

$$E\{\tilde{x}'^r\} = E\{(\tilde{x}'')^r\} - \left( \sum_{\substack{m=1 \\ m \neq r-1}}^r \binom{r}{m} (1 - 2^{1-m}) B_m q^m E\{(\tilde{x}'')^{r-m}\} \right). \quad (\text{ET.2.1})$$

- T.3** Evaluate the error in the covariance expression (B.25), in page 611, and the error in the kind correction (T.28), in page W81, for Gaussian distribution with  $q_1 < \sigma_1$ ,  $q_2 < \sigma_2$ , and  $|r_{12}| < 0.9$ .
- T.4** Derive the general expression of the two-dimensional kind corrections (express the moment  $E\{\tilde{x}_1^{r_1} \tilde{x}_2^{r_2}\}$  with the moments  $E\{(\tilde{x}'_1)^{r_1} (\tilde{x}'_2)^{r_2}\}$ ), using the so-called Bernoulli numbers (see Eq. (T.4.FN1)).

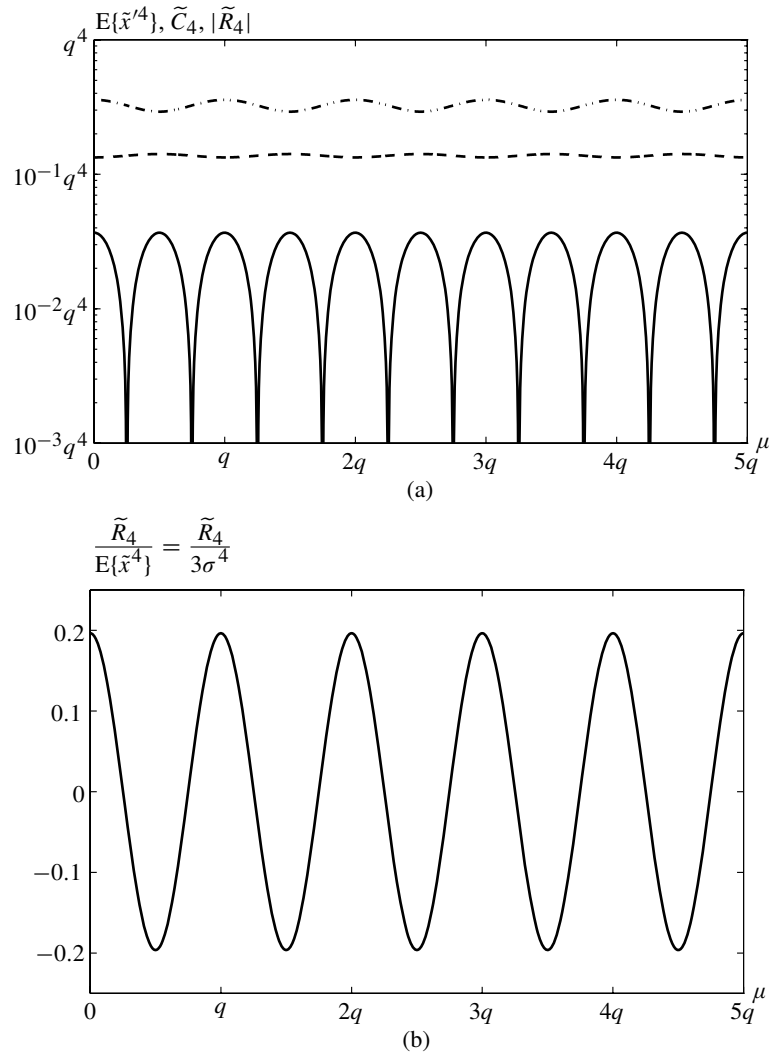


**Figure T.9** The fourth centralized moment of the quantizer output, the fourth Kind correction, and its error for Gaussian input,  $q = 2$ ,  $\sigma = 1$ : (a) the fourth centralized moment of the output (dash-dot), Kind correction (dashed), residual error of the correction (continuous line); (b) relative error of the fourth centralized moment.

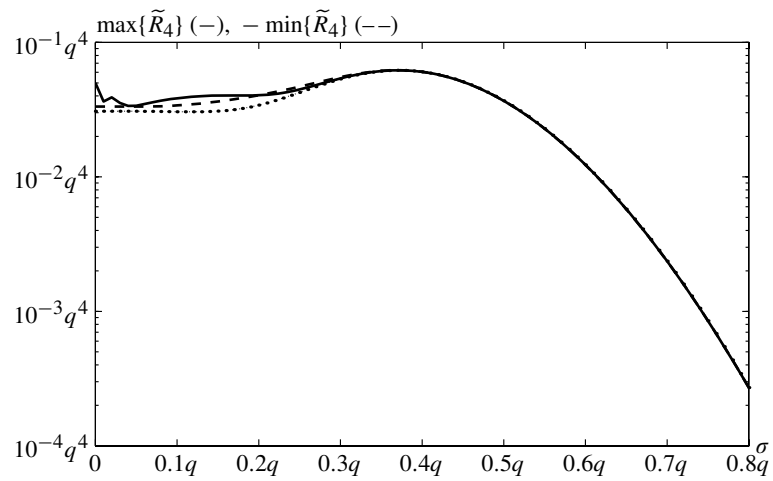


**Figure T.10** Maximum and minimum values of the residual error of the fourth Kind correction for Gaussian input, as a function of  $\sigma$ . The continuous line illustrates the exact value of the maximal residual error, the dashed line shows  $(-1)$  times the minimum error. The dotted line is calculated from the approximation by the  $l = 1$  terms (T.27).



## Addendum U

---

# ***Comparison of the Engineers' Fourier transform and the Definition of the Characteristic Function***

Some uncertainties in the precise forms of the formulas may stem from the slightly different definitions of the Fourier transform in engineering, and in mathematics. In this appendix, the most important differences are listed.

In the engineering definition, either the variable  $f$  or the variable  $\omega$  is used in the frequency domain. Their relation is  $\omega = 2\pi f$ . This small difference causes the appearance and disappearance of factors  $1/(2\pi)$  in a few formulas.

In the mathematicians' definition of the characteristic function,  $u$  is used, which corresponds to  $\omega$ , but a positive sign is used in the exponent of the kernel of the forward transform. This causes slight changes in a few formulas only.

The differences in the properties of the transform pairs are illustrated in the following expressions.

Definition:

$$\begin{aligned} X(f) &= \int_{-\infty}^{\infty} x(t)e^{-j2\pi ft} dt & \Phi(u) &= \int_{-\infty}^{\infty} f(x)e^{jux} dx \\ X_{\omega}(\omega) &= \int_{-\infty}^{\infty} x(t)e^{-j\omega t} dt \end{aligned} \tag{U.1}$$

Inverse:

$$\begin{aligned}
 x(t) &= \int_{-\infty}^{\infty} X(f) e^{j2\pi ft} df & f(x) &= \frac{1}{2\pi} \int_{-\infty}^{\infty} \Phi(u) e^{-jux} du \\
 x(t) &= \frac{1}{2\pi} \int_{-\infty}^{\infty} X_{\omega}(\omega) e^{j\omega t} d\omega & &
 \end{aligned} \tag{U.2}$$

Shifting:

$$\begin{aligned}
 x(t-a) &\leftrightarrow e^{-j2\pi fa} X(f) & f(x-a) &\leftrightarrow e^{jua} \Phi(u) \\
 x(t-a) &\leftrightarrow e^{-j\omega a} X_{\omega}(\omega) & & \\
 e^{j2\pi bt} x(t) &\leftrightarrow X(f-b) & e^{-jbx} f(x) &\leftrightarrow \Phi(u-b) \\
 e^{j\omega b t} x(t) &\leftrightarrow X_{\omega}(\omega-b_{\omega}) & &
 \end{aligned} \tag{U.3}$$

Negative argument:

$$\begin{aligned}
 x(-t) &\leftrightarrow X(-f) & f(-x) &\leftrightarrow \Phi(-u) \\
 x(-t) &\leftrightarrow X_{\omega}(-\omega) & &
 \end{aligned} \tag{U.4}$$

Negative argument (for real  $x(t)$  and real  $f(x)$ ):

$$\begin{aligned}
 x(t) &\leftrightarrow \overline{X(-f)} & f(x) &\leftrightarrow \overline{\Phi(-u)} \\
 x(t) &\leftrightarrow \overline{X_{\omega}(-\omega)} & & \\
 x(-t) &\leftrightarrow X(-f) = \overline{X(f)} & f(-x) &\leftrightarrow \Phi(-u) = \overline{\Phi(u)} \\
 x(-t) &\leftrightarrow X_{\omega}(-\omega) = \overline{X_{\omega}(\omega)} & &
 \end{aligned} \tag{U.5}$$

Integral:

$$\begin{aligned}
 \int_{-\infty}^{\infty} x(t) dt &= X(0) & \int_{-\infty}^{\infty} f(x) dx &= \Phi(0) = 1 \\
 \int_{-\infty}^{\infty} x(t) dt &= X_{\omega}(0) & & \\
 x(0) &= \int_{-\infty}^{\infty} X(f) df & f(0) &= \frac{1}{2\pi} \int_{-\infty}^{\infty} \Phi(u) du \\
 x(0) &= \frac{1}{2\pi} \int_{-\infty}^{\infty} X_{\omega}(\omega) d\omega & &
 \end{aligned} \tag{U.6}$$

Derivatives:

$$\begin{aligned}
 (-j2\pi t)^n x(t) &\leftrightarrow \frac{d^n}{df^n} X(f) & (jx)^n f(x) &\leftrightarrow \frac{d^n}{du^n} \Phi(u) \\
 (-jt)^n x(t) &\leftrightarrow \frac{d^n}{d\omega^n} X_\omega(\omega) \\
 \frac{d^n}{dt^n} x(t) &\leftrightarrow (j2\pi f)^n X(f) & \frac{d^n}{dx^n} f(x) &\leftrightarrow (-ju)^n \Phi(u) \\
 \frac{d^n}{dt^n} x(t) &\leftrightarrow (j\omega)^n X_\omega(\omega) & &
 \end{aligned} \tag{U.7}$$

Moments:

$$\begin{aligned}
 (-j2\pi)^n \int_{-\infty}^{\infty} t^n x(t) dt &\leftrightarrow \frac{d^n}{df^n} X(f) \Big|_{f=0} & (j)^n \int_{-\infty}^{\infty} x^n f(x) dx &\leftrightarrow \frac{d^n}{du^n} \Phi(u) \Big|_{u=0} \\
 (-j)^n \int_{-\infty}^{\infty} t^n x(t) dt &\leftrightarrow \frac{d^n}{d\omega^n} X_\omega(\omega) \Big|_{\omega=0} & &
 \end{aligned} \tag{U.8}$$

Convolution:

$$\begin{aligned}
 x_1(t) \star x_2(t) &\leftrightarrow X_1(f) X_2(f) & f_1(x) \star f_2(x) &\leftrightarrow \Phi_1(u) \Phi_2(u) \\
 x_1(t) \star x_2(t) &\leftrightarrow X_{\omega_1}(\omega) X_{\omega_2}(\omega) \\
 x_1(t) x_2(t) &\leftrightarrow X_1(f) \star X_2(f) & f_1(x) f_2(x) &\leftrightarrow \frac{1}{2\pi} \Phi_1(u) \star \Phi_2(u) \\
 x_1(t) x_2(t) &\leftrightarrow \frac{1}{2\pi} X_{\omega_1}(\omega) \star X_{\omega_2}(\omega) & &
 \end{aligned} \tag{U.9}$$

An alternative definition is given with  $1/\sqrt{2\pi}$  terms in both directions (a unitary transform):

$$X_2(\omega) = \frac{1}{\sqrt{2\pi}} \int_{-\infty}^{\infty} x(t)e^{-j\omega t} dt, \quad x(t) = \frac{1}{\sqrt{2\pi}} \int_{-\infty}^{\infty} X_2(\omega)e^{j\omega t} d\omega \quad (\text{U.10})$$

For this, the above properties are similar, with the following differences:

Integral:

$$\int_{-\infty}^{\infty} x(t) dt = \sqrt{2\pi} X_2(0), \quad x(0) = \frac{1}{\sqrt{2\pi}} \int_{-\infty}^{\infty} X_2(\omega) d\omega \quad (\text{U.11})$$

Derivatives:

$$(-jt)^n x(t) \leftrightarrow \frac{d^n}{d\omega^n} X_2(\omega), \quad \frac{d^n}{dt^n} x(t) \leftrightarrow (j\omega)^n X_2(\omega) \quad (\text{U.12})$$

Moments:

$$\frac{(-j)^n}{\sqrt{2\pi}} \int_{-\infty}^{\infty} t^n x(t) dt \leftrightarrow \frac{d^n}{d\omega^n} X_2(\omega) \Big|_{\omega=0} \quad (\text{U.13})$$

Convolution:

$$\begin{aligned} x_1(t) \star x_2(t) &\leftrightarrow \sqrt{2\pi} X_{\omega_1}(\omega) X_2(\omega) \\ x_1(t)x_2(t) &\leftrightarrow \frac{1}{\sqrt{2\pi}} X_{\omega_1}(\omega) \star X_{\omega_2}(\omega) \end{aligned} \quad (\text{U.14})$$